Patterns of Skeletal DNA Preservation and the Influence of Post-mortem Microbial Communities

A Dissertation Presented for the
Doctor of Philosophy
Degree
The University of Tennessee, Knoxville

Alexandra Leah Emmons
August 2019

DEDICATION

I dedicate this work to my family. Without their love and support, I would never have made it this far.

ACKNOWLEDGEMENTS

Thank you to my chair, Dr. Amy Mundorff and my committee, Dr. Jennifer DeBruyn, Dr. Dawnie Steadman, Dr. David Carter, and Dr. Alex Bentley, for their help and guidance. Thank you to the Department of Anthropology at the University of Tennessee and to staff and volunteers at the Forensic Anthropology Center. Thank you to the donors, for without them this research would not be possible. Lastly, thank you to various alumni and friends of the university (the Thomas family, Walter Leitner, and Simon Beckett), and external funding agencies (the National Institute of Justice and National Science Foundation) for financially supporting various aspects of this work.

ABSTRACT

DNA analysis plays an important role in forensic identification, particularly when remains are heavily decomposed. In such instances, extracting DNA from skeletal/dental remains may be necessary to obtain an identification, yet there is no consensus regarding which skeletal elements should be sampled for DNA testing. Previous research examining intra/inter-individual skeletal preservation in surface deposited remains found that small cancellous bones outperformed dense, cortical bones in human DNA quantity and quality, a pattern that held true in individuals with PMIs up to 21 years. In this dissertation, I expanded on this research by examining whether the same pattern would result in buried remains, with the goal of relating observed patterns to changes in soil geochemistry and microbial ecology.

Chapter II presented a characterization of the microbes capable of colonizing bone from surface deposited remains using next generation sequencing methodologies, thereby addressing the gap in what is known about microbial skeletal degradation. Chapter III focused on patterns of intra/inter-individual skeletal DNA preservation in a multi-individual burial and the impact of the burial environment, including moisture and microbial loading. Chapter IV directly compared microbial communities in buried remains to those from the surface, and further related changes in microbial community composition and structure to changes in bone organic content (i.e., human DNA), soil microbiology and geochemistry, and the *in vivo* gut ecosystem.

Bones of the foot showed similarly high human DNA typing success from buried and surface environments. The cuneiforms showed consistently high human DNA yields from all three interred individuals. Bone microbial loading was not a reliable predictor of human DNA concentration. Rather, specific bacteria including *Clostridium* spp., which includes known collagenase-producers, and a suite of other taxa from the phyla Bacteroidetes, Proteobacteria, Planctomycetes, Firmicutes, and Actinobacteria, have demonstrated inverse relationships with human DNA concentration. The deposition environment (e.g., site hydrology) had a noticeable impact on patterns of skeletal DNA preservation. This research complements previous work by Mundorff and Davoren [5] and Hines et al. [9], while redressing gaps in the existing body of knowledge regarding skeletal DNA degradation, the microbial ecology of bone, and the effects of the burial environment.

TABLE OF CONTENTS

LIST OF TABLES

LIST OF FIGURES

CHAPTER 1
INTRODUCTION, BACKGROUND, AND RESEARCH QUESTIONS

DNA analysis plays an important role in forensic identification, particularly when lengthy post-mortem intervals and advanced decay are considered (e.g.,[1–4]). In such instances, extracting DNA from skeletal or dental remains may be necessary to obtain an identification. However, this process is not without its shortcomings. Few laboratories possess the expertise necessary to deal with challenging post-mortem samples such as degraded skeletal remains. Moreover, skeletal elements contain differing concentrations of human DNA pre-degradation due to intrinsic differences, and because DNA does not degrade evenly throughout the skeleton, some bones may prove more reliable for DNA recovery over increasing post-mortem intervals than others. The purpose of this dissertation was to understand patterns of skeletal DNA preservation in buried remains, focusing on inter-individual and intra-individual variation, and how these patterns differ from surface remains. The goal is to not only document observed patterns of skeletal DNA preservation but also to relate these patterns to changes in soil geochemistry and microbiology. Currently, the procedures used to test bone and teeth are costly; therefore, this knowledge may help avoid wasting valuable time and money sampling skeletal elements that fail to yield adequate DNA results.

By comparing DNA degradation among skeletal elements within a single individual and then assessing consistency across three individuals, Mundorff and Davoren [5] ranked skeletal elements based on their overall DNA yield and ability to ascertain a full forensic profile (i.e., 16 STR loci). The authors found that small cancellous bones, on average, yielded greater amounts of higher quality DNA than their larger, denser cortical bone counterparts. They further tested the most successful elements, as well as commonly sampled bones (i.e., the femur and tibia), which were not among the most successful elements, from an additional 12 individuals, up to 21 years post-mortem. The pattern of small cancellous bones out-performing dense, weight-bearing cortical bone maintained over time [5]. However, these results were obtained using skeletal elements from individuals who decomposed on the ground surface; none were buried.

Decomposition is highly variable and influenced by a number of environmental factors. Patterns established on the surface may not be representative of a burial context. Certain data on DNA degradation in skeletal elements recovered from the ground surface conflict with data from buried remains (e.g., [5–9]). The difference between findings may be due, in part, to differences in the elements tested in these studies. For example, phalanges and tarsal bones were ranked as some of the most successful elements by Mundorff and Davoren [5] but were not reported on by Milos et al. [8] or Edson et al. [6]. In fact, many of the most successful elements reported on by Mundorff and Davoren [5] comprise elements rarely sampled for DNA, and therefore ones with limited reports of success. Whether the above findings conflict because of sample composition or because of differences in surface and subsurface decomposition, points to a gap in the existing knowledge base that can only be bridged through a controlled study focusing on testing all skeletal element types from buried human remains. This will directly contribute to our understanding of the susceptibility of DNA to degradation.

Additionally, it is crucial to not only uncover patterns in DNA degradation but also environmental and edaphic influences. Soil is a dynamic environment with multiple interacting chemical (e.g., soil pH, soil moisture, ion exchange capacities, redox potentials, and oxygen content), physical (e.g., soil minerology), and biological factors (e.g., microbes)[10]. These interacting features constrain or augment the decomposition of carrion within a burial

environment. Soil provides a challenging environment for skeletal DNA survival. Bone decay mechanistically proceeds via chemical degradation of the organic and inorganic components of bone and/or biogenic (microbial) degradation [11]; the latter of which, is a key focal point of this dissertation. The soil harbors microbial taxa that efficiently break down labile organic matter, including DNA, for nutrient uptake and cycling [12,13]. More recalcitrant material is also degraded by soil decomposers, albeit at a slower rate.

During decomposition, both endogenous microbes from the body and microbes from the surrounding grave soil can invade exposed bones [14] by exploiting the natural microanatomy of bone including void space or other points of access such as Volkmann's canals or Haversian systems [15,16]. Because of this, we expect intrinsic differences related to bone morphology and function to affect the degree of microbial invasion and the types of microbes capable of bone colonization and subsequent degradation. An understanding of both the intrinsic (bone tissue type and morphology) and extrinsic (microbial presence, composition, and structure) factors affecting DNA preservation is essential to extending our findings to other decomposition scenarios. Therefore, a large focus of this dissertation was devoted to understanding changes in the living bone ecosystem in post-mortem human remains, characterizing differences in microbial communities in surface and buried remains and how these communities change by anatomical region, individual, and bone type.

Organization

The contents of this dissertation follow a manuscript policy outline. Following a literature review on the decomposition of buried remains, post-mortem human microbial ecology, skeletal biology, and skeletal DNA preservation, as well as an overview of the sample/site description and research objectives, this dissertation will proceed as follows. Chapter II, entitled *Patterns of microbial colonization of human bone from surface-decomposed remains* presents a characterization of the microbes capable of colonizing bone from remains that had decomposed on the surface using next generation sequencing methodologies. Chapter II also addresses the gap in what is currently known about microbial skeletal DNA degradation by assessing changes in bacterial loading and attempting to predict taxa associated with increases or decreases in human skeletal DNA concentration. Chapter III, entitled *Inter and intra-individual variation in skeletal DNA preservation in buried remains* focuses on patterns of intra-individual and inter-individual skeletal DNA preservation in a multi-individual burial and how these patterns are shaped by burial factors, including moisture and microbial loading. This chapter complements existing research by Mundorff and Davoren [5]. Chapter IV, entitled *The post-mortem bone microbiome: implications for DNA survivability in buried remains,* directly compares microbial communities in buried remains to those from the surface, and further relates changes in microbial community composition and structure to changes in organic content, specifically human DNA, soil microbiology and geochemistry, and the *in vivo* gut ecosystem. The final chapter, Chapter V, synthesizes this information, providing overarching conclusions, limitations, and areas for further research.

Literature Review

Decomposition of Buried Human Remains

Factors that modulate the rate and trajectory of decomposition differ between a buried and surface environment. On the surface, decedents are exposed to more variable environmental conditions including changes in temperature, humidity, rain levels, insect activity, UV exposure, and scavenging. Temperature is the most important factor regarding the rate of decomposition [17,18]. Increases in temperature result in increased insect and microbial activity. According to Van't Hoff's rule, the velocity of an enzymatic reaction increases by a factor of two or three for every ten degree Celsius temperature increase [19]. Surface decomposition is variable with changes in daily and seasonal temperature fluctuations. Insects are impacted by temperature and other changes in climate including the frequency of precipitation events, and are the second most important factor related to the rate of decomposition [20]. Without insects, decomposition progresses at a slower rate and is dominated by decay and dehydration [21]. Though the order Diptera may be active at 5-13 degrees Celsius, their activity is drastically reduced, and at temperatures below 0 degrees Celsius, their eggs and larvae die. This is in contrast to optimal temperatures, during which, Diptera have been known to consume 50% of carcass biomass using a small mammal model (*Rattus rattus)* [22]. Similarly, without scavenging, the rate of decomposition will also decrease [17], yet increased temperatures, insect activity, and microbial activity constrain the influence of scavengers by limiting temporal bioavailability [23].

Other factors that affect the rate of decomposition include the presence of clothing or other coverings, trauma, pH, embalming, ground surfaces (e.g., concrete vs. soil), and seasonality [17]. The degree to which these variables affect the rate of decomposition is an area of extensive and ongoing research. For example, though trauma provides alternative points of access to insects and has demonstrated anecdotal increases in the rate of decomposition [17], other research has suggested that it has no effect on the rate of decomposition [24]. Likewise, reports that clothing both increase [17] and decrease [25] the rate of decomposition exist. Other coverings, including sheets and tarps, alter the trajectory of decomposition (mummification vs. liquefaction vs. adipocere formation) based on the degree of permeability. For example, cotton sheets are more likely to promote desiccation, possibly by limiting insect activity and scavenging, but maintaining air flow, while plastic tarps stimulate adipocere formation [26].

Burials are effectively a type of covering, in which soil composition, moisture, depth, and other edaphic parameters influence the degree of oxygen availability. Decomposition in a buried environment progresses at a much slower rate, reportedly eight times slower than decomposition in an open-aired, oxic environment in East Tennessee [27]. Burials exclude access by scavengers and insects and minimize temperature effects [27,28]. At increased depths, temperatures stabilize and fluctuate less diurnally, though they continue to shift seasonally [28]. Rodriguez and Bass [28] compared cadaver decomposition at different depths (1 ft, 2ft, and 4ft). They observed daily and seasonal temperature fluctuations at depths of 1ft and noted ongoing scavenging and necrophagous insect activity. Both insect activity and scavenging were no longer present at depths of 2 ft and greater, which showed decreased rates of decomposition [28]. Though, the coffin fly has reportedly accessed cadavers at depths up to 2 m [29].

As alluded to above, the physical and biogeochemical environment of the burial (e.g., rate of oxygen diffusion, moisture content, soil texture, and redox potential) also influences the rate and trajectory of decomposition. Using 216 soil microcosms and a small mammal model (*Rattus rattus*), Carter et al. [30] examined the relationship between moisture content, soil pH,

nitrogen reactive ninhydrin, CO_2-C evolution, microbial biomass carbon, and enzymatic activity (protease and phosphodiesterase). Three soil textures (i.e., sandy loam, sand, and medium clay) were equilibrated to three matric potentials, representing wet, moist, and dry soils. Coarse textured soils with low moisture contents resulted in reduced decomposition rates. These soils have high gas diffusivities, but lack optimal moisture levels, resulting in low microbial motility and low hydrolytic enzyme activity. In contrast, wet fine textured soils (more clayey) resulted in reduced decomposition rates by limiting oxygen availability. The combination of low gas diffusivity with increased microbial biomass constrained the rate of oxygen exchange, shifting the environment to anaerobic processes and reducing microbial activity [30].

Both surface and subsurface microbial communities, within the decaying organism and in the underlying soil continually shift in structure and composition throughout decomposition [31,32], dictated by changes within the environment. This is important because microbial communities produce a number of compounds and enzymes not only helpful for the catabolism of macromolecules but also for competitive interactions with other microbes, insects, and scavengers [33], which will affect the progression of decomposition. Whether the environment, either subsurface or surface, is reducing or oxidative, impacts the decomposition rate by placing selective pressures on microbial communities and their metabolic strategies. Reducing, or anoxic environments, promote decomposition by anaerobic microbes (either facultative anaerobes or obligate anaerobes), which are less efficient decomposers than their aerobic counterparts [18]. In contrast, oxidative environments, or oxic conditions, promote aerobic decomposition.

Reducing conditions also affect the likelihood of adipocere formation [31]. Adipocere, a white substance known as grave wax, results from the hydrolysis of triglycerides into free fatty acids and is primarily composed of myristic, palmitic, and stearic acids. Adipocere has preservative effects on human tissues [31,32]. Though burial is not a requirement for the formation of adipocere, its formation on buried carrion/cadavers is a common occurrence. Plastic and synthetic coverings or wrapping [33] as well as neutral to alkaline pHs have also been associated with adipocere formation. Though moisture is required for the hydrolysis of triglycerides, the body's own moisture is sufficient for this process to occur in poorly drained soils [31]. Adipocere formation should not be considered a terminal state of decomposition; reversion to an aerobic environment can lead to its degradation [32].

Microbes in Human / Carrion Decomposition Research

Microbes are important for both surface and subsurface decomposition. Putrefaction, which is dominated by anaerobic bacteria and fermentative metabolic pathways, is the degradation of tissues by enteric gut microorganisms [19]. This occurs early in decomposition simultaneous to autolysis. The catabolism of large macromolecules (e.g., proteins, fats, and carbohydrates) produces acids (e.g., propionic, butyric, acetic, acetoacetic, and lactic acid) and gases (e.g., methane, carbon dioxide, ammonia, and hydrogen sulfide) and results in distention or bloating of the abdomen, face, and scrotum [18,34]. The role of endogenous and exogenous microbes continues throughout decomposition, even after skeletonization [14,35], yet, research on the human post-mortem microbiome, as it pertains to forensic science, has only gained traction in recent years. Though research pertaining to microbial ecology and decomposition is not a new area of research, as soil organic matter decomposition has been a long-studied area in microbiology, its potential in human decomposition research has not yet been fully explored.

As research on the post-mortem microbiome has expanded within the fields of anthropology, entomology, and ecology, an evolution of terminology has followed. Multiple

terms specific to post-mortem microbial communities have been established and used by different research groups. The *necrobiome* was coined as an inclusive descriptor of postmortem microbial communities referring to the communities of microbial prokaryotes and eukaryotes associated with a "decomposing heterotrophic biomass", thereby excluding the decomposition of plant matter but including microbes, necrophagous insects, and scavengers [36]. Other terminology has also developed to reference specific regions of decomposing carrion. For example, Pechal et al. [37] defined the *epinecrotic community* as the community of organisms that live or move on the surface of decomposing carrion, generally referring to the skin or mucosal membranes, and including protists, bacteria, archaea, and fungi, while the *thanatomicrobiome* has been used to refer to the microbiome of internal organs after death [38].

The primary goals of post-mortem microbiome research in forensic science has been to (1) understand the ecology and biochemistry of carrion decomposition and (2) to identify indicator taxa that can be used to estimate the post-mortem interval, or the time between death and discovery of a decedent (e.g., [37,39–45]). Though this research has focused on a number of different substrates such as the skin [37,41,43], mouth [37,46,47], gut [37,41,43–46], internal organs [38,48,49], and bone [14], much of this research has focused on the soil either directly or indirectly [43,50–54]. Together, this research, which is cursorily summarized below, has evoked questions related to seasonality, individual variability, edaphic/environmental influences, and interkingdom dynamics.

Though enteric microbes were known to be important to the process of putrefaction, the role of soil microorganisms has been a focus of increased research, most notable over the last ten years. Importantly, using a murine model (n = 80) and two soil types, sterilized and unsterilized, Lauber et al. [55] demonstrated that decomposition progresses 2 to 3 times slower in sterilized soil versus unsterilized soil. This is likely a contributing factor as to why cadavers placed on different surface materials (e.g., concrete vs. soil) decompose at different rates [17]; the microbes capable of colonizing those surfaces are integral to the decomposition process. In the same study, key saprophytic and ureolytic taxa recognized as potential carrion decomposers were identified using 16S rRNA and 18S rRNA gene sequencing, including soil eukaryotes (e.g., *Mucoromycotina* and *Eurotiomycetes*) and soil prokaryotes (e.g., *Morganella* and *Proteus*) [55].

While soil microbial communities did not have a significant effect on skin microbial communities, and gut microbial communities did not have a significant impact on soil microbial communities [55], other research has contradicted this pattern [41,50,56]. Metcalf et al. [41] observed a convergence of soil and skin communities in the late stages of decomposition using a murine model, which the authors hypothesized to be related to low skin biomass in comparison to the soil, while others have observed the persistence of a human-associated gut bacteria, *Bacteroides* sp., well after skeletonization [56] and even the collection of remains [50].

Postmortem microbial communities change in consistent and reproducible ways throughout decomposition [41], even across seasons, soil types, and host species [43]. Soil microbial communities in decomposition begin to change following the introduction of cadaveric material in soil; this coincides with purge and a transition from bloat to active decomposition [50,57]. Cadaver-associated soil microbial communities have shown decreases in diversity, evenness, and richness across time [36]. Following rupture, or the release of cadaver-derived nutrients due to cracks and tears from increased pressure during bloat, Cobaugh et al. [50] observed increases and dominance in the relative proportions of two phyla, Proteobacteria and Firmicutes in cadaver-associated soils, which coincided with a simultaneous decrease in the relative abundance of Acidobacteria. In contrast, the authors did not see a significant change in

the proportions of Bacteroidetes, likely related to the release of human-associated bacteria into the surrounding environment (i.e., *Bacteroides* sp.*)* [50]. Metcalf et al. (2013) observed similar patterns; post-rupture soils saw a decline in Acidobacteria (an oligotrophic group) and a shift to more copiotrophic groups such as Alphaproteobacteria (e.g., Rhizobiales). In addition, they observed that facultative and obligate anaerobes dominated the gut microbiome of mice throughout bloat, including Firmicutes and Bacteroidetes, followed by a shift to more aerobic bacteria or facultative anaerobes during active decay [41].

A second major shift in microbial community structure and function has been seen in the transition from active decay to advanced decay, as the decomposition rate slows. During this time, Cobaugh et al. [50] saw a small spike in microbial respiration and a reduction in biomass production and ammonia concentrations, which is suggestive of a more oligotrophic community functionality. The phylum Firmicutes dominated the advanced stage of decomposition with noticeable shifts from aerobic to anaerobic taxa, including human-specific bacteria; changes which were consistent with an anoxic environment [50]. Metcalf et al. (2013) observed increased proportions of Bacteroidetes, Alphaproteobacteria, and Betaproteobacteria during advanced decay, with a restoration of microbial community richness and diversity in the final stages of decomposition.

Using these observations, researchers hypothesized that the succession from oligotrophic to copiotrophic taxa and back could be used to develop models for PMI estimation. For example, using random forest models, a supervised learning technique, Metcalf et al. [41] developed PMI models with a minimum mean absolute error of 3.30 +/− 2.52 days using skin and soil communities, which were successful within 34 days post-mortem. Using quantitative PCR (qPCR) to quantify changes in human gut bacteria, Hauther et al. [44] identified two taxa potentially useful for PMI estimation with PMIs less than 20 days, *Bacteroides* and *Lactobacillus. Bacteroides* remained a potential PMI biomarker following 16S rRNA community analysis, which also unveiled a potential role for *Parabacteroides* in PMI estimation [45]. *Lactobacillus* has also been identified as an important PMI biomarker in decaying organ tissues and blood, along with *Clostridium* and *Prevotella* [38,49]. In particular, by applying random forest models to microbial taxa recovered from decaying organs, *C. novyi* was more predictive of late PMIs, while unclassified *Clostridium* was more predictive of early PMIs [49].

Other interesting research has focused on seasonality, temperature, and insect activity, important regulators of the decomposition rate. For example, Carter et al. [57] focused on seasonal changes in soil microbial communities associated with *Sus scrofa* remains, finding that while bacterial soil communities significantly differed between summer and winter, soil microbial eukaryotes were more stable. In addition, they identified seasonal indicators including Chitinophagaceae during the summer and *Psychrobacter* during the winter [57]. Tibbett et al. [59] used buried skeletal muscles from *Ovis aries* to examine the effects of temperature on microbial activity and the decomposition rate, demonstrating unsurprisingly that microbial respiration and the rate of tissue decomposition increased with increasing temperatures and decreased with decreases in substrate availability (Also see [60]). Other research has pointed to blow flies as an important source of human decomposer microbes [43], likely related to the observation that larger body masses attract greater attention from various arthropod species [61]. Evidence suggests that not only do insects play a role in the dispersal of bacteria, but they also rely on bacteria to locate carrion sources by responding to the quorum signaling behavior of bacteria [62].

Most carrion/cadaver associated soil studies have involved surface decomposition. There is a paucity of data on grave soil communities associated with buried remains, likely because burial disturbance during sampling would artificially impact observed patterns. Nevertheless, differences in alpha diversity metrics between soils recovered during surface decomposition and those associated with subsurface decomposition have been noted, with richness decreasing in the former and increasing in the latter [58]. However, soils in this study and a follow-up study were collected directly above remains, at a maximum depth of 30 cm [53,58], which is less likely to be affected by decomposition byproducts due to gravity. Because of this, it was unsurprising that Thomas et al. [53] concluded that soils collected above dry human remains were similar to untreated (no decomposition) soils.

Similarly, research on postmortem microbial eukaryotic communities has also been limited. Though research has examined changes in both 16S rRNA and 18S rRNA genes, 16S rRNA research has dominated. Nevertheless, changes in microbial eukaryotic communities have been equally informative in PMI estimation models [41], and soil nematodes [41,63], microbivorous arthropods [64], and protozoa [65,66] have shown significant responses to pulses in cadaveric inputs and concomitant microbial blooms.

Bone as an Environment

Most decomposition research terminates with the skeletonization of remains. However, unless fossilized, which is rare, bone continues to decay following soft tissue decomposition. Decomposition proceeds via multiple co-occurring processes, physical, chemical, and biological. Autolysis, the self-degradation of the body via its own mechanisms of cellular death, and putrefaction, or the degradation of the body by enteric micro-organisms occur simultaneously [18]. These processes are further influenced by scavenging, changes in temperature and humidity, environmental microbiota, arthropod activity, and a suite of other factors related to the condition of remains at the time of death and deposition. These processes continue to have an affect beyond skeletonization. Bone is not only susceptible to chemical modifications, with influences from the physical environment, but is also susceptible to biological modification from microbial decomposers from a number of potential sources (e.g., the decaying individual, scavengers, arthropods, and the surrounding soil) and physical modification from scavenging macrofauna and growing vegetation [11,67]. In this way, decaying remains, including skeletal material, can be considered ecological inputs (e.g., nutrient sources / habitats) capable of supporting a dynamic ecosystem of both microscopic and macroscopic scavengers and other incidental taxa.

Bone Preservation

Bone is an interesting material, not only because it is made up of both inorganic and organic components but also because of its multiple structural/functional roles (i.e., protection, hematopoiesis, and homeostasis) [68]. The inorganic phase (~30-50% by volume, ~65% by weight) comprises the majority of bone, while the organic phase (~30-45% by volume, 20-25% by weight), and water (~10% by weight) make up the remainder [68,69]. The inorganic phase includes a calcium phosphate material ($Ca_{10}(PO_4)(OH)_2$), most similar to hydroxyapatite, known as bioapatite, that is non-stoichiometric with the surrounding environment [70]. Being non-stoichiometric has *in vivo* advantages, allowing bone to store and release calcium, sodium, and other trace elements important for biosynthesis with continual turnover [71,72]. Bioapatite also includes phosphate, hydroxy ions, carbonate, pyrophosphate, magnesium, and potassium [72].

The organic component of bone consists of 90-95% Type I collagen, primarily made up of glycine, proline, and hydroxyproline (Gly-X-Y), with minor contributions from other non-collagenous proteins (e.g., proteoglycans, glycoproteins, osteocalcin, and osteonectin) as well as lipids, mucopolysaccharides, and carbohydrates [35,73].

Type I collagen is a highly organized hierarchal protein. At the base of this hierarchy lies tropocollagen, which has a triple helix conformation; these molecules aggregate and organize into bundles known as microfibrils, which are stabilized by aldehyde cross-links and other intramolecular hydrogen bonds between molecules. These then organize further into fibrils and then fibers [67,69]. Bone mineral is in close association with collagen, deposited between collagen molecules laterally and longitudinally at gap ends. Bone mineralization is stimulated by osteoblasts and regulated by a suite of non-collagenous proteins and signaling cascades. Mineralized fibrils are further organized into sheets known as lamellae. This organization is structurally dependent on the applied loading force or stressor, compression versus tension [68].

There are two main types of bone: cancellous (i.e., spongy bone or trabecular bone) and cortical bone (i.e., compact bone). Cortical bone generally forms the outer layers of bones and is the primary bone type of the diaphyses of long and short bones of the arms and legs. Trabecular bone is generally found in marrow spaces, including the metaphyses of long bones, vertebrae, and ribs as well as in the flat bones of the cranium, ilium, and sternum [67,74]. Red marrow is continually produced in these regions throughout life, and with age, progenitor cells can differentiate into adipocytes instead of red marrow, causing a divergence to yellow marrow in the diaphyses of long bones with age [68]. The density of mineralized tissue necessitates that bone cells be in close proximity to blood vessels [68]. Haversian systems form the center of osteons, around which are found bone cells, or osteocytes. The osteocytes are connected by canaliculi (~200nm), while Haversian systems are connected by Volkmann's canals (both ~50-250 μm in diameter); through these connections run blood vessels and nerves [67,75].

Bone diagenesis is the postmortem alteration of bone by various chemical, physical, and biological factors that result in the modification of the original material [72]. The mechanics of bone diagenesis is not well understood but proceeds via two overarching and interdependent processes, chemical and microbial degradation [11,67]. When not in equilibrium with the surrounding environment, dissolution and recrystallization of bioapatite occurs, allowing microorganisms and enzymes access to the organic phase, resulting in degradation. Similarly, as the organic component degrades by either chemical or biological means, bioapatite becomes more vulnerable to environmental fluctuations and dissolution of the lattice structure is more probable due to new voids in the crystal lattice [11,35,72,76–78]. Dissolution promoted by the presence of water and low pH is not the only way for microbial taxa to gain access to tightly bound collagen. Microbes may also degrade hydroxyapatite directly through the production of organic acids [79]. Microbially mediated degradation is an important mechanism of skeletal degradation. To become fossilized, bone must remain relatively free of microbial influence. Mechanistically, collagen degradation in fossilizing bone likely occurs over long time periods by abiotic processes [80].

Additionally, bacteria, archaea, and microbial eukaryotes including fungi exploit the existing microanatomy of bone, porosity and vascularization, to colonize and degrade organic and inorganic material [16]. Though fungal activity has been implicated in bone degradation since the 1800s [67], attributed to Wedl (1864), and the role of bacteria in putrefaction has been emphasized for decades, the impact of microbes on human bone throughout decomposition, including post-skeletonization, is not well understood. Classically, the microbial modification of

bone has been the focus of bone histological research within the disciplines of archaeology, paleoecology, and paleontology, including but not limited to methods such as light microscopy, scanning electron microscopy (SEM), backscatter electron microscopy (BSE-SEM), and mercury intrusion porosimetry [75]. The histological manifestation of microbial degradation presents as differences in tunneling behavior, bone boring, and other resorptive changes; together, destructive changes to bone are referred to as microscopic foci destruction [81]. Types of tunneling include Wedl, Hackett, linear longitudinal, budded, and lamellate. In general, Wedl and Hackett tunneling are characterized by the presences of fungi or Cyanobacteria, while the latter three are the result of bacterial modification [75].

Interestingly, observations of microscopic focal destruction on bone in the archaeological record indicate that microbial activity disproportionately impacts human bone degradation over animal bone. This could be related to butchery practices, as there would be a lack of putrefactive bacteria in deposited butchered remains [16]. Alternatively, it could also relate to differences in bone maturity and density, as most animals are butchered shortly after reaching maturity [67]. However, others have also emphasized the importance of enteric microbes in bone degradation [82–84]. White and Booth [82] observed an early form of non-Wedl tunneling in pig remains, which they explained as an indicator of putrefactive bacterial bioerosion early after death (3 – 5 months). In addition, still born neonates showed no evidence of bacterial degradation, likely related to the sterility of their gut microbiomes, while buried remains showed more extensive alterations, potentially related to the persistence of gut microbes in burials [82]. Booth [83] suggested that funerary practices could be reconstructed based on the degree of bacterial bone degradation in a given sample; greater bioerosion indicated prolonged exposure to putrefactive bacteria. Similar to pig neonates, human neonates from cemeteries with otherwise extensive bacterial skeletal alterations were relatively free of bacterial influence.

The rate at which bone is impacted microscopically by microbial influence has also been questioned. Bell et al. [84] examined the rate of diagenetic change postmortem in the skeleton by examining forensic bone with different post-mortem intervals and deposition environments. Post-mortem change, in the form of destructive foci, were observed as early as 3 months after death but were attributed to and influenced by gut demineralization (digestion). Bacterial signs of skeletal alterations were not observed until 15 months at the earliest followed by 2 years. In contrast Marchiafava et al. [79] observed fungal tunneling, as a result of *Mucor* activity, in as little as 15 days using defleshed bone. Given that putrefactive bacteria may substantially contribute to post-mortem bacterial skeletal degradation, it is possible that bacteria infiltrate the skeleton early in the decomposition process via translocation to bone through nutrient arteries and then spreading intra-cortically by way of Haversian systems, as speculated by Bell et al. [84]. By inoculating mice nares with fluorescently labeled bacteria, Burcham et al. [85] observed bacterial migration into various organ systems one hour following death; translocation increased over the next three to fourteen days. While bone was not the focus of their study, enteric microorganisms likely contribute to microbial bone degradation.

Many collagenase-producing microbes found in the human gut and in soil and have been hypothesized to be important bone degraders [70]. Collagenases are proteolytic enzymes specific to the degradation of collagen; they are most efficient at neutral pHs (Child 1995). Collagenase producing bacteria isolated from bone have included *Alcaligenes pichaudii, Bacillus subtilis, Pseudomonas fluorescens, Clostridium histolyticum,* among others [86] and fungal species such as *Penicillium chrysogenum* and *Penicillum expansum* [70,87]. Other collagenase-producing bacteria enriched from human bone from multiple archaeological sites include *Pseudomonas*,

Xanthomonas, *Fusarium*, *Cladosporium*, *Aeromonas*, and *Trichonella* [70], and fungal genera from the phyla Ascomycota, Basidiomycota, and Mucoromycota [70,87]. Interestingly, Cyanobacteria are also thought to be important bone degraders and have been implicated in marine bone diagenesis [88], generally resulting in bone destruction progressing from the outer surfaces inward [67]. While collagenase producers may not be the only bone degraders, evidence of greater bone preservation in the absence of culturable collagenase producing microbes suggest they play an important role [70]. *Mucor*, a fungal taxon, has been linked to microscopic bone matrix degradation, creating boring tunnels and resorptive pits, within bone medullary cavities via experimental histological research [79]. The authors speculated on the ability of *Mucor* to solubilize apatite crystals through the production of organic acids [79]. Both bacteria and fungi are likely able to exploit the inorganic content of bone, particularly phosphates.

To understand specific organisms microscopically altering bone, culture-based methods have generally been employed. However, only a small subset of environmental microbes can be cultivated in the laboratory [89]. Limited research [14,90,91] has been conducted since the advent of high throughput sequencing technologies that allow us to characterize microbes without cultivation, while other research has used Sanger sequencing of cloned PCR products [87]. Damann et al. [14] examined changes in bacterial community composition in human rib samples from twelve individuals that had decomposed at the Anthropology Research Facility (ARF). Microbial community composition became increasingly reflective of the surrounding soil environment with increased post-mortem intervals. Partially skeletonized remains showed greater contributions from Firmicutes, while fully skeletonized remains saw increased proportions of Bacteroidetes, and dry remains had greater proportions of Actinobacteria and Acidobacteria [14].

Mircea et al. [88] examined fungal presence in bones from three Transylvanian archaeological sites using both Sanger sequencing and culture-based methods. Following storage, *Stachybotrys chartarum*, *Penicillium chrysogenum*, *Aspergillus versicolor*, and *Pseudogymnoascus pannorum* were consistently isolated from bones from multiple sites, whether they were contaminants from storage or from the soil was unknown. Only a single microscopic focal destruction, noted as a 6 μm pit, was observed. Only a single microscopic focal destruction, noted as a 6 μm pit, was observed. Though the authors suggested that the pit could have resulted from several fungal species (*Stachybotris chartarum*, *Alternaria alternata*) or algal species (*Spongiocloris spongiosa* and *Chlorosarcinopsis eremi*), they also admitted that it could have been bacterially produced. In addition, though *Penicillium chrysogenum* has collagenolytic activity, no evidence of active bone degradation by this species was presented [87].

Reeb et al. [90] characterized the "hidden" microbial community within bison bone at Yellowstone National Park. The bison had died during harsh winter conditions. The authors uncovered a diverse microbial community comprised of 18 bacterial, 7 fungal, and a single algal phylotype(s). Bone colonization was hypothesized to be related to the harsh exterior environment, though several of the taxa were likely contributing to bone degradation [90]. Hollund et al. [91] explored bone diagenesis across multiple regions of a single bone (periosteal surface, the middle cortex, and the endosteal surface); only three bones (medieval cattle femora) were included in their analyses. Community composition data was relegated to the supporting information, but the authors did note that observed microbial bioerosion was coupled with increased bacterial diversity [91].

Other areas of research pertaining to bone biodegradation include whale fall ecology and medical research. Evidence from whale falls, marine sites of decomposing whale carcasses, suggest that bone lipid content relates to skeletal element preservation [92]. Whale falls have been studied as large nutrient sources in deep-sea marine environments, which are usually nutrient-limiting. Initially, whale carcasses serve as labile sources of organic material, but following tissue removal, whale skeletons continue to provide nutrients to more specialized/oligotrophic communities. Interestingly, researchers have observed a link between skeletal element survival in whale carcasses and bone lipid content. The degradation of high lipid content bone fuels chemoautotrophs, resulting in the formation of sulfur-oxidizing bacterial mats on deep sea whale skeletons. This has resulted in an inverse relationship between lipid content and microbial bioerosion of whale bones, which may indicate an inhibitory relationship between increased sulfide levels and microbial bioerosion. In contrast, juvenile whales, which have a much lower lipid content, generally degrade much faster [92]. Yellow marrow in human bone, which is high in lipids, is likely degraded quickly by lipolytic bacteria. Nevertheless, this importantly points out the dynamism of microbial communities; microbial interactions could be key to unveiling patterns among decomposers.

Moreover, a bone devouring gastropod, *Rubyspira osteovora*, found in association with decaying whale carcasses, has allowed researchers to identify important gastro-endosymbionts related to bone digestion. Three operational taxonomic units (OTUs) belonging to the genera *Mycoplasma*, *Psychromonas*, and *Psychrilyobacter* were identified as key bone digesters in *Rubyspira osteovora*. Though these OTUs were neither found in marine sediments or bone, they have been associated with the digestion of other recalcitrant material including wood. *Psychromonas* has also been isolated from deep sea leeches associated with whale bones [93].

Research on microorganisms associated with osteomyelitis is also useful to the study of post-mortem microbial skeletal degradation. Recently researchers have examined the abilities of biofilms to directly resorb hydroxyapatite without stimulating inflammation and osteoclastogenesis from host cells [94,95]. Rat jaw bones and hydroxyapatite discs were inoculated with *Staphylococcus aureus*, *Pseudomonas aeruginosa*, *Candida albicans*, and *Streptococcus mutans* in the presence of multiple growth media types. All organisms tested were able to form biofilms on experimental surfaces, which resulted in destruction characteristic of pathological specimens from osteomyelitis patients [94].

Microbial degradation acts in concert with chemical modification. Soil geochemistry and site hydrology are equally important to microbial degradation [11,67] and can influence the composition and abundances of microbes present in a given environment [35]. The mechanisms that regulate bone recrystallization in life are no longer present after death. Dissolution in a soil environment is probable with increased moisture levels. Water infiltrates bones through existing pore spaces and vascular networks, through which the diffusion rate is generally slow. Dissolution in saturated environments is limited by the local diffusion gradient. While continuous saturation has limited dissolution potential, frequent hydrologic fluctuations can be devastating to bone [67]. In a sample of 138 bones from seven sites across Europe, histological preservation was the greatest from water-logged or completely dry sites, while fluctuating water levels produced the poorest indices of preservation [96].

This interaction with the environment is further mediated by pH. Hydroxyapatite is stable at a neutral, slightly alkaline pH (~7.8). Acidic environments encourage hydroxyapatite dissolution, while alkaline environments have a preservative quality [67]. Water also promotes collagen degradation. By encouraging dissolution of the inorganic phase, the collagen is more

accessible to hydrolytic enzyme activity by microbial collagenases. Without mineral dissolution, collagen is virtually inaccessible to enzymatic degradation. Extremely acidic environments (pH 1-2) and alkaline environments (pH > 7.5) increase the rate of collagen hydrolysis [67].

Skeletal DNA Degradation, Skeletal Sampling, and Rank Order Testing

Density has been the primary intrinsic factor related to skeletal preservation (Galloway et al. 1997). However, other intrinsic factors including skeletal morphology, microanatomy, pathology, trauma, age, trace element composition, and sex are also important. Extrinsic factors act in association with intrinsic factors to promote or inhibit skeletal degradation. These include UV irradiation, water presence, humidity, pH, cleaning and processing techniques, carnivore and rodent damage, trampling, vegetation, [97,98], and microbial damage [35]. Though physical bone preservation is linked to molecular preservation, this relationship is not simple. In some cases, indices of gross skeletal preservation have been well correlated with DNA survival [99], while in others gross bone preservation and weathering have been shown to be unrelated to DNA preservation [15].

Time has not been a good indicator of DNA preservation [100]. Larger DNA fragments preferentially degrade over smaller DNA fragments with time, but this relationship has shown minimal predictive success [101,102]. Though cellular location and copy number influence DNA preservation, with greater preservation from mitochondrial DNA [103], DNA degradation, in general, is influenced primarily by environmental factors [97] and begins within minutes of death. Enzymes released during autolysis result in increased fragmentation of cellular DNA. Shortly thereafter and in combination with autolysis, enteric microorganisms proliferate and further catabolize accessible macromolecules into smaller subunits, including DNA [104,105]. Decay will continue with effects from the environmental influences discussed above; the impact of which will differ based on differences in the deposition environment (surface vs subsurface vs submerged) and intrinsic factors.

Once deposited in the environment, bone undergoes diagenesis. Throughout this process, skeletal DNA preservation appears to relate to the integrity of the mineral lattice structure [76,77]. DNA can bind to hydroxyapatite and gain protection from environmental destruction. However, if the mineral component is breached, dissolves, and recrystallizes due to environmental disequilibrium, bound DNA will be released from the mineral structure and become available for environmental destruction (accessible to soil microbes) [76]. As a labile polymer composed of repeating units of phosphate groups, sugars, and nitrogenous bases, DNA can be readily assimilated by microbes. If not destroyed by microbes, long-term environmental factors can incite oxidative or hydrolytic damage and subject the DNA to physical forces that can cause further mechanical shearing [13,104]. Therefore, to survive, extracellular DNA must obtain physical protection from environmental factors that cause its degradation (i.e., temperature, UV damage, hydrolytic damage (water), and enzymatic damage (via microbial activity and related to water content). Survival within osteocytes or other remnant tissues (e.g. from the red bone marrow) may also be possible [106,107].

Though there seems to be conflicting patterns, skeletal element type plays a role in DNA preservation and degradation (e.g., [5–9,108,109]). Whether this has to do with differences in cortical/compact and cancellous bone composition is debated, which could be linked to microbial presence. Multiple studies have observed high amounts of microbial DNA co-extracted with human DNA [7,8,110]. More porous elements are more likely to be affected by exogenous contamination [111]. Increased concentrations of microbial DNA and other environmental

substances (e.g., humic acids) can act as potential PCR inhibitors, which can lead to failed DNA testing [112].

As decomposition progresses, it becomes more difficult to establish a positive identification visually or using fingerprints, leaving dental matching and DNA comparison as the most reliable methods available to identify skeletal remains [3,113]. Yet, there is no consensus regarding which skeletal elements should be sampled for DNA testing. Only a few studies have focused on differential DNA preservation in bone, the majority of which examine previously generated data [6–8,108,109]. Lauded for its large sample size and uniform testing methods, one of the most comprehensive studies examined 11,650 skeletal DNA tests [9]. The results of Hines et al. [9] showed that the talus and other tarsal bones out-perform dense long bones. They further reported good results from other small cancellous bones, such as the patella, however the sample sizes were too small to include in overall analyses [9]. Edson et al. [6] reported the greatest success from the femur and tibia, but also noted high success rates for the metatarsals. Fairly high success rates (greater than 70%) were also observed in the clavicle, scapula, humerus, radius, and mandible. Similarly, Leney [7] reported high success rates among the femur, tibia, mandible, and first metatarsal. In contrast to Edson et al [6], Leney [7] observed a high rate of success from the pelvis. Milos et al. [8] described the highest success rates from the femoral midshaft and teeth; the authors noted that general success decreased with decreasing bone density, suggesting that dense, cortical bones are better for DNA analysis. However, these retrospective analyses were limited by the composition of their datasets. All element types were not systematically tested. Moreover, while these studies benefited from the use of large sample sizes, other variables were difficult to control, such as the post-mortem interval, burial location, and environment.

The above studies compared DNA degradation across elements from different individuals, but dataset limitations prevented comparison of variation within a single individual. Understanding intra-individual variation may be equally as informative as inter-individual variation, even when large sample sizes are considered. When comparing all element types within a single individual, Mundorff and Davoren [5] demonstrated that small cancellous elements, especially from the foot, outperformed large, dense cortical elements in the quantity and quality of extracted human DNA. More recent research supports this conclusion. As mentioned above, the talus and other tarsals were reported as the second most successful bone type, after teeth, by Hines et al. [9]. Ferreira et al. [114] and Ferreira et al. [115] have successfully utilized metatarsals and phalanges in DVI situations, promoting their use in certain postmortem circumstances. Nevertheless, it is possible that the mechanism of DNA degradation and the pattern of DNA preservation shifts over extended PMIs. Skeletal DNA sampling strategies for forensically relevant remains likely diverge from those applied to ancient remains. For example, the petrous portion of the temporal bone, the densest region in the human skeleton, is the preferred element of choice in ancient DNA research [116–119].

Lastly, bone processing techniques including soft tissue maceration and standard osteological analysis procedures (e.g., X-rays and CT scans) can impact the degree of DNA degradation in bone. When testing exhumed and surface remains for DNA following boiled and unboiled treatments, Iwamura et al. [106] found that boiling practices were related to osteon fragmentation and DNA degradation. Frank et al. [120] tested the effects of processing techniques such as CT scans and X-rays, concluding that these techniques can have additive effects on DNA degradation.

Purpose, Objectives, and Goals

The purpose of this dissertation research was two-fold: (1) to empirically assess patterns of human DNA preservation from buried (subsurface) skeletal remains and determine how such patterns relate to patterns previously observed in remains that had decomposed on the ground surface, and (2) to relate patterns in skeletal DNA preservation in buried remains to site-specific taphonomic variables, focusing on microbial influence. The objectives were threefold: (1) to determine whether the patterns of DNA preservation previously observed in skeletal elements associated with surface processes of decomposition (i.e., [5]) hold true in a burial context; (2) to determine if there is enough variability to develop a rank order of skeletal elements based on DNA yield and STR profile completeness, and (3) to relate patterns of skeletal DNA degradation to microbial composition and structure in the soil and within the bone itself. Results complement existing research on bone sampling strategies for skeletal remains recovered from the ground surface to develop a bone sampling selection method for disinterred skeletal remains.

Currently, practitioners focus on sampling dense, cortical bones (i.e., the femur and tibia), a labor intensive and time-consuming process. If smaller bones produce equal or higher DNA yields, a re-evaluation of sampling strategies to maximize success while minimizing resource expenditure may be beneficial in medico-legal contexts. In addition, this study contributes to the growing body of knowledge on the interacting physical, biological, and chemical processes in the soil during cadaver decomposition and adds to the limited research on microbial communities directly associated with bone and thought to have a direct impact on the survivability of skeletal DNA.

Research Questions and Hypotheses

The following research questions were addressed: (1) Does the deposition environment (surface vs. subsurface) relate to patterns of DNA degradation? (2) Do human DNA testing success rates in subsurface bones deviate from previous studies that did not consider small, cancellous bones? (3) Is susceptibility to microbial invasion related to DNA preservation? (4) Does skeletal DNA preservation persist in a patterned or stochastic manner in subsurface decomposition? (5) What microbes are capable of colonizing bone and does this differ between surface and buried remains? Lastly, (6) Does skeletal DNA degradation and/or microbial community composition relate to soil geochemical or edaphic conditions? The following hypotheses were addressed:

> *Hypothesis I*: The pattern of human DNA quantities, measured as nanograms per gram of bone powder, and quality, measured by the degradation index (small autosomal target / large autosomal target) and STR amplification success, will be different between surface and subsurface remains due to significant changes in the decomposition environment. As discussed above, a surface environment is prone to extreme environmental fluctuations in temperature, UV exposure, humidity/moisture, etc., which would likely inhibit the growth and activity of certain microbial taxa [68]. In addition, we expect oxygen availability to be a dominant factor influencing the types of microbes in contact with and capable of colonizing bones in these environments, which is expected to relate to burial depth. If microbes are influencing bone degradation, community differences between subsurface and surface remains should be associated with differential decomposition / decay.

Hypothesis II: Human skeletal DNA quantity and quality from predominantly cancellous elements will be lower than DNA recovered from predominantly cortical elements in subsurface remains. Though the opposite was observed by Mundorff and Davoren [5], the stability of the subsurface environment is expected to encourage increased microbial bone degradation, especially from gut derived microbes. Greater porosity in cancellous bone relative to cortical bone increases its susceptibility to microbial colonization and degradation. In addition, though DNA preservation results from a combination of factors, evidence points to a close association between DNA survival and DNA binding to hydroxyapatite [76,77]. Therefore, we expect skeletal elements with greater density and increased inorganic content to preserve better throughout the duration of interment (4 years).

Hypothesis III: DNA quality and quantity from buried skeletal remains will relate to microbial community composition, abundance, and other geochemical factors, especially site hydrology. Soil pH and site hydrology are known factors related to DNA degradation. While microbial communities are known bone degraders and have been co-extracted in high concentrations along with DNA [110], their role in DNA degradation is mediated, in part, by environmental conditions. Therefore, the environment and the microbes within that environment are crucial determinants of DNA degradation (and thus preservation).

Sample Description

To understand patterns of DNA preservation and their relationship with taphonomic and edaphic parameters and microbial ecology, three sets of samples were used: (1) surface remains, (2) buried (subsurface) remains and associated soils, and (3) human gut samples from living donors.

Surface Remains

Three male individuals that had decomposed on the ground surface at the University of Tennessee (UTK) Anthropology Research Facility (ARF) in 2009 were examined for patterns of human DNA preservation and associated changes in microbial community composition and structure. Remains were collected from the ground surface following complete skeletonization. Remains were gently cleaned at UTK's Forensic Anthropology Center (FAC), and 55 bone and tooth samples from each individual (n = 3) were sampled following mechanical and chemical cleaning, resulting in a total skeletal sample size of n = 164. Total DNA was extracted and human DNA quantity and quality were assessed at Bode Cellmark Forensics, Lorton, Virginia. Methods encompassing bone sampling and DNA extraction and analysis were previously described in detail in Mundorff and Davoren [5]. Total DNA extracts from Mundorff and Davoren [5] were used in Chapter II to assess microbial loading via qPCR and microbial community composition and structure following next generation sequencing of the 16S rRNA and 18S rRNA genes. No soil or gut samples were collected prior to placement of individuals at the ARF, and no soil or other cadaver-associated samples were collected throughout the decomposition process. All bone samples represent a single time point. Samples from the same three individuals were also used as a comparative sample in Chapter IV; individuals were renamed ("SA", "SB", and "SC") in chapter IV to differentiate from buried individuals ("A", "B", and "C") in the same chapter.

Buried Remains

Three individuals, disinterred after a period of four years, from a single grave at UTK ARF were assessed for patterns of human DNA preservation, bacterial and archaeal community structure, composition, and abundance, as well as changes in the soil environment. Because environmental differences often result in differential decomposition, the decision to test three skeletons from within a single grave was made to minimize the effects of environmental differences. Individuals were stacked at the time of disinterment to replicate a realistic burial event. A 2 x 2 m grave was excavated and disinterred in February 2017, four years after interment. Because individuals were stacked, with individual C on the top, oriented West to East, B in the middle, placed North to South, and A at the grave base, oriented West to East, individuals exhibited differential states of decomposition at the time of disinterment (Figure 1.1-1.3). During disinterment, soils were collected with depth throughout the grave and along lateral transects extending away from the grave to establish geochemical and microbial profiles within and extending outward from the grave. Details on soil sampling and geochemical methods, analysis, and results are available in Keenan et al. [56].

To ensure consistency and to directly compare disinterred remains to those that decomposed on the ground surface [5], the same methodologies from Mundorff and Davoren [5], with only minor differences, were used to assess inter-individual and intra-individual variation in human skeletal DNA from buried individuals. To compare DNA yields from all skeletal element types within a single individual and between individuals, the same representative selection of 49 bones were sampled from each skeleton. This approach limited unnecessary destructive sampling and additional costs by avoiding duplicate (rights vs. lefts) and redundant (e.g., ribs) elements. Representative element selection was decreased from 55 in Mundorff and Davoren [5] to 49; teeth were not included, as the focus was on patterns of DNA preservation in human bone. We did, however, increase the number of samples per bone for subsets of selected elements to assess variation between sampling sites on a single bone. Based on previous observations [5], 19 elements were sampled across two sites, while the femur, tibia, and humerus were selected for additional sampling across 3 sites. Technical replicate variation was also assessed to understand the variation in samples recovered from a single sampling site; to this end, the three sites sampled on the femur, tibia, and humerus were sampled twice (Figure 1.4). Individual bones were marked at the sampling site, photographed, and re-photographed again after sampling. Similar to surface remains, remains disinterred from the multi-individual burial were mechanically and chemically cleaned prior to sampling using a 3/8” drill bit. Total DNA was extracted from bone samples using a complete demineralization protocol [122]; DNA extracts were used for human and microbial DNA quantitation and 16S rRNA gene sequencing. Detailed methods regarding total DNA extraction, total DNA quantitation, human DNA quantification, and microbial DNA quantification are presented in Chapter III. Detailed methods relating to 16S rRNA sequencing and analysis are available in Chapter IV.

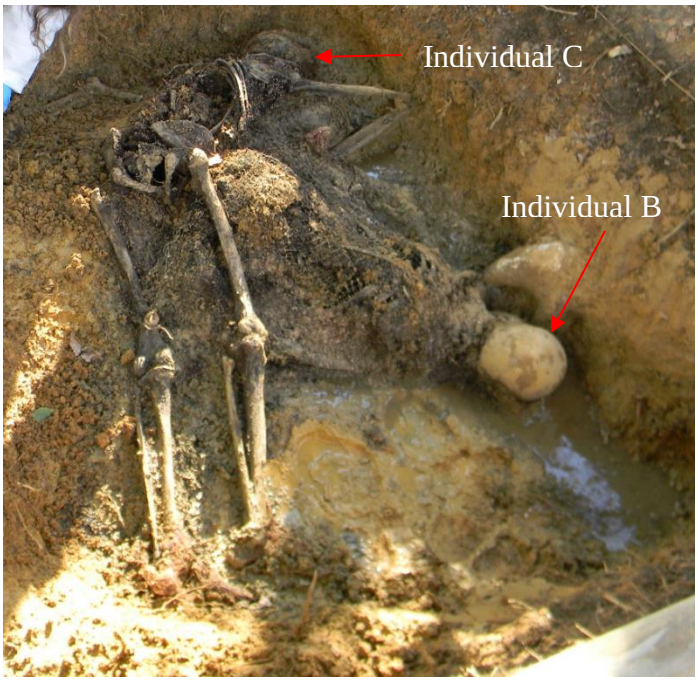

Figure 1.1: Individual C at the time of disinterment. C was skeletonized with minimal adipocere formation and remaining tissue.

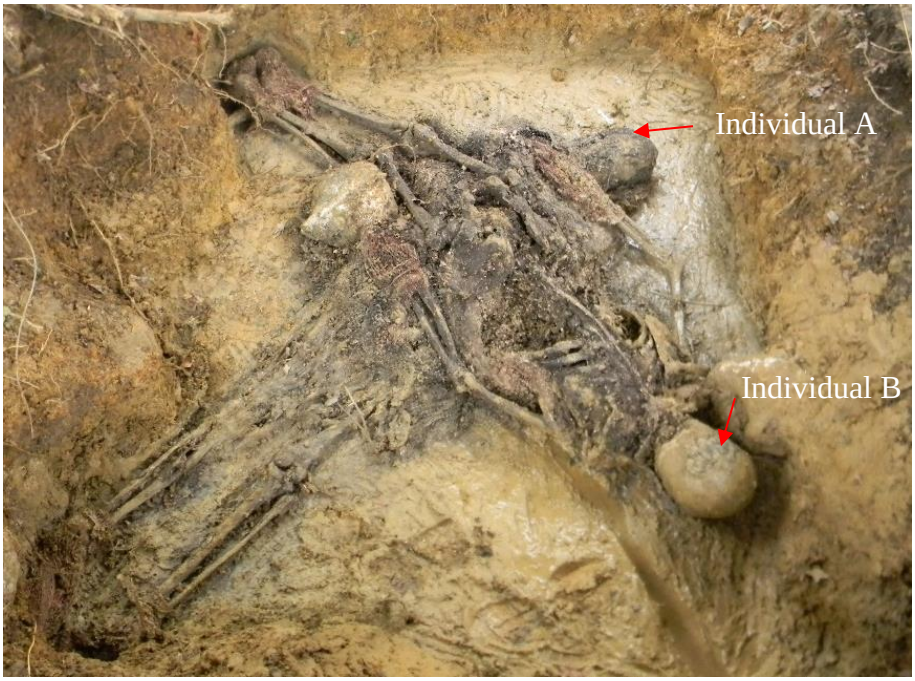

Figure 1.2: Individual B at the time of disinterment. B was mostly skeletonized with moderate adipocere formation, especially in the region of the torso.

Figure 1.3: Individual A at the time of disinterment. Individual A experienced extensive adipocere formation, with preserved tissue underneath. Only the distal extremities were fully skeletonized.

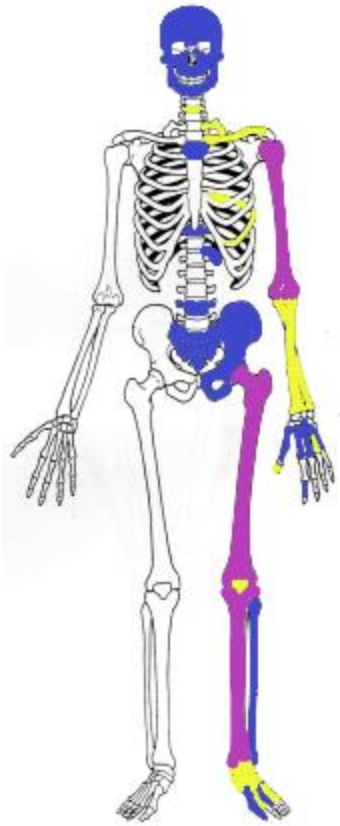

Figure 1.4: Subsurface bone selection. All representative bones were sampled from the left side of the body. Bones are highlighted based on the number of samples taken per element. Blue represents a single sampling site. Yellow indicates two sampling sites, and purple indicates 6 sampling sites.

American Gut Project

The American Gut Project (AGP) is a civilian / scientist sourced project that began in 2012 as a collaborative effort between the Earth Microbiome Project (EMP) and the Human Food Project (HFP) to understand population diversity in the human gut microbiome [123]. The data is open-source and freely available. To better understand the sources of microbial populations in post-mortem human bone, we accessed a total of 62 samples from the AGP to directly compare to surface and subsurface bone communities. Samples from human feces (n = 53), sebum (n = 2), saliva (n = 6), and hair (n = 1) and associated metadata were accessed from the American Gut Project (AGP) (Qiita Accession ID 10317); samples were chosen based on age (between 50-70 yrs.) and residence (TN, GA, AL, WA, and VA) to reflect demographic information from deceased individuals involved in surface and subsurface decomposition. Sample and prep IDs as well as other demographic information are available in Chapter IV.

ARF and Grave Site Geochemistry

The Anthropology Research Facility (ARF), founded in 1980, is a 2 acre outdoor facility dedicated to actualistic decomposition research [124]. Individuals used in this study, excluding those from the AGP, were deposited either on the ground surface or in a burial at the ARF. Buried individuals were interred in a more recently acquired section of the facility, and thus were thought to be deposited in soil not previously exposed to human decomposition.

A soil biology and geochemical profile of the grave has been established previously by Keenan et al. [56]. Soil geochemical parameters within the grave and extending laterally out from the grave were tested, including pH, gravimetric moisture, microbial respiration, dissolved organic carbon, dissolved organic nitrogen, and extracellular enzyme potentials, among others. Soil biology characterization included nematode composition and microbial. Soil at the ARF is composed of clay and channery clay loam overlain with a 10 cm top horizon, rich in soil organic matter [56]. Soil samples were collected at depths of 0-5 cm, 30-35 cm, 70 -75 cm, and 85-90 cm; an additional sample was collected at 40 cm from within the rib cage of individual C.

Laterally, extending out from the grave, soils at depths of 0-5 cm and 30-35 cm were not significantly impacted by decomposition. In contrast, within the grave, depths of 30-35 cm and 70-75 cm demonstrated significant soil geochemical changes in response to ongoing human decomposition. Elevated nitrification potentials and nitrate concentrations as well as increased fungal presence were observed at 30-35 cm, which coincided with a decline in nematode diversity and evenness. A sample taken from within the rib cage of individual C at 40 cm, which was composed of mixed soil and decomposition products, included the highest enzyme potentials of leucine aminopeptidase and phosphodiesterase, indicating a more copiotrophic functionality at this depth. Below 40 cm, at 70 -75 cm, grave soil samples shifted to a mostly anoxic environment. This was the only depth at which a human-associated obligate anaerobe, *Bacteroides* sp., was detected. In addition, this depth regime saw elevated microbial respiration rates, dissolved organic carbon, dissolved organic nitrogen, ammonium, conductivity, and pH as well as increased N-acetyl-β-glucosaminidase enzyme potentials. Despite high levels of labile organic sources, enzyme potentials indicate a more oligotrophic functionality at 70-75 cm [56].

Analytical Terms and Methods

This research included the analysis of large, multidimensional microbial datasets, which at times required the use of esoteric ecological metrics and analytical tools. Some of these tools / methods require further explanation, as summarized below.

Measures of ecological diversity include two concepts, species richness and evenness. Species richness is the number of species in a sample / site, while evenness refers to the equitability in species abundance within a sample / site [125]. Two categories of diversity are commonly used to understand community dynamics and were used in this dissertation: (1) alpha diversity and (2) beta diversity. Alpha diversity refers to within sample diversity, while beta diversity represents between community diversity [125]. There are a number of different metrics used to calculate diversity and all have positive and negative attributes. This research used Inverse Simpson (1/D) to assess within habitat diversity (i.e., alpha diversity). Inverse Simpson is easily quantified but is sensitive to highly abundant species. Simpson's D as an estimate for "finite samples" is calculated as follows, "with n_i the number of clones in the *i*th OTU" [126], or amplified sequence variant (ASV):

$$D = \sum \left(\frac{n_i(n_i - 1)}{N(N - 1)}\right)$$

Observed richness, or the total number of OTUs / ASVs or species in a sample was used to calculate species richness.

Beta diversity metrics used to understand between community differences included Bray-Curtis dissimilarity and weighted UniFrac. Bray-Curtis is a non-Euclidean dissimilarity metric based on both compositional and abundance data. Resulting values range from zero to one, with zero indicating complete similarity and one indicating complete dissimilarity [127]. Similarity percentages (SIMPER) [128] use Bray-Curtis dissimilarities to identify taxa driving community differences. Non-metric multidimensional scaling (NMDS) is a common ordination technique used to represent distances and dissimilarities due to its ability to preserve rank orders while reducing dimensions [128,129]. Resulting stress with each iteration of the NMDS demonstrates goodness of fit; low stress indicates that the data is well represented by the ordination [129].

UniFrac is a relatively recent distant metric that is based on phylogenetic distance (i.e., phylogenetic tree branch lengths) [130]. The idea is that two distinct environments would have disparate evolutionary histories. Its strength is that "it exploits the different degrees of similarity between [16S rRNA] sequences." Weighted UniFrac is a quantitative measure of UniFrac that also takes into consideration abundance [131].

Random forest regression models were used in Chapters II and IV to identify important taxa related to human skeletal DNA concentration. Random forest (RF) regression is a machine learning approach that has gained traction in human decomposition research to estimate the post-mortem interval [40,43]. RF is easily implementable and can be applied to a wide range of data. RF models construct and combine results from decision trees fitted to a training set to increase accuracy. RF modeling is fairly robust to overfitting and outputs important features to the model [132,133].

Significance of Research

Missing persons investigations place hefty demands on the U.S. criminal justice system financially and in human effort. From a molecular anthropology perspective, this research has the potential to advance criminal justice policy and practice in the United States by refining skeletal sampling protocols for DNA analysis, thus reducing the time, labor, and financial costs

of DNA analysis while maximizing identification rates of skeletonized remains. This project complements previous work by Mundorff and Davoren [5] and Hines et al. [9], while redressing gaps in the existing body of knowledge regarding skeletal DNA degradation and the effects of the burial environment. The greatest potential contribution of this research is the development of a DNA sampling rank-order of success for all skeletal element types specific to human remains recovered from a buried context.

From a microbial ecology perspective, this research relates patterns of skeletal DNA preservation to site specific taphonomic variables, particularly microbial influence, which is crucial to understanding how these patterns in DNA survivability arose, thereby expanding the applicability of this research to multiple environments. Moreover, microbial bone degradation is an important component of bone diagenesis and preservation. To date, the majority of research on microbes associated with bone decay has been limited to histological and culture-based studies. This research adds to the growing body of literature on the microbial ecology of bone.

CHAPTER 2
PATTERNS OF MICROBIAL COLONIZATION OF HUMAN BONE FROM SURFACE-DECOMPOSED REMAINS

A version of this chapter has been submitted for publication by Alexandra L. Emmons, Sarah W. Keenan, Jennifer M. DeBruyn, Jonathan Davoren, Janna Andronowski, David Carter, and Amy Z. Mundorff

Citation: TBD

Publication Statement:

This is a research chapter. In addition to conducting the majority of research analyses presented herein, I am the original and primary author of this chapter. Co-authors provided funding, guidance, conceptualization, and editing. Data on percent cortical content was collected by a co-author, and methods related to the collection of that data were also written by the same co-author.

Abstract

Microbial bone colonization plays a role in post-mortem skeletal degradation, as heterotrophic bacteria and fungi readily degrade organic material, including DNA. However, the types and distributions of bone-colonizing microbes are not well characterized; in particular, it is unknown if microbial communities vary in abundance or composition between bone types. If differences exist, it may help explain patterns of human DNA preservation. Therefore, the goals of the present study were to (1) identify the types of microbes capable of colonizing different bone types and (2) relate microbial abundances, diversity and community composition to bone type and DNA preservation. DNA extracts from 164 bone and tooth samples from three individuals were assessed for bacterial loading using qPCR to quantify gene abundances; 16S rRNA and 18S rRNA gene amplicon sequencing were used to examine differences in microbial community composition and structure. Random forest models were applied to predict operational taxonomic units (OTUs) associated with human DNA concentration. Dominant bacterial bone colonizers included OTUs from the phyla Proteobacteria (36%), Actinobacteria (23%), Firmicutes (13%), Bacteroidetes (12%), and Planctomycetes (4.4%). Eukaryotic bone colonizers included OTUs belonging to Ascomycota (40%), Apicomplexa (21%), Annelida (19%), Basidiomycota (17%) and Ciliophora (14%). Microbial communities demonstrated significant differentiation by individual and anatomical region. Bacterial loading was not a significant predictor of human DNA concentration in two out of three individuals. Though random forest models models were minimally successful in identifying microbes related to patterns of DNA preservation, models were complicated by differences between individuals and body regions. This work expands on our understanding of the types of microbes capable of colonizing human bone and contributing to microbial human skeletal DNA degradation.

Introduction

Skeletonization is the final “stage” of human decomposition, exposing bone to the exogenous environment [134]. Once the body has progressed to a skeletonized state, teeth and bone become the only materials that can be used for human identification. However, while bone is more recalcitrant than soft tissues, it is not stable; it continues to decay over time. With death, bone undergoes decomposition and diagenesis, the postmortem alteration of bone by chemical,

physical, and biological factors that result in modification of the original bone material [72]. Time is not a good indicator of skeletal DNA preservation [100]; instead bone diagenesis and DNA survival is highly dependent on the depositional environment, including microbial activity [97,135].

Bone decay mechanistically proceeds via chemical and/or biogenic (microbial) degradation of the organic and inorganic components of bone [11]. Microbes are capable of colonizing and degrading human bone, and microbial DNA is often co-extracted with human DNA and interferes with downstream processes [7,8,110]. The organic component of the bone consists of 90-95% type I collagen (primarily made up of glycine, proline, and hydroxyproline), with minor contributions from other non-collagenous proteins (e.g., osteocalcin, osteoponin, and osteonectin) as well as lipids, mucopolysaccharides, and carbohydrates [73]. The inorganic or mineral component is most similar to hydroxylapatite and consists of calcium, phosphate, carbonate, hydroxide, and to varying degrees sodium [35,72,136]. Bone apatite, or bioapatite, can be described as 'nature's trashcan,' as infiltration and substitutions from environmental elements are common. One of the main requirements for lasting preservation via fossilization is a complete shift from the bioapatite mineral lattice to a fluorinated apatite or fluorine- and carbonate-enriched apatite[71,72].

When not in equilibrium with the surrounding environment, dissolution and recrystallization of bioapatite occurs, allowing microorganisms and enzymes access to the organic phase, resulting in degradation. Similarly, if the organic component degrades by either chemical or biological means, bioapatite becomes more vulnerable to environmental fluctuations and dissolution of the lattice structure is more probable due to new voids in the crystal lattice [11,35,72,76–78]. For example, wet environments demonstrate increased rates of DNA degradation because water allows for mineral dissolution and increased hydrolytic damage [137]. The interdependence between the mineral and organic phases of bone supports the idea that greater porosity or increased void space increases the susceptibility of bone to environmental influences [15,138], both chemical and biological.

Though the reservoir for long-term DNA preservation in bone remains unclear, the binding of DNA to bioapatite crystallites seems to be crucial for long-term DNA survival [76]; persistence within osteocytes or other remnant tissues (e.g., from the red bone marrow) may also be possible [106,107]. Gross bone preservation and weathering has been shown to be unrelated to DNA preservation or degradation in some cases [15], while in others, indices of gross preservation are better correlated [16,99]. Differences in DNA preservation and degradation by bone type have been observed, though patterns are not consistent between studies (e.g., Leney, 2006; Milos et al., 2007; Edson et al., 2009; Mundorff et al., 2009; Hines et al., 2014; Mundorff and Davoren, 2014). Whether this has to do with differences in cortical and cancellous bone composition is debated. More porous elements are thought to have increased bacterial presence [76], but increased presence does not necessarily mean increased degradation, as certain microbial taxa may be better adapted to exploiting skeletal material than others.

In archaeology, microbial degradation of bone has been studied primarily through histological research, focusing on regions of microscopic focal destruction [16,81–83,139]. However, culture-based research has shown that collagenase-producing bacteria can use mammalian bone as a substrate (e.g., *Alcaligenes pichaudii*, *Bacillus subtilis*, *Pseudomonas fluorescens*, *Clostridium histolyticum*) [86]. Others have shown greater DNA preservation from archaeological sites with bones lacking culturable collagenase producing bacteria [70]. These observations suggest that DNA preservation within a bone may be partially dependent on the

amount and/or type of microbes colonizing the bones. Genera including *Pseudomonas*, *Xanthomonas*, *Fusarium*, and *Trichonella* have been cultured from bones from diverse archaeological sites [70]. Experimental research has also shown macroscopic destruction phenomena consistent with fungal degraders, specifically from the genus *Mucor* [79], while others have cultured genera from the phylum Ascomycota [70]. Research to date has primarily been limited to culture-based methods, and we know that only a small subset of environmental microbes can be cultivated in the laboratory. Only a few studies [14,90] have been conducted since the advent of high throughput sequencing technologies that allow us to characterize microbes without cultivation. Thus, there is a gap in knowledge regarding the types of microbes capable of colonizing and degrading human bone.

The purpose of the current study was two-fold: to (1) identify the types of microbes capable of colonizing different bone types using next generation sequencing methodologies and (2) relate microbial abundances, diversity, and community composition to bone type and patterns of human DNA preservation We expected total bacterial gene abundances, as a proxy for overall bacterial presence or loading, to increase with decreasing human DNA quantity and quality. We also expected to see shifts in microbial populations with changes in bone morphological and microstructural properties (i.e., bone type and cortical content).

Materials and Methods

In 2009, three male individuals were placed outside on the ground surface to decompose naturally at the Anthropology Research Facility (ARF) at the University of Tennessee, Knoxville (UTK) (Table 2.1). Following complete skeletonization (13 – 23 months), the same 55 bone and tooth samples representing all skeletal element types from each individual (total n = 165) were collected and gently washed at the Forensic Anthropology Center (UTK) (Table S2.1; Table 2.2). Prior to sampling, the external surface of each bone was cleaned by mechanically removing 1-2 mm of the outer surface of bone, followed by chemical cleaning via bleach, ethanol, and sterile water. Bones were sampled using a drill and masonry bit at slow speeds (< 100 rpm); DNA was extracted from sampled bone powder using a complete demineralization protocol [122]. Methods encompassing bone sampling and DNA extraction and analysis were previously described in detail in Mundorff and Davoren (2014). Human DNA quality and quantity were examined to elucidate patterns of DNA preservation by bone type (Mundorff and Davoren, 2014). These same skeletal DNA extracts were used in the present study to assess microbial loading via qPCR and microbial community composition and structure using next generation sequencing of the 16S rRNA and 18S rRNA genes.

Microbial and Human DNA Quantitation

As a proxy for total bacterial abundance and colonization of bone, qPCR was used to quantify 16S rRNA gene abundances [140] using the Femto™ Bacterial DNA Quantification Kit. Assays were conducted as per manufacturer instructions using a BioRad CFX Connect™ Real-Time PCR Detection System. Samples were quantified in triplicate, while standards were quantified in duplicate, and a minimum of three no template controls were included in each 96-well plate. Data are presented as gene copy number per gram of bone powder (gene copies gbp^{-1}) and log gene copy number per gram of bone powder. Human DNA was quantified using the Quantifiler™ kit from Life Technologies (Qf); methods and data are reported in (Mundorff and Davoren, 2014).

Table 2.1: Donor Information for the three individuals placed at ARF 2009

Individual	Ancestry	Sex	Weight (kg)	Medical History	Length of Placement
A	European	Male	104.3	Diabetes, Alcoholism, Substance abuse	13 months
B	European	Male	80.3	High cholesterol, Arthritis	16 months
C	European	Male	127.0	Diabetes, Cardiac	23 months

Table 2.2: Number of bones sampled by body region for each of the three individuals

Body Region	*Sample Quantity per Individual*
Skull	6
Teeth	7
Trunk	13
Leg	4
Arm	3
Hand	8
Foot	14
Total	55

Total DNA Quantitation

Total DNA was quantified using the Quant-iT™ PicoGreen™ dsDNA Assay Kit (Invitrogen™) using a 200 µL total volume on a 96 well microplate reader. Samples and standards were run in duplicate, with standards ranging from 0 µg mL^{-1} to 1.0 µg mL^{-1}. Total DNA concentrations are reported as nanograms per gram of bone powder (ng gbp^{-1}).

Percentage Cortical Content

Clinical CT scans of each element were acquired using a Siemens Biograph mCT 64 slice scanner. Scans involved helical acquisition using a 0.6 mm slice thickness, 500 mAs, 120 kV, and bone window with kernel B70s. Data were stored on compact discs and transferred to workstations with image processing software (OsiriX 5.6, Geneva, Switzerland). The DNA sampling site on each element was digitally measured using ImageJ (National Institutes of Health). A macro was created to detect and measure the areas of cortical and cancellous bone (mm) on each CT slice where the sampling site appeared. Measurements of cortical width and height and cancellous width and height were taken separately for each cortical and cancellous bone region for all bones. Average cortical and cancellous bone width and height measurements were then computed for each site. Due to issues with scan quality, ten of the original 129 samples were removed from the analysis. Percentiles of cortical and cancellous bone were computed from each DNA sampling site for all elements.

Mean percentiles of cortical bone composition at each sampling site were divided into seven categories by skeletal element: (1) 80-100%, (2) 70-79%, (3) 60-69%, (4) 50-59%, (5) 40-49%, (6) 30-39%, and (7) 20-29%. The first category consists of bones whose sampling sites did not contain any cancellous bone, including the humerus, radius, ulna, femur, and tibia. The second, third, and fourth categories contained only three elements with sampling sites that were composed of over 50% cortical bone. Percentile data were further averaged from each element type across all individuals. The majority of element types revealed consistent measurements between individuals, with standard deviations of 10% or less. Three element types (temporal, occipital, cervical vertebra) exhibited high variability between the three individuals in the relative amount of cortical and cancellous bone removed from the sampling sites.

Next Generation Sequencing Analysis

Total DNA extracts from bone were sent to Hudson Alpha Institute of Biotechnology Genome Services Laboratory (Huntsville, AL) for sequencing of the V3-V4 region of the 16S rRNA gene and V4-V5 of the 18S rRNA gene using 300 PE chemistry on an Illumina MiSeq instrument. Library preparation was performed by Hudson Alpha according to Illumina protocols. Primers for the 16S rRNA gene consisted of S-D-Bact-0564-a-S-15 and S-D-Bact-0785-b-A-18 from Klindworth et al. (2013); primers for the 18S rRNA gene were 574f and 1132r from Hugerth et al. (2014).

Adapters were removed by Hudson Alpha prior to data distribution. Read quality was assessed using fastqc (v. 0.11.7) and multiqc (v. 1.5). Primers were removed using cutadapt (v. 1.14) [143], and reads were quality trimmed using trimmomatic (v. 0.36) [144]. Data were further trimmed, aligned, and classified using mothur (v. 1.39.5) according to the mothur SOP [145]. 16S rRNA and 18S rRNA sequences were aligned and classified into operational taxonomic units (OTUs) at 97% sequence identity, using the SILVA ribosomal RNA database (v. 128). Statistical analyses and visualizations were conducted in R (v. 3.4.1) [146], primarily using phyloseq (v.1.20.0) [147] and dependencies.

Samples with less than 5,000 reads were removed from analyses, and samples were rarefied to even depth by the smallest library (16S rRNA min. library = 48,288 reads; 18S rRNA min. library = 5,368 reads) prior to alpha and beta diversity measurements including ordination methods and visualizations based on ordination methods (Figures S2.1, S2.2). Bray-Curtis dissimilarities were computed for all ordinations. Alpha diversity metrics, including Inverse Simpson and observed richness, were computed using a subsampling approach, in which richness and diversity metrics were computed for a total of 100 iterations, each scaled to even depth.

Sequence Quality Analysis

Two samples failed to sequence using 16S rRNA primers, while twenty samples failed to sequence using 18S rRNA primers. Extensive trimming was undertaken due to the increased error rate associated with 300 PE chemistry. Fastqc and multiqc demonstrated high quality reads in the forward direction, with a significant drop in mean quality Phred scores in the reverse direction at an approximate base pair position of 200 (Phred Score < 25). Following cutadapt and trimmomatic, total 16S rRNA contigs were reduced by 46%. This was further reduced by an additional 14% following further processing in mothur, resulting in a total read loss of 60% (from 37,185,525 to 14,958,201 sequences). This left a total of 14,958,201 sequences, of which 692,709 were unique.

18S rRNA sequences presented an additional challenge; using 300 PE chemistry, forward and reverse reads overlapped by ~59 base pairs (bp). Fastqc and multiqc showed a significant reduction in mean base quality in both forward and reverse reads. Forward reads showed a drop in mean quality scores at an approximate position of 250 bp (Phred scores < 25), the same drop in quality was observed in reverse reads at ~200 bp. As a consequence, trimming to remove low quality base pairs resulted in a dramatic loss of reads. Following cutadapt and trimmomatic, total 18S rRNA contigs were reduced by 46%, and after further processing in mothur, sequences were further reduced by 49%, resulting in a total read loss of 95% (from 30,253,173 sequences to 1,518,971). This left a total of 1,518,971 sequences, of which 181,486 were unique. Due to poor read quality, individual A was removed from additional data analysis in phyloseq, resulting in a remaining 7,901 OTUs across 90 samples.

Data Analysis

All data analyses, excluding random forests tests, were conducted in R (v.3.4.1). Two-factor analysis of variance tests (ANOVAs) were used to examine differences in log transformed human DNA concentrations by individual and body region. Assumptions such as normality and homogeneity of variance were tested using D'Agostino's normality test (package = fBasics v. 3042.89) (Wuertz et al., 2017) and Levene's test (package = car v. 3.0.2) respectively. Regression analysis was then used to assess the relationship between human DNA concentrations from bone samples and hypothesized predictor variables (i.e., bacterial DNA gene abundances, total DNA concentrations, and percentage cortical content). Human DNA concentrations, bacterial gene abundances, and total DNA concentrations were log-transformed prior to linear regression. Multiple regression analysis was also performed, treating log transformed human DNA as the dependent variable and log transformed bacterial gene abundances, log transformed total DNA, and percentage cortical content as independent variables, including their various interactions. Assumptions including heteroskedasticity, normality, autocorrelation, and multicollinearity were tested using the R package sjstats (v. 0.17.0).

Kruskal-Wallis tests were used to assess statistical significance in alpha diversity metrics, followed by multiple comparisons with false discovery rate adjusted p-values. Permutational multivariate analysis of variance tests (PERMANOVAs), applying 999 permutations, were used to assess statistical significance in beta diversity between categorical variables of interest including body region (i.e., head, upper torso, arm, hand, lower torso, leg, foot), individual (A, B, and C), human DNA category, and cortical category. These same variables were tested for homogeneity of multivariate dispersion, using 999 permutations. Human DNA category was an arbitrary categorical variable created by dividing a continuous variable, human DNA concentration, by quartiles, each quartile defining a category used for factor analysis. Cortical category was established by using the mean percentiles of cortical bone composition at each sampling site as described above [0 (Teeth), 1 (80-100%), 2 (70-79%), 3 (50-59%), 4 (40-49%), 5 (30-39%), 6 (<39%)]. In addition, SIMPER, similarity percentages, followed by non-parametric Kruskal-Wallis tests with false discovery rate (FDR) corrected p-values, were used to determine OTUs significantly contributing to differences between individuals and human DNA category (seq-scripts release v. 1.0) [148]. Random forest models were generated using Python (v. 3.5.2) and scikit-learn (v. 0.19.2) to identify OTUs contributing to patterns of human DNA preservation. OTUs were merged at the genus level, and all samples were used to generate the model (bacteria, n = 162; microbial eukaryotes, n = 71; combined datasets, n = 71). Data were randomly split into training (3/4) and testing (1/4) sets.

Results

Bacterial and Human Quantification via qPCR

Though bacterial gene abundances, which was used as a proxy for bacterial loading, were often high when human DNA quantities were low, for example in the teeth, upper torso, lower torso, and in the hand, this relationship was not consistent across all body regions. Despite bones of the feet having some of the highest human DNA quantities, these also corresponded with high bacterial gene abundances (Figure 2.1). While bones with high cortical content generally demonstrated lower bacterial infiltration, bacterial gene abundance was not a significant predictor of percent cortical content (adjusted R^2 = -0.03) (Figure 2.2A). Total DNA was, however, a significant predictor of percent cortical content ($p < 0.001$, F = 71.43, DF = 1, 33, adjusted R^2 = 0.67); as the percentage of cortical bone decreased, total DNA increased (Figure 2.2A).

When excluding teeth, human DNA quantities were significantly different by individual ($p < 0.001$, F = 12.06, DF = 2) and body region (DF = 6, $p < 0.01$, F = 4.52), with a significant interaction between body region and individual ($p < 0.05$, F = 1.87, DF = 12). On average, individual B had greater concentrations of human DNA than A or C, while individual A had the lowest concentrations of human DNA. Therefore, to test the effects of various predictor variables on human DNA recovered from bone, individuals were assessed independently. Bacterial gene abundance did not significantly predict human DNA concentration in two out of three individuals (A, $p = 0.12$; B, $p = 0.05$), while bacterial gene abundance demonstrated a positive relationship with human DNA concentration in individual C ($p = 0.01$, F = 6.85, adjusted R^2 = 0.113) (Figure 2.2B). A similar relationship was observed for total DNA, which also showed a positive relationship with human DNA concentration for individual C ($p = 0.001$, F = 12.41, adjusted R^2 = 0.199). In addition, percent cortical content was a significant predictor of human

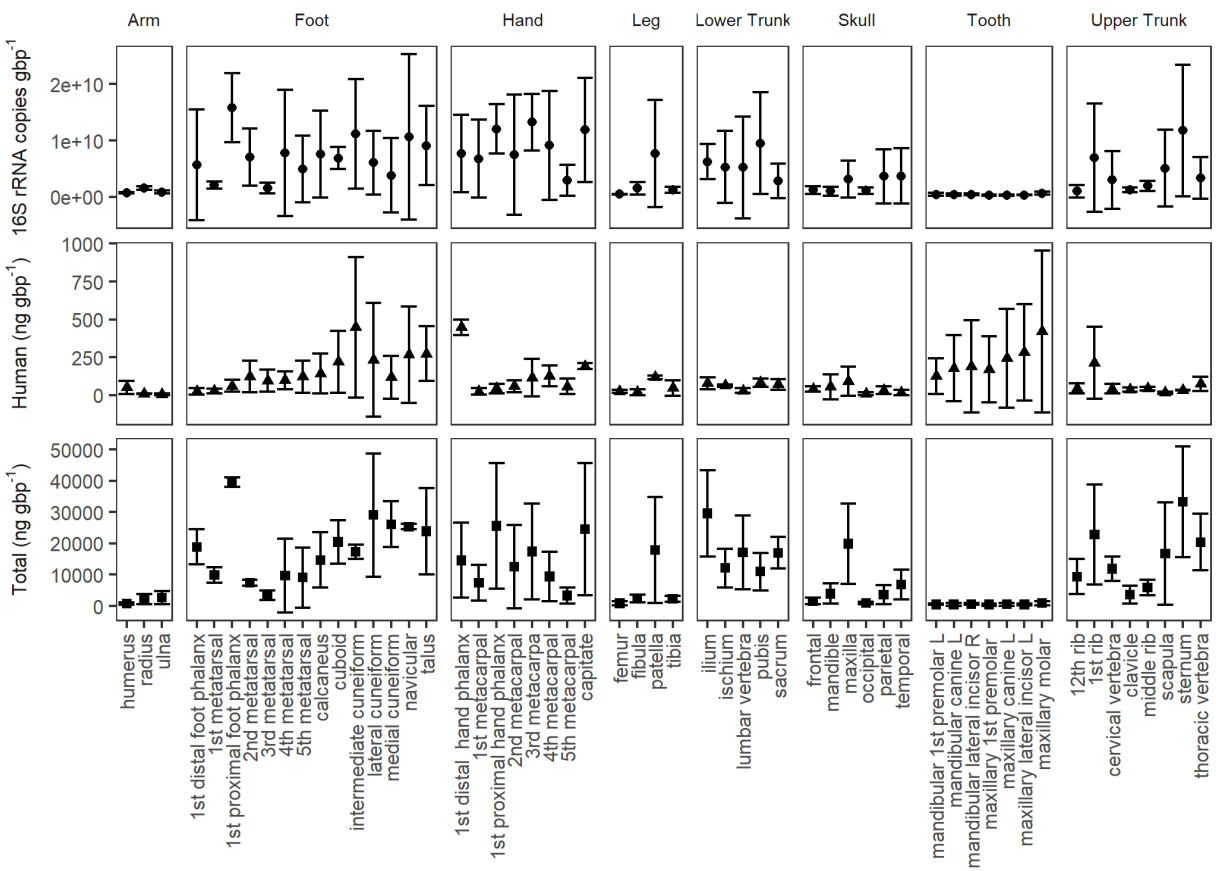

Figure 2.1: Mean total DNA (Total (ng gbp^{-1})) or the concentration of DNA extracted, mean human DNA concentration (Human (ng gbp^{-1}), as quantified using qPCR, and bacterial gene copies (16S rRNA copies gbp^{-1}), as quantified using qPCR by bone type (n = 3 individuals). Concentrations are presented as nanograms (ng) per gram of bone powder (gbp^{-1}). Bars represent standard deviations where n = 3.

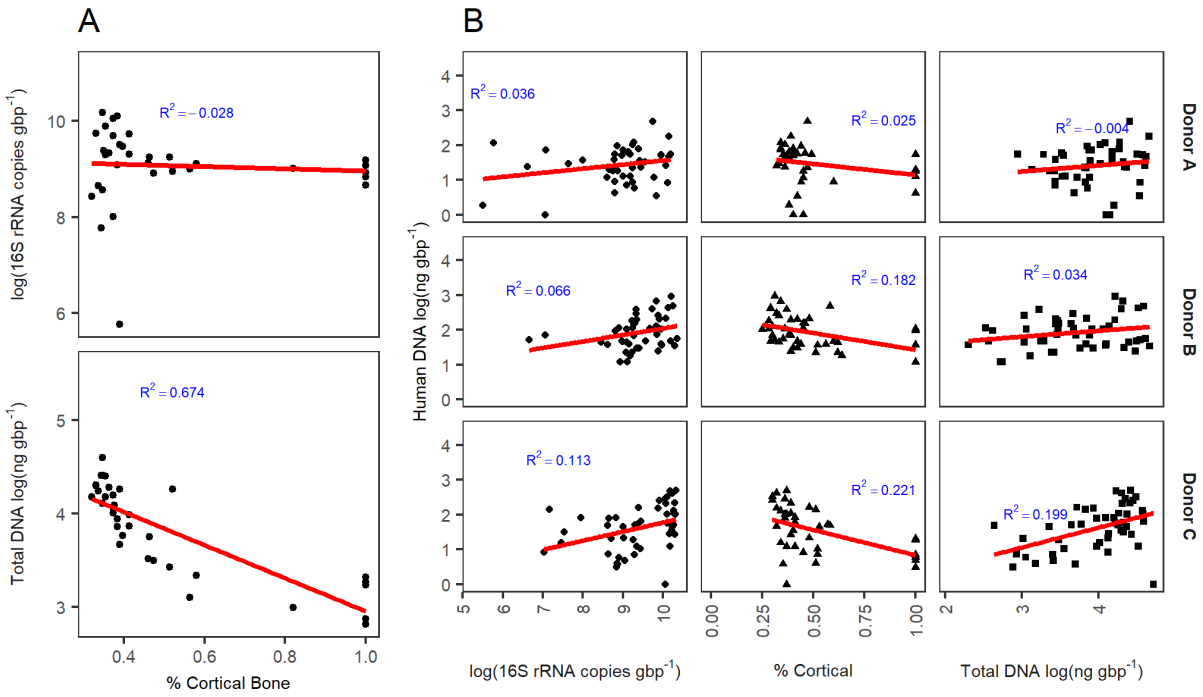

Figure 2.2: (A) Percent cortical content compared with log-normalized bacterial gene abundances and log-normalized total DNA, averaged by bone type (n = 3). (B) Bacterial gene abundances, percent cortical content, and total DNA compared with human DNA concentrations by individual (A, B, C). Raw data is shown. The red line demonstrates the best fit linear regression.

DNA concentration in two out of three individuals (B, $p = 0.003$, F = 10.33, DF = 1, 41, adjusted $R^2 = 0.182$; C, $p = 0.002$, F = 11.75, DF = 1, 37, adjusted $R^2 = 0.221$).

When including all predictors (i.e., bacterial gene abundance, total DNA concentration, and percent cortical content) in a single model, the assumption of multicollinearity was not met, indicating that predictor variables were highly correlated.

Bacterial Community Analysis

Bacterial communities showed contributions from 47 phyla; of these, only 12 demonstrated greater than 2% relative abundance when averaged by bone type: Proteobacteria (20 – 57%), Actinobacteria (4 - 37%), Firmicutes (2 – 35%), Bacteroidetes (2 – 21%), Planctomycetes (0.2 – 11%), Saccharibacteria (0.2 – 12%), , Chloroflexi (2.8 - 7.8%), Verrucomicrobia (0.05 - 4.7%), Chlamydiae (0.02 - 3.9%), Acidobacteria (0.04 – 2.2%), BRC-1 (0.009 - 2.3%), and Deinococcus-Thermus (0 - 7.0%) (Figure 2.3).

Bacterial communities significantly differed by individual ($p = 0.001$, F = 11.08, DF = 2) (Figure 2.4), body region ($p = 0.001$, F = 3.99, DF = 7), human DNA concentration ($p = 0.02$, DF = 3, F = 1.48), and cortical bone content ($p = 0.003$, F = 1.28, DF = 5). There was a significant interaction between body region and individual ($p = 0.001$, F = 2.70, DF = 14) and body region and cortical content ($p = 0.02$, F = 1.23, DF = 4). Heterogeneous multivariate dispersion was observed by individual ($p = 0.016$), body region ($p = 0.001$), and cortical category ($p = 0.001$), but not human DNA ($p = 0.27$); bacterial communities from individual A and C clustered more tightly compared with individual B (Figure 2.4). When examining individuals independently, body region remained significant (A, $p = 0.001$; B, $p = 0.001$; C, $p = 0.001$) (Figure 2.5), while cortical content remained significant in individuals B and C (B, $p = 0.003$; C, $p = 0.03$) but not A ($p = 0.63$).

Diversity was significantly different by individual ($p < 0.01$, DF = 2); individual A had the lowest diversity (mean = 30.0), while individual C had the greatest diversity (mean = 46.9) (Figure S2.3). When each individual was considered independently, diversity also significantly differed by body region (A: $p < 0.01$, $X^2 = 19.0$, DF = 7; B: $p < 0.0001$, $X^2 = 34.6$, DF = 7); C: $p < 0.001$, $X^2 = 24.9$, DF = 7) (Table S2.2; Figure S2.4); body regions from A followed a different trend in diversity than B or C. Richness did not show significant differences by individual ($p > 0.05$, $X^2 = 3.97$, DF = 2), but did significantly differ by body region ($p < 0.0001$, $X^2 = 46.0$, DF = 7). Observed richness was greatest in the upper and lower torsos (Figure S2.5).

OTUs driving differences between individuals included predominantly soil taxa from the following families: Streptosporangiaceae, Nocardiaceae, Comamonadaceae, Pseudomonadaceae, Xanthomonadaceae, Clostridiaceae, Brevibacteriaceae, Streptomycetaceae, Intrasporangiaceae, unclassified Thermomicrobia, and Mycobacteriaceae. Notably, OTUs identified as *Simplicispira* and an unclassified member of Streptosporangiaceae were found at greater abundances in A, while *Stenotrophomonas* and *Rhodococcus* showed greater abundances in individual C; *Brevibacterium*, an unclassified member of Thermomicrobia, *Pseudomonas*, and *Clostridium* were greatest in B (Figure S2.6). Although three OTUs significantly contributed to differences by human DNA category (two *Streptomyces* and one *Mycobacterium*), these OTUs did not remain significant after correcting p-values using FDR.

Random forest models were used to identify bacterial OTUs associated with differences in human DNA concentrations. The initial model generated had a mean absolute error of 91.7 ($p = 0.03$, adjusted $R^2 = 0.09$), with 30 predictor OTUs identified (Figure S2.7). Important predictor OTUs were represented by Actinobacteria (importance = 30%), Bacteroidetes (17%), Firmicutes

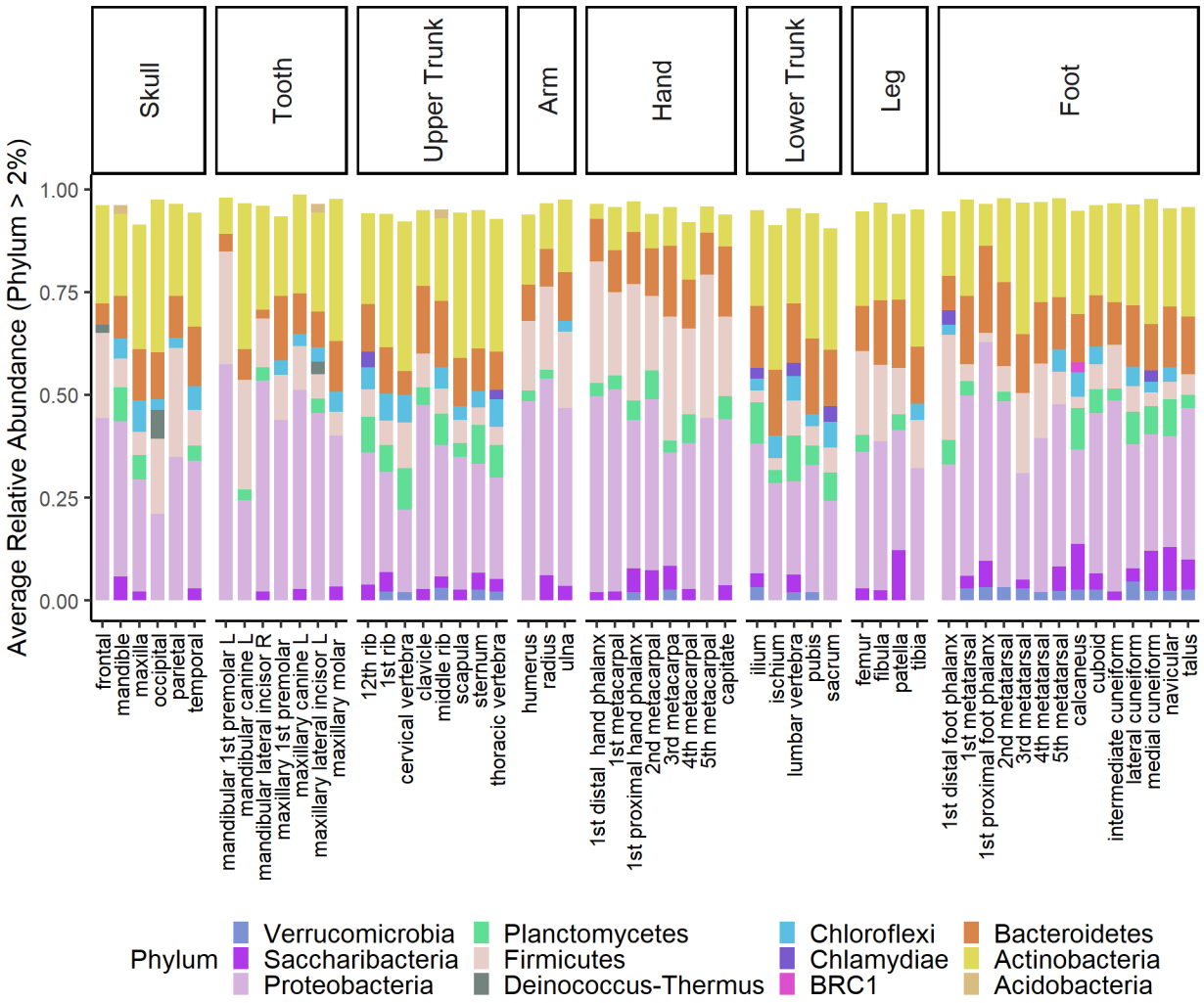

Figure 2.3: Bacterial phylum-level community membership. Mean relative abundances greater than 2% for all individuals combined. Bone phyla membership was averaged by bone type (n = 3), except in the case of the navicular, occipital, and sternum (n = 2).

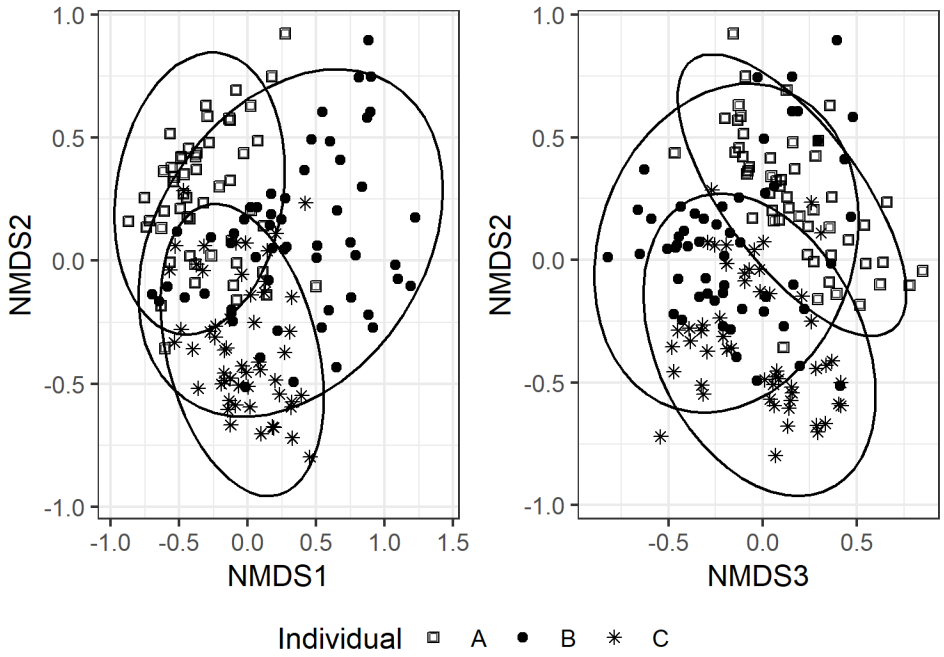

Figure 2.4: Non-metric multidimensional scaling (NMDS) ordination performed on Bray-Curtis dissimilarities of bone bacterial communities (n =162) and visualized by individual. Stress = 0.14 and k = 3; ellipses represent 95% confidence intervals.

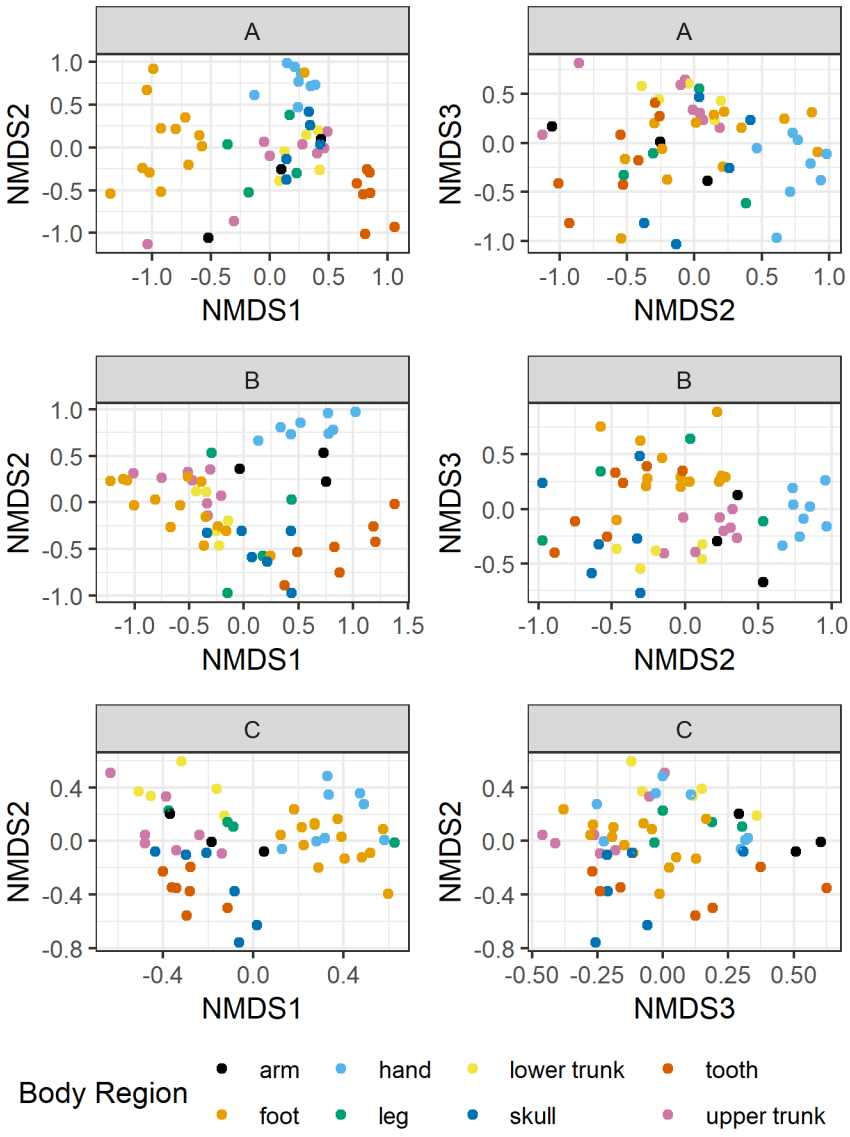

Figure 2.5: Non-metric multidimensional scaling (NMDS) ordinations on Bray-Curtis dissimilarities of bone bacterial communities. Ordinations were conducted independently by individual (A: n = 53, B: n = 55, C: n = 54) and visualized by body region (A: stress = 0.14, k = 3; B: stress = 0.10, k = 2; C: stress = 0.10, k = 3). The letters "A", "B", and "C" above figure panels refer to individuals.

(23%), and Proteobacteria (30%). Contributing OTUs greater than 1% included the genera *Clostridium*, unclassified Dermacoccaceae, *Paracoccus*, and *Actinotalea* (Figure S2.7A). The model only slightly improved when excluding teeth from the analysis (mean absolute error = 72.5, $p = 0.02$, adjusted $R^2 = 0.12$). When teeth were excluded, the top five predictor OTUs became unclassified Dermacoccaceae (14%), unclassified Desulfuromonadales (9%), *Clostridium* (3%), unclassified Gaiellales (3%), and unclassified Mollicutes (3%).

Eukaryotic Community Analysis

Microbial eukaryotic communities showed large contributions from Ascomycota (mean relative abundance 40%), Apicomplexa (21%), Annelida (19%), Basidiomycota (17%), Ciliophora (14%), and enigmatic Eukaryota (including *Incertae sedis*) (14%), with additional contributions from Cercozoa (9%) Peronosporomycetes (8%), Nematoda (7%), and Cryptomycota (6%) (Figure 2.6). While Apicomplexa had a high mean relative abundance (21%), this was dominant in a single sample, a fibula from individual B.

Microbial eukaryotic communities showed similar patterns in beta diversity compared to bacterial communities. When testing differences between body region, individual, human DNA quartiles, and cortical content, microbial eukaryotic communities significantly differed by individual ($p = 0.001$, $F = 8.69$, $DF = 1$), body region ($p = 0.001$, $F = 2.83$, $DF = 7$), human DNA ($p = 0.02$, $F = 1.41$, $DF = 3$), and cortical content ($p = 0.001$, $F = 1.60$, $DF = 5$), with a significant interaction between body region and individual ($p = 0.001$, $F = 4.08$, $DF = 3$), body region and human DNA ($p = 0.02$, $F = 1.25$, $DF = 4$), and individual and cortical content ($p = 0.008$, $F = 1.72$, $DF = 1$). Due to sequence loss, alpha diversity metrics were not computed.

A random forest model was also applied to the microbial eukaryotic dataset to identify OTUs contributing to patterns of human DNA preservation. The resulting model was not significant, with a mean absolute error of 171.96 ($p = 0.14$, adjusted $R^2 = 0.07$). The most important predictor taxon identified (OTU0003), contributing to 33% of the model, was an unclassified member of Saccharomycetales. Microbial eukaryotic and bacterial OTU data were combined and a random forest model was constructed for shared samples to predict human DNA concentrations. The resulting model was significant (mean absolute error = 175.71, $p = 0.03$, adjusted $R^2 = 0.21$). Again, the top predictor taxon was OTU0003 with an importance value of 10% or 0.1; this Saccharomycetales OTU decreased in abundance in the skull of individual B as human DNA concentrations increased (Figure S2.8). Other important contributors, with importance values greater than 1% or 0.01, included bacterial genera from the phyla Actinobacteria (*Microbacterium*, 6%, Gaiellales uncultured, 5%, *Leifsonia*, 2%, *Williamsia*, 2%), Proteobacteria (*Stenotrophomonas*, 2%), Firmicutes (Clostridiales Family XI uncultured, 2%), Gemmatimonadetes (unclassified Gemmatimonadaceae, 2%), and Planctomycetes (*Zavarzinella*, 2%).

Discussion

Characterizing the Postmortem Bone Microbiome

The post-mortem bone microbiome is diverse and variable in the human skeleton two years after death. Though bone bacterial communities included a wide-array of taxa, bacterial communities were primarily dominated by six phyla (Actinobacteria, Bacteroidetes, Firmicutes, Proteobacteria, Planctomycetes, and Saccharibacteria). Excluding Planctomycetes and Saccharibacteria, these taxa were also shown to dominate human rib samples from twelve

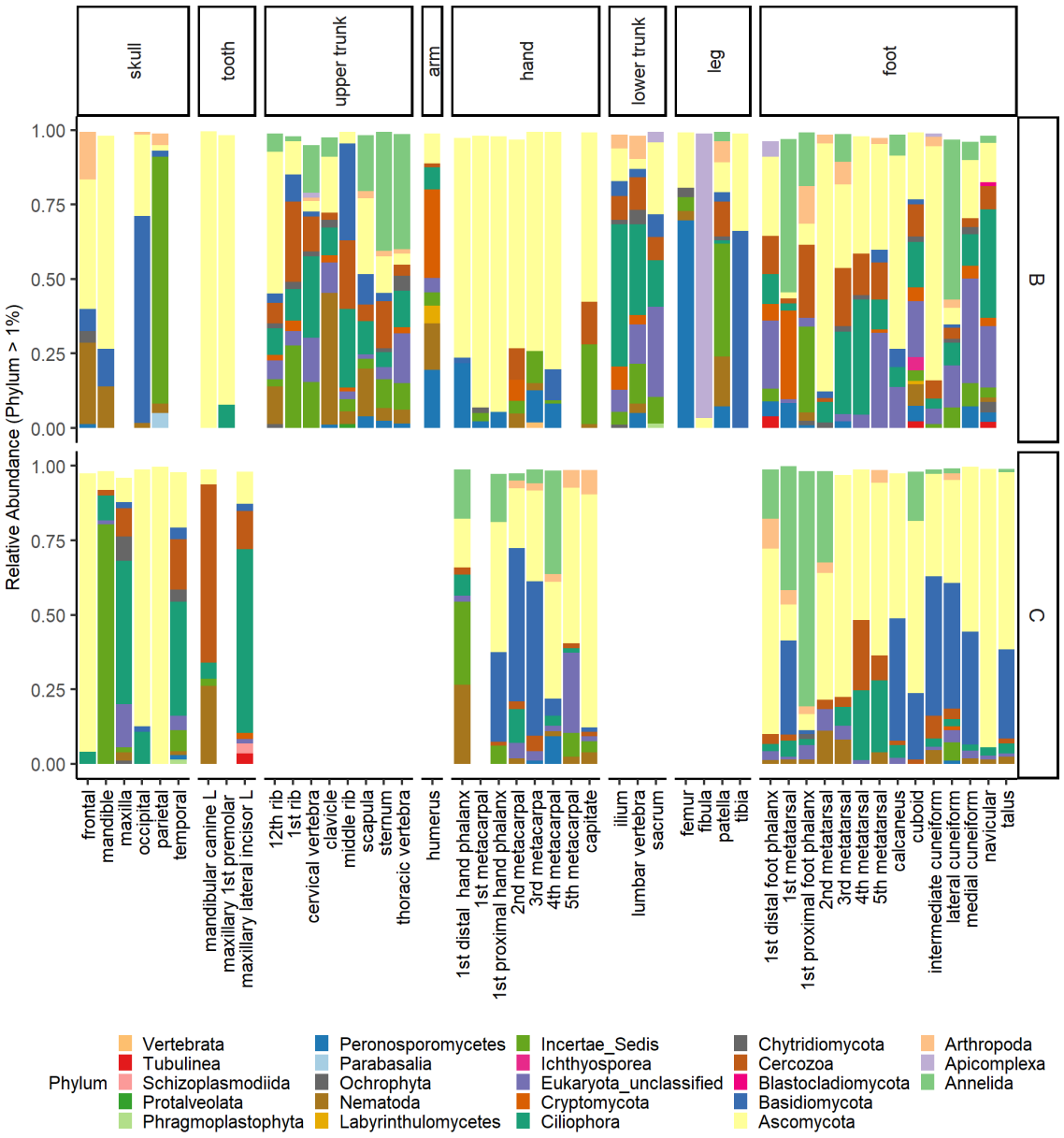

Figure 2.6: Relative abundance of eukaryotic phyla by bone type and individual. Relative abundance is shown for only those phyla with greater than 1% relative abundance, and for two of the three individuals (B and C). Data were not averaged by bone type.

individuals that had also decomposed at the ARF [14]. Damann et al. [14] observed changes in proportions of these dominant taxa and Acidobacteria, with increasing post-mortem intervals (PMIs). Partially skeletonized remains showed greater contributions from Firmicutes, while fully skeletonized remains saw increased proportions of Bacteroidetes, and dry remains had greater proportions of Actinobacteria and Acidobacteria [14]. Rib samples from the current study most closely resembled dry remains in phyla-level contributions [14], but unlike taxa proportions observed in Damann et al. [14], rib samples from this study also contained greater than 2% from Verrucomicrobia, Saccharibacteria, Planctomycetes, Chloroflexi, and Chlamydiae (Figure S2.10). Discrepancies in observed taxa may be due to differences in sample size and sequencing analysis methodologies. While Plactomycetes, a phylum commonly associated with aquatic environments, and Saccharibacteria, a phylum containing multiple environmental taxa, were not observed by Damann et al. [14] in abundances greater than 1%, these phyla have been observed in multiple studies focused on gravesoils [50,54].

Ascomycota, observed in 100% of samples (71 of 71) in the eukaryotic dataset, and Basidiomycota, observed in 55% of samples, were the dominant microbial eukaryotes in this study. This was unsurprising, as these fungal phyla contain multiple saprophytic groups that have previously been observed in association with decomposing carrion [149]. In addtion to fungi, multiple phyla of protists were also detected, including Apicomplexa (5 of 71 samples), Ciliophora (49 of 71 samples), and Cercozoa (49 of 71 samples). Protists found in association with bones may be opportunistic, potentially transferred to remains via soil, scavengers, insects, rain water, and run-off and may be active fungal and bacterial consumers. For example, the genus *Rhogostoma*, which was prevalent in samples from indiviudals A and B, has been involved in experiments in which they consumed both fungal and bacterial species [150]. Similarly, Nematoda were detected, with the majority of sequences belonging to the family Rhabditidae, which contains bacterivorous members, previously observed in decomposition research [41,56,63,151]. Other bacterivores detected within human bones included Tubulinea, Cercozoa, and Apicomplexa, which have also been found in association with soils underlying human remains [151]. Cercozoa and other testate amoeba are extremely sensitive to environmental change, and generally decrease in the soil with cadaveric inputs [65]. While certain species have responded with positive growth during late stage decomposition (from 1 month to 1 year post-mortem) [66], their presence in bones over a year after death likely reflects a shift back to more oligotrophic conditions.

Presence of Deinococcus-Thermus, a phylum well-represented by thermophiles [152], at greater than 1% relative abundance in 6% of samples, is suggestive of a harsh environment. Bones deposited on the soil surface are exposed to sharp temperature contrasts daily and annually. East Tennessee experiences freezing temperatures in the winter and temperatures greater than 37°C in the summer, which can influence moisture availability. As indicated Reeb et al. [90], bone may provide shelter from a harsh exterior environment, likely defined by low moisture and variable temperature extremes by season. Individual C had greater abundances of Deinococcus-Thermus than B and A (Figure S2.11), likely due to the greater length in the time in which this individual was exposed to environmental fluctuations in temperature and precipitation (Figure S2.9). On a similar note, the majority of samples with abundances greater than 1% were from the skull including cranial elements and teeth. The cranium is one of the first body regions to skeletonize during decomposition due to low tissue biomass and high larval presence. It is likely that this skeletal region also experiences greater intervals of environmental exposure [17].

Community Differences by Individual and Anatomical Region

Beta diversity analyses showed differences in bone microbial communities, including both prokaryotes and eukaryotes, by individual and body region. This is unsurprising, as there is extensive research on the human microbiome and a multitude of variables that relate to differences in microbial community structure and composition between individuals including life history (e.g., health and diet) [153–155]. Two of the three individuals had a history of diabetes (Individual A and C), which may have contributed to differences in microbial community structure and composition [156]. Moreover, the duration of placement at the ARF, which was also influenced by differences in temperature and precipitation, likely contributed to differences observed between individuals. In particular, bacterial alpha diversity was lowest in individual A and greatest in C, reflecting differences in exposure duration (Figure S2.3; Figure S2.9).The impact of the soil microbiota is expected to increase overtime, with prolonged soil contact [14]. Because of this, we hypothesize that differential rates in skeletonization likely influence bone microbial composition and structure at any given time point.

Recently, Pechal et al. (2018) showed microbial differentiation by anatomic region (i.e., external sites from the auditory canal, eyes, nose, mouth, umbilicus, and rectum) up to 48 hours after death. Though they speculated that this pattern would likely attenuate with longer post-mortem intervals, this has yet to be tested. Here, bone microbial communities retained differences by anatomic location in individuals with post-mortem intervals greater than 1 year. Micro-environmental differences in soil communities as well as differences in enteric microorganisms and their abilities to compete and persist with soil microorganisms colonizing the body likely contributed to spatial differences observed in anatomic regions and between different individuals. Research on the human microbiome has shown the uniqueness of microbial communities by not only individual but also body site and time [158,159], which has recently gained utility in microbial forensics [160,161].

Nicholson et al. (1996) demonstrated that bones in similar environments showed drastic differences in bone preservation, despite similarities in soil pH and drainage. This evokes the question - if not the environment, what is the source of these differences? Enteric/putrefactive bacteria have been posited as the primary source of macroscopic biogenic decomposition in pig remains; neonatal pig remains demonstrated no evidence of microbial degradation, which researchers hypothesized as being related to the relative sterilitiy of infant guts compared with adults [82]. While the source of bacteria in this study remains unknown, as we have no gut or soil samples prior to placement to track bacterial translocation, we suspect that both soil and gut microbes are able to colonize and aid in bone biodegradation (e.g., Metcalf et al., 2016). We have previously demonstrated that human-associated *Bacteroides*, an obligately anaerobic member of the human gut microbiome, can persist for long periods of time in the soils impacted by decomposing human remains (Cobaugh et al. 2015, Keenan et al. 2018), providing evidence that these gut microbes are present in the decomposition environment and thus have the potential to colonize bone. The extent to which enteric microorganims are able to move throughout the body is likely limited, and distance from the gut may be a crucial factor controlling differences in microbial communities by body region. However, Pechal et al. (2018) recently observed an increase in gene abundance associated with bacterial motility during decomposition, so this is an area of postmortem microbiology that merits further study.

Bone microstructure (i.e., the percentage of cortical content) also influenced differences in microbial communities. Communities differed by cortical bone percentage likely due to the presence of greater void space in cancellous bone compared with cortical bone, facilitating ease

of invasion, especially for incidental taxa or soil contaminants (e.g., potentially Verrucumicrobia). However, this may also be related to nutritive differences; cancellous elements may harbor more labile material in the form of surviving remnant tissues such as red marrow [107], while cortical bone may be considered more recalcitrant. This may account for patterns observed in total DNA concentrations and bacterial gene abundances. Bacterial gene abundance was not a significant predictor of human DNA concentration, and cases in which bacterial gene abundance did significantly predict human DNA (i.e., individual C), the relationship was positive, indicating that the degree of microbial loading does not negatively impact the pattern of skeletal DNA preservation in remains with environmental exposure up to two years. Rather, the presence of specific taxa likely has a greater impact on skeletal integrity.

Additionally, presence from both aerobic and anaerobic genera, points to the existence of micro-spatial differences within a single bone. This phenomenon is also observed in soils where, for example, anaerobic microsites can persist within a well-drained, well-aerated soil. Extracellular polymeric substances were observed surrounding living cells on bison bone at Yellowstone National Park, using scanning electron microscopy [90]. This highlights the importance of biofilm production in microbial bone colonization. Though microscopy was not performed in the current study, biofilm production combined with increases in microbial biomass during decomposition are hypothesized to play an important role in the development of micro-spatial differences in oxygen access and respiration strategies.

Microbial Taxa Associated with Skeletal DNA Preservation

Random forest models were minimally successful in identifying microbes related to patterns of DNA preservation, however, they were likely complicated by microbial community differences by individual and body region. While bacterial OTUs produced more accurate random forest models than eukaryotic OTUs, the best model resulted when combining both bacterial and eukaryotic data sets, with a Saccharomycetales OTU identified as the most important contributor to the model. Saccharomycetales are commonly associated with the oral microbiome of healthy humans [163]. This taxon decreased in abundance with increased human DNA concentrations in the cranium of individual B; this may indicate that oral microbes can persist throughout decomposition and may have implications for DNA survival. Alternatively, this could implicate a phosphate solubilizing fungi.

Similarly, bacterial random forest models were conflated by body region; genera *Actinotalea* and *Paracoccus*, showed increased abundances with human DNA concentrations in teeth, while Dermacoccaceae demonstrated increased abundances in the feet. Importantly, increased abundances of *Clostridium sp.*, a genus that contains known collagenase producers [35], were observed when human skeletal DNA concentrations decreased. Though Clostridium spp. is ubiquitous in both the soil environment and the human gut, its presence in surface remains, lends weight to a gut origin. The foot is the farthest anatomical region from the gut, and interestingly, bones of the feet had some of the highest human DNA concentrations. Distance from the gut as an important factor related to human DNA degradation requires further testing. Though predictor taxa could be identified using random forest models, their functional role in DNA degradation, if any, remains unclear. The variation seen by body region and individual may be passified by increasing the research sample size.

Conclusions

Most of what is known regarding the biogenic degradation of bone is from histological research concerning archaeological bone (e.g., Child, 1995b; Nielsen-Marsh and Hedges, 2000; Trueman and Martill, 2002; Booth, 2016; Hollund et al., 2017). The current study used next generation sequencing technologies to provide a survey of bacteria, fungi, and protists capable of bone colonization. Though specific taxa were correlated to patterns of human DNA preservation using random forest models, the functional role of identified bone microbes remains unknown. Because the target of this study was DNA, which provides information regarding presence rather than activity, it is difficult to discern incidental taxa, i.e. taxa that are present and inactive, from taxa that are actively degrading bone. This is an issue that has long plagued microbial ecology – linking structure and function. Remnant extracellular DNA of microbial origin is a problem [166], and microbial DNA can bind to hydroxyapatite similar to human DNA [167,168], further complicating observed differences in community composition and structure. Nevertheless, the current study presents a first step in characterizing microbial differences with morphological and microstructural differences by bone type within and between individuals following skeletonization. Ultimately this provides a foundation for understanding postmortem colonization of bone by microbes and the subsequent effects on bone stability and human DNA preservation over time.

Acknowledgements

Thanks to Mundorff and DeBruyn lab members for their support and guidance in this research. In addition, the authors would like to thank Dr. Yong Bradley for providing access to the clinical CT scanner at the University of Tennessee Medical Center, and to Shelley Acuff for operating the CT system and assisting with bone set-up prior to scanning.

Funding

This work was partially funded by the National Institute of Justice grant 2010-DN-BX-K229 and the National Science Foundation Award 1549726 to JMD

Appendix I

Table S 2.1: Bones sampled from each of the three individuals (Mundorff and Davoren, 2014)

Bone Type	Sample Quantity per Individual
Skull	
Frontal	1
Temporal	1
Parietal	1
Occipital	1
Maxilla	1
Mandible	1
Teeth	
Maxillary lateral incisor **Maxillary canine**	1
Maxillary 1st premolar **Maxillary molar**	1
Mandibular lateral incisor **Mandibular canine**	1
Mandibular 1st premolar	1
Trunk	
Cervical vertebra	1
Thoracic vertebra	1
Lumbar vertebra	1
1st Rib	1
Middle rib	1
12th Rib	1
Sternum	1
Sacrum	1
Clavicle	1
Scapula	1
Ilium	1
Ischium	1
Pubis	1
Leg	
Femur	1
Tibia	1
Fibula	1
Patella	1
Arm	
Humerus	1
Radius	1
Ulna	1

Table S 2.1 (continued)

Bone Type	Sample Quantity per Individual
Hand	
Metacarpals 1–5	5
1st Proximal phalanx	1
1st Distal phalanx	1
Capitate	1
Foot	
Metatarsals 1–5	5
1st Proximal phalanx	1
1st Distal phalanx	1
Calcaneus	1
Talus	1
Navicular	1
Cuboid	1
Medial Cuneiform	1
Intermediate Cuneiform	1
Lateral Cuneiform	1
Total	55

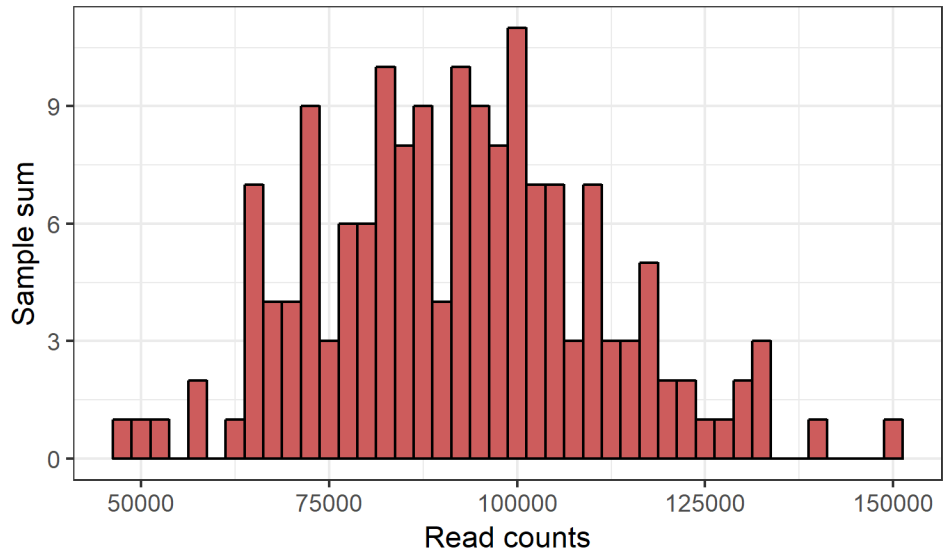

Figure S 2.1: 16S rRNA targeted metagenomics read distribution. The minimum library size was 48,288 reads, while the mean library size was 92,334.6 reads; the maximum library was 150,228 reads.

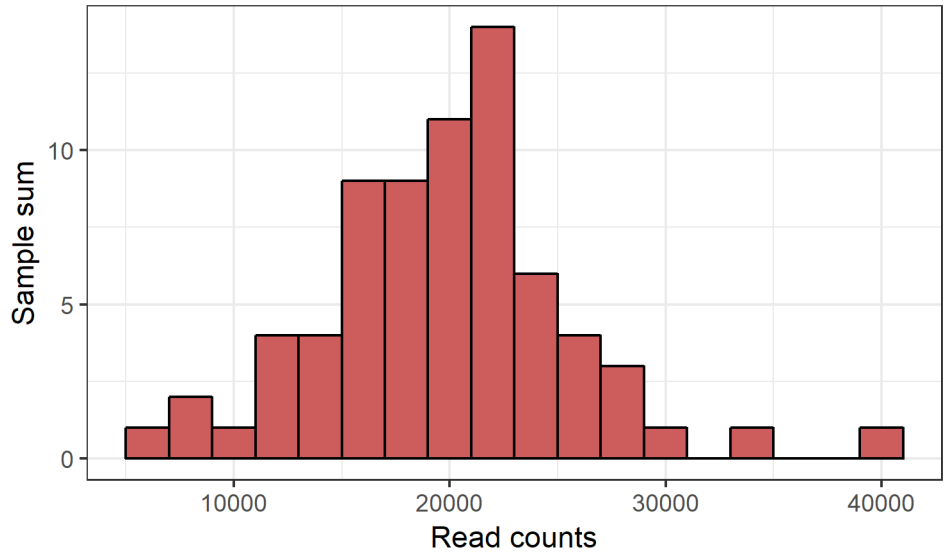

Figure S 2.2: 18S rRNA targeted metagenomics read distribution. The minimum library size was 5,368 reads; the mean library size was 19,853 reads, and the maximum library size was 40,977 reads.

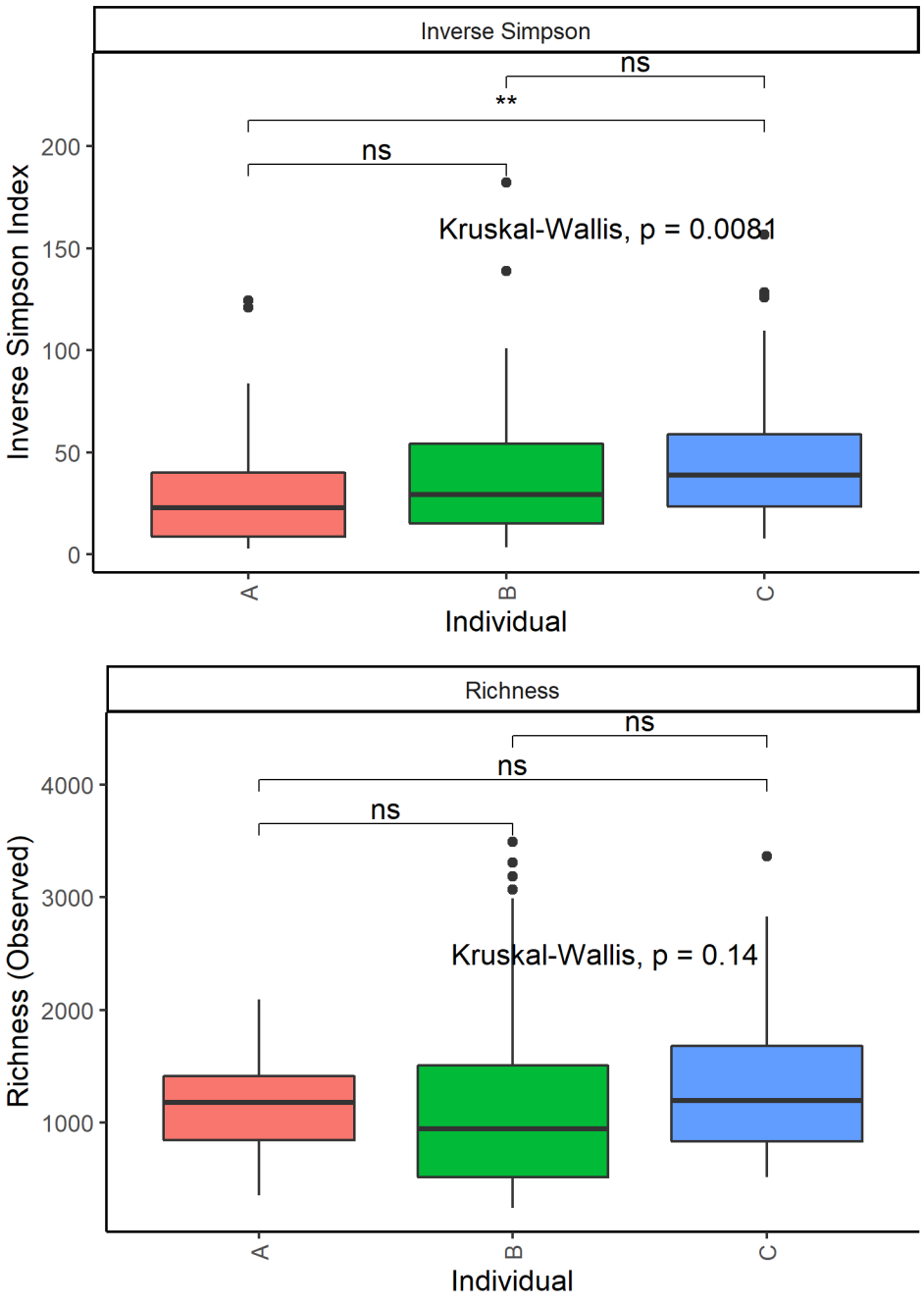

Figure S 2.3: Bacterial alpha diversity (Inverse Simpson) and richness (observed) by individual. **Indicate significance below an alpha value of 0.01. No significance is denoted by "ns".

Table S 2.2: Bacterial alpha diversity metrics including observed richness and diversity (Inverse Simpson). Data was separated by individual, and the mean and standard deviation was computed by body region. Significance levels are represented by asterisks (*$p < 0.05$; **$p < 0.01$); multiple comparison tests by individual were only conducted using Inverse Simpson indices. Lower case letters in parenthesis refer to body regions. A body region with an exponent corresponding to another body region indicates that those two regions have significantly different diversity indices.

Individual	Body Region	Inverse Simpson (mean)	Sd. Dev.	Richness (mean)	Sd. Dev.
A	Arm (a)	35.9	6.6	309.1	1100.4
A	Foot (b)	24.2	14.0	420.1	1045.7
A	Hand (c)	57.3	35.1	332.9	1509.6
A	Leg (d)	36.5	21.3	310.1	1252.5
A	Lower trunk (e)	23.6	30.3	232.8	1403.3
A	Skull (f)	34.3	48.9	484.0	1273.9
A	Tooth (g)^{c*}	9.2	6.4	168.3	699.5
A	Upper trunk (h)	26.2	25.9	327.7	1168.9
B	Arm (a)^{c*,h*}	19.3	3.8	213.9	757.9
B	Foot (b)^{c**,g*}	63.0	49.0	970.4	1915.6
B	Hand (c)^{a*,b**,d*,e*,f*,h*}	6.1	2.1	203.5	478.0
B	Leg (d)^{c*}	37.2	31.4	368.7	789.5
B	Lower trunk (e)^{a*,c*,f*,g*}	59.0	12.0	276.5	1363.4
B	Skull (f)^{c*,e*}	28.3	10.5	235.2	807.1
B	Tooth (g)^{b*,e*,h*}	15.9	11.0	156.4	397.5
B	Upper trunk (h)^{c*,g*}	61.3	27.9	653.9	1848.9
C	Arm (a)	25.5	9.4	410.4	944.0
C	Foot (b)^{g*}	44.7	24.5	335.1	1078.0
C	Hand (c)	34.3	14.4	212.1	979.9
C	Leg (d)	41.3	18.2	569.4	1348.6
C	Lower trunk (e)	91.0	43.1	533.3	1824.3
C	Skull (f)	45.8	36.5	689.5	1400.9
C	Tooth (g)^{b*,h*}	14.5	7.4	422.9	1005.3
C	Upper trunk (h)^{g*}	79.8	47.8	574.5	2302.5

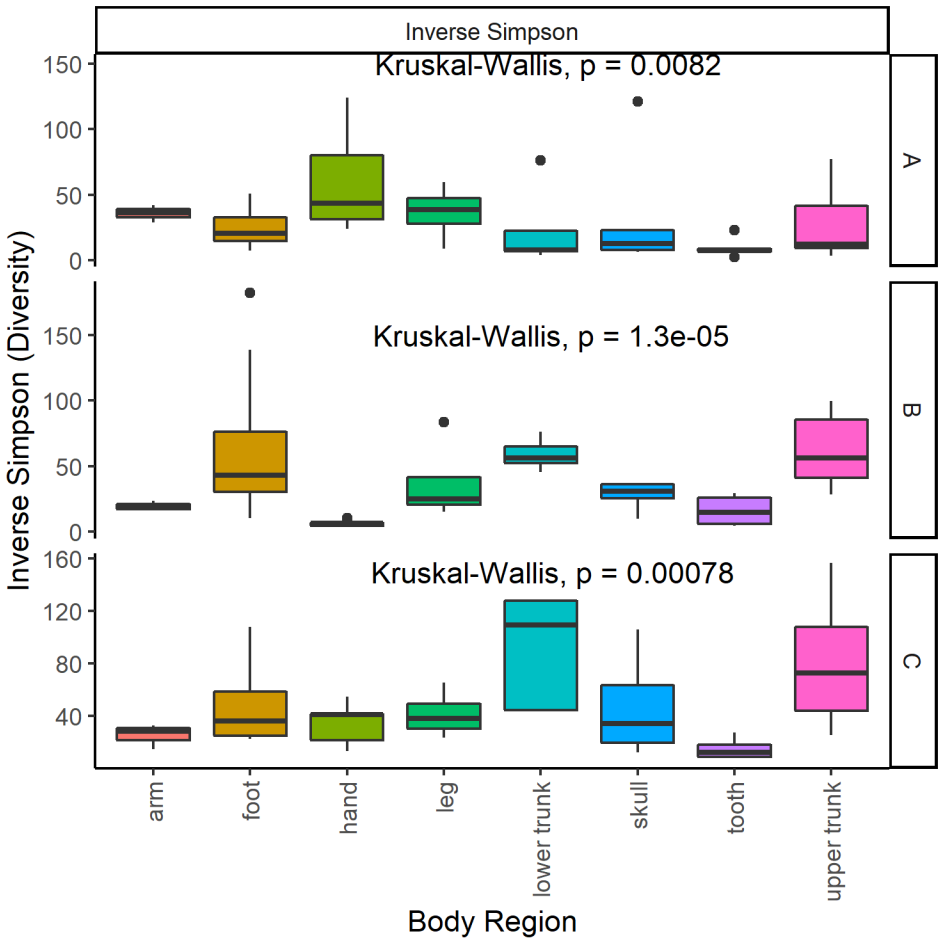

Figure S 2.4: Inverse Simpson (diversity) calculated from the bacterial dataset. Individuals ("A", "B", and "C") were assessed independently.

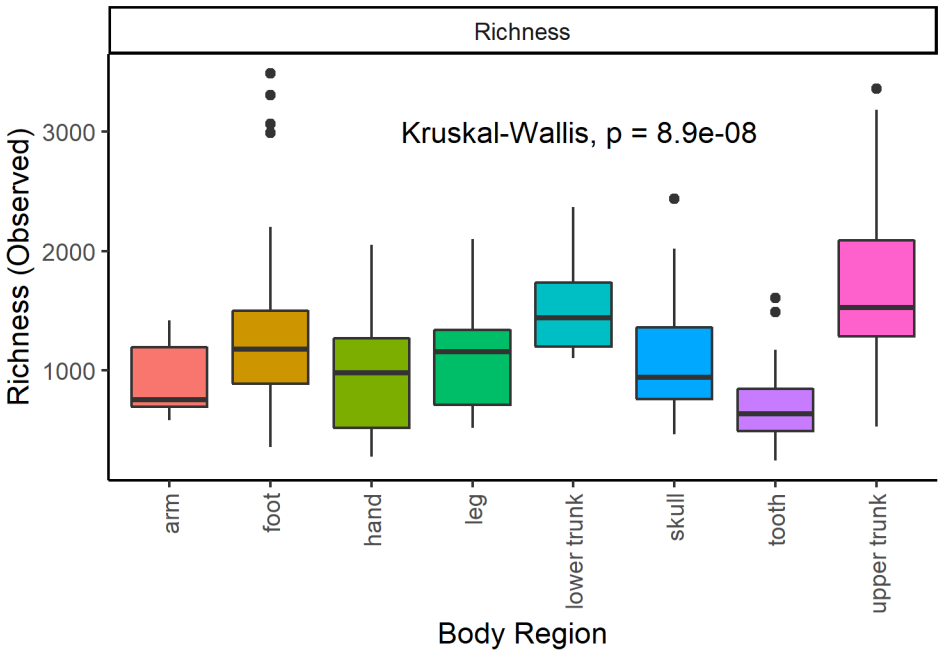

Figure S 2.5: Richness (observed) calculated from the bacterial dataset; individuals were combined.

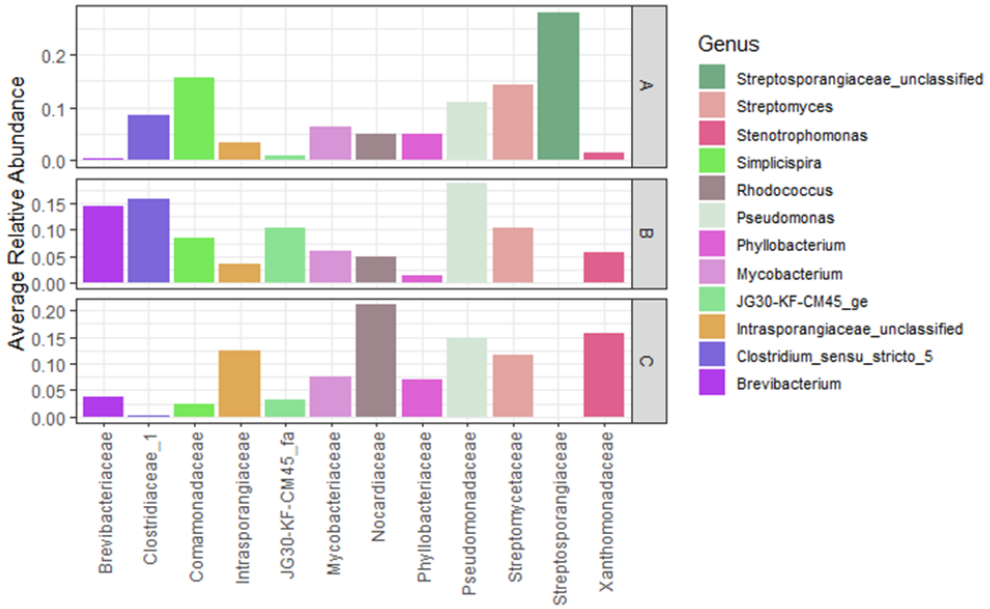

Figure S 2.6: SIMPER results by individual (A: n=53, B: n=55, C: n=54). Results include only those OTUs that demonstrated a significant difference by individual following SIMPER. All OTUs of a given genus are not represented here. The x-axis contains information on the taxonomic identification of these OTUs at the family level.

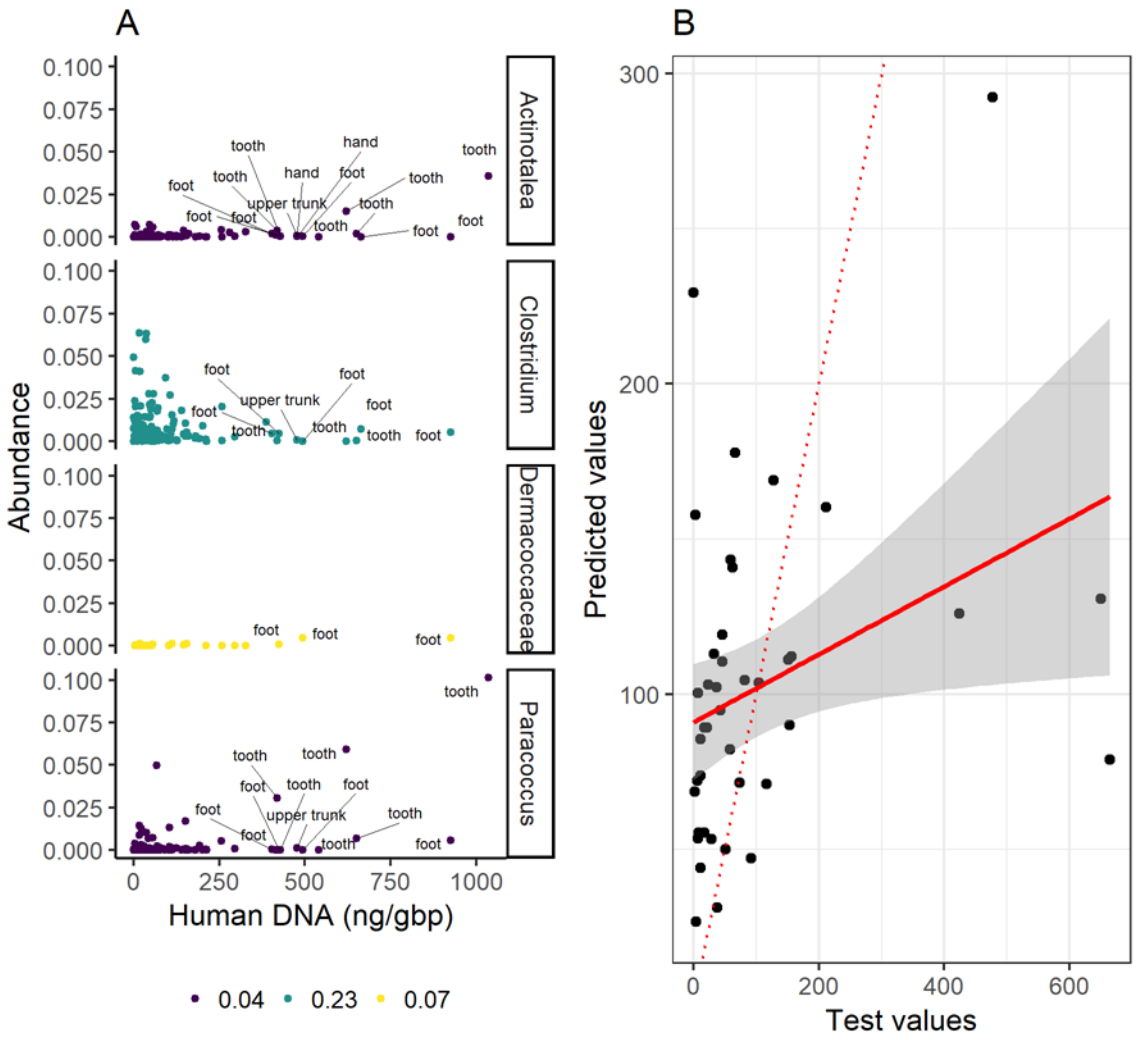

Figure S 2.7: Random forest regression. (A) Bacterial OTUs important for predicting human DNA concentrations. Importance, as a value between zero to one, is represented in color. Human DNA concentrations greater than 400 ng gbp^{-1} are labeled by body region. Abundance refers to relative abundance by bone sample, represented by values zero to one. (B) Model accuracy as a function of test values versus predicted values. The solid red line represents the modeled data; the dotted line represents an expected model if 100% accuracy.

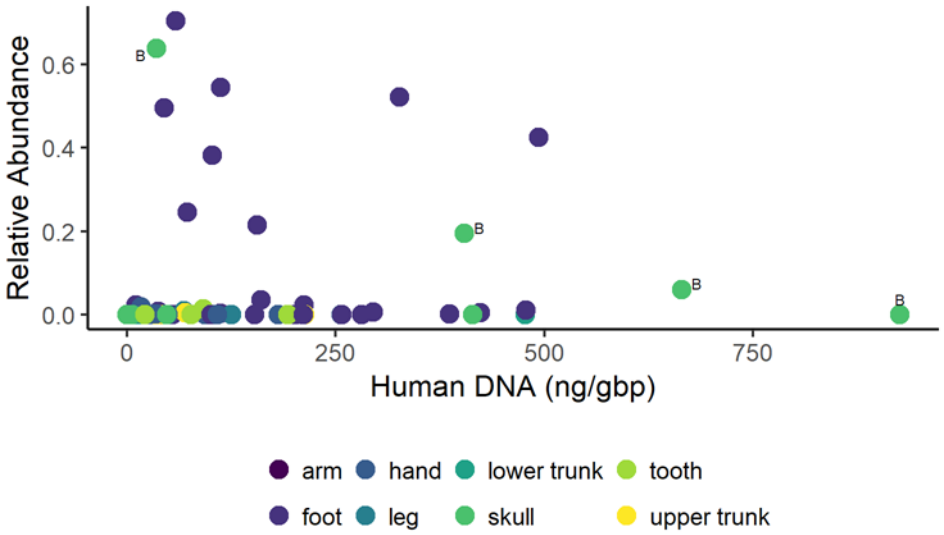

Figure S 2.8: Relative abundance of the unclassified Saccharomycetales OTU plotted against human DNA concentration. The label "B" refers to individual B.

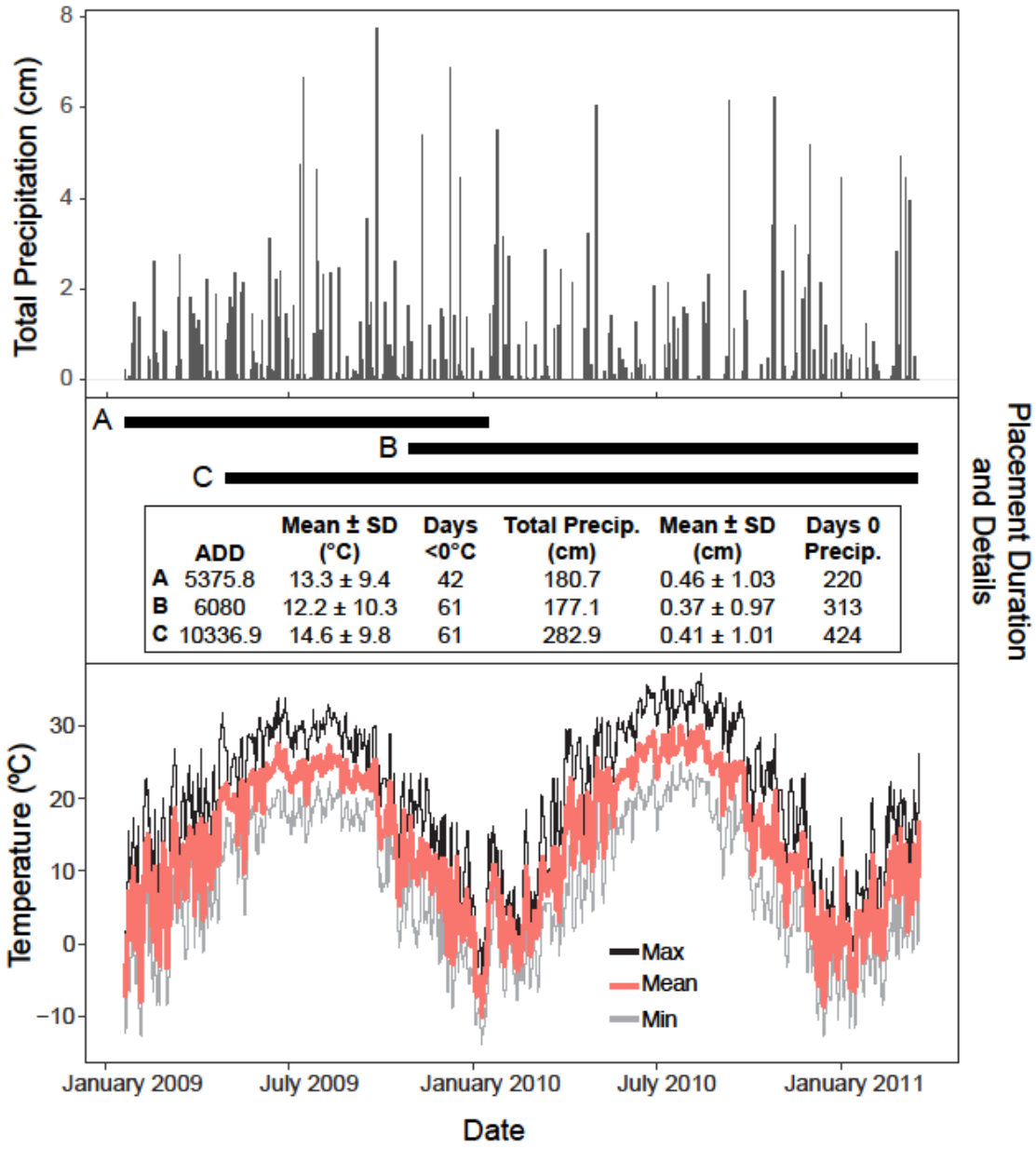

Figure S 2.9: Changes in temperature and precipitation for the duration of deposition of each donor. Donors are labeled "A", "B", "C", and "ADD" refers to accumulated degree days, an indicator of both time and temperature. Data obtained from NOAA (https://www.noaa.gov/). Figure courtesy of Sarah Keenan (co-author).

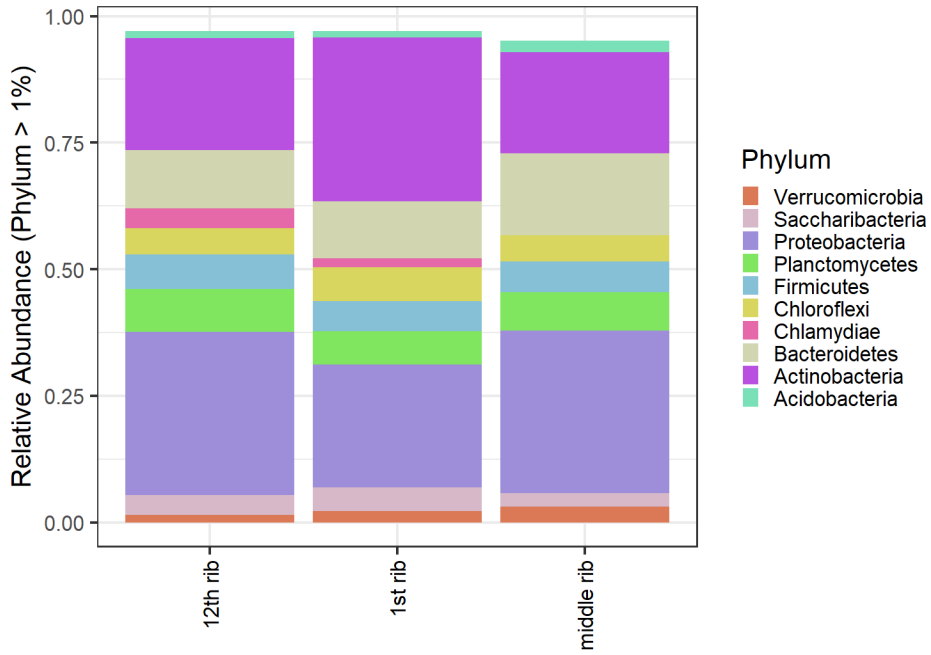

Figure S 2.10: Phylum-level bacterial community membership in human rib samples. Relative abundance was averaged by bone type, combining results from three individuals (n = 3). Only taxa with average relative abundances greater than 1% are shown.

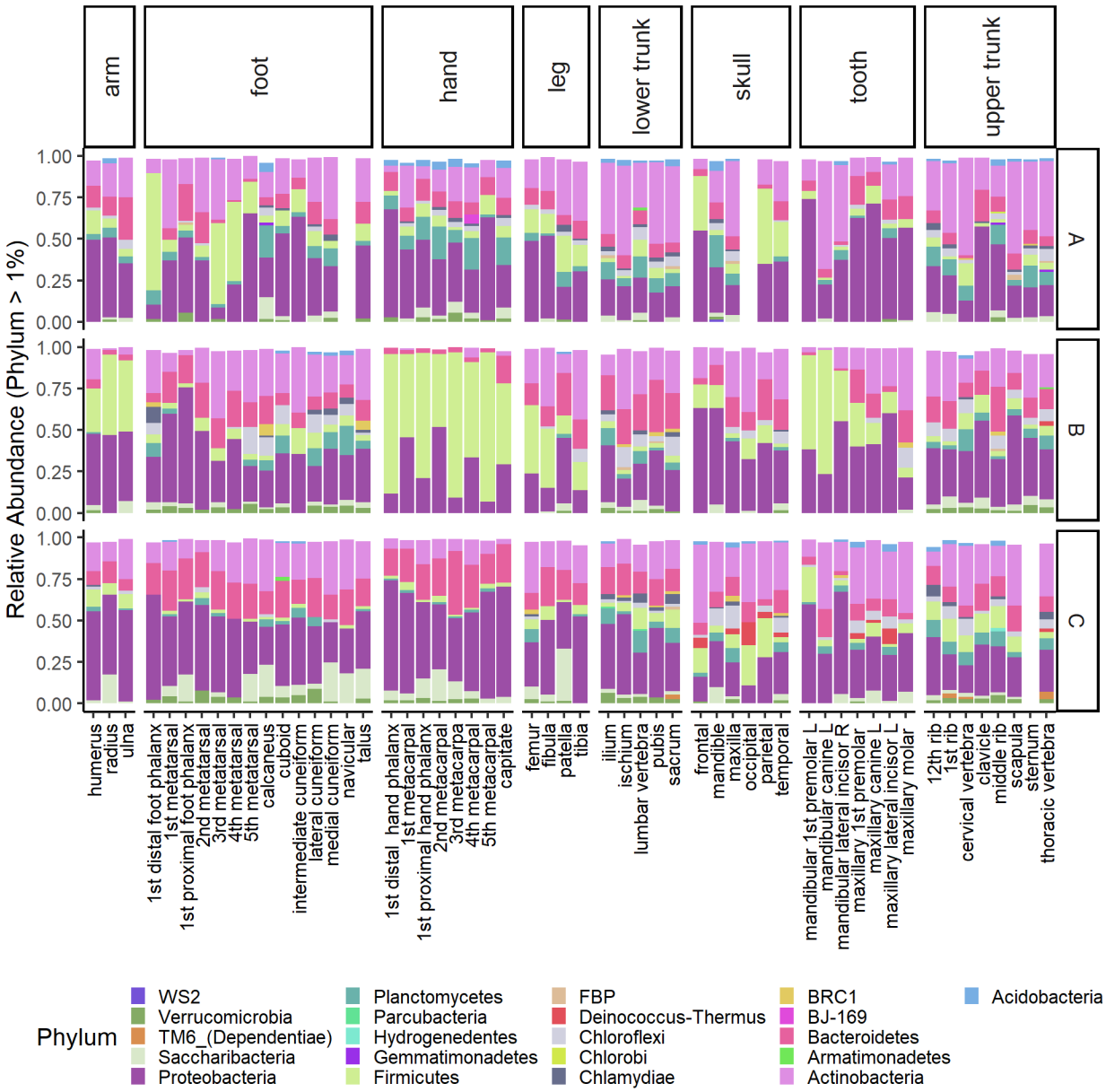

Figure S 2.11: Bacterial community phylum-level contributions visualized by individual ("A", "B", and "C") and body region (arm, foot, hand, leg, lower trunk, skull, tooth, upper trunk). Only relative abundances greater than 1% are displayed.

CHAPTER 3
INTER AND INTRA-INDIVIDUAL VARIATION IN SKELETAL DNA PRESERVATION IN BURIED REMAINS

A version of this chapter has been submitted for publication by Alexandra L. Emmons, Jonathan Davoren, Jennifer M. DeBruyn, Amy Z. Mundorff

Citation: TBD

Publication Statement:

This is a research chapter. Aspects of this research were conducted by me and others were conducted by co-authors. I analyzed most of the data and am the original and primary author of this chapter. Co-authors provided funding, guidance, conceptualization, and editing.

Abstract

Our ability to identify skeletal remains often relies on the quality and quantity of DNA extracted from bone and teeth. Current research on buried remains has been retrospective, and no study to our knowledge has comprehensively assessed both intra-individual and inter-individual variation in human skeletal DNA from all representative skeletal element types recovered from a burial. Three individuals were interred together in a single grave for four years. Following disinterment, skeletal DNA was extracted, quantified, and GlobalFiler™ results were produced from 49 bones per skeleton, representing all bone types. Multiple sites per bone were also tested to determine intra-bone variability. Co-extracted bacterial and fungal DNA were quantified to determine microbial loads in the bones. Results show that the small, cancellous bones of the feet outperformed other bones in terms of DNA yield, measured as nanograms per gram of bone powder, and STR completeness. The cuneiforms, in particular, had consistently high human DNA yields for all three individuals. DNA yield varied by individual and depth within the grave, with the shallowest individual demonstrating the highest DNA yields While the feet exhibited the greatest variation in DNA yield across bone type and sampling site, they also demonstrated some of the highest DNA yields and the most complete STR profiles, evoking a re-evaluation of their use for skeletal DNA sampling and analysis.

Introduction

DNA extracted from bone or teeth is an important source for forensic identification [1–4,169], particularly when remains are decomposed or skeletonized. Though DNA testing has become routine in forensic practice, degraded DNA, which is common with extended postmortem intervals, requires specialized expertise found at few laboratories. Additionally, skeletal DNA does not degrade evenly across the human skeleton [5,170], and because of this, skeletal selection for DNA sampling can be challenging, informed by anecdotal evidence and limited research [e.g., 7–12].

Multiple recommendations and guidelines currently exist for DNA sampling, especially in the context of disaster victim identification (DVI) [171–174], however, to our knowledge, only one guideline [i.e., 16] provides detailed DNA sampling recommendations for skeletal remains. The International Commission of Missing Persons (ICMP) [174] provides information detailing which bones should be prioritized in sampling, namely teeth followed by femora, tibiae, and pelvic bones. The ICMP also provides regional sampling guidelines for partial remains, describing which element to sample when only a particular region of the body (e.g., leg, arm, thorax, etc.) is present. Moreover, the ICMP works with remains from many different

depositional contexts, and therefore, is one of few published guidelines that considers circumstances of buried and commingled remains.

Recommendations published by ICMP [174] are based on research conducted by Hines et al. [9], which ranked osseous remains as follows: 1) teeth, 2) talus, 3) other tarsals, 4) petrous portion of the temporal bone, 5) femur, 6) vertebrae, 7) tibia, and 8) metatarsals. This study benefited from a large sample size and less biased sampling practices – earlier DNA testing generally focused only on specific bone types, ignoring small or predominantly cancellous bones such as the tarsals. Research was based on 11,650 DNA tests conducted on remains recovered from the Western Balkans (18 - 21 years post-mortem) [9]. Despite observing high DNA typing success from small foot bones, the authors recommended the sampling of dense, weight bearing bones such as the femur due to other considerations including ease of sampling, diagnostic ability, and potential for re-association when working with large commingled collections, as foot bones are notoriously difficult to re-associate to the skeleton [9].

Others have also advocated for the prioritization of weight bearing bones (i.e., the femur and tibia) in skeletal DNA sampling and testing, including earlier research conducted on remains from the former Yugoslavia [8], as well as research generated from the Armed Forces DNA Investigative Laboratory (AFDIL), which regularly processes recovered remains of missing U.S. servicemen from WWII, Vietnam, and Korea for mitochondrial DNA testing and analysis [6,7,108]. However, these studies used a sampling approach that preferentially selected dense cortical bones, leading to biased sample sizes by bone type. For example, tarsals were not included in tests by Leney [7], Edson et al. [6], or Milos et al. [8]. Extraction protocols also varied between these studies, rendering results less comparable. Differences in extraction methodologies can impact all other downstream processes and can impact final human DNA yields [77].

Small bones of the hands and feet have shown utility in specific DVI scenarios. Sample types including knee cartilage, phalanges, and metatarsals have shown efficacy in DNA testing and identification in disasters in Rio de Janeiro, Brazil, including floods, mudslides, and plane crashes. These smaller elements were easy to remove from individuals using disposable equipment; further sampling did not require large bone saws and other equipment that necessitate decontamination protocols prior to each sampling event [114,115]. Mundorff et al. [109] also observed high DNA typing success in patellae and other small bones including the tarsals and metatarsals in identifying remains recovered from the World Trade Center disaster. In a study looking at both intraindividual and interindividual variation in human skeletal DNA preservation following surface decomposition, Mundorff and Davoren [5] found that small cancellous bones, on average, yielded greater amounts of better quality DNA than larger, denser cortical bones, a pattern that held true in remains with extended postmortem intervals, up to 21 years.

The extent to which this pattern persists in a burial environment remains unclear. Nevertheless, just as the relative ease of sampling and reduced risk of contamination lends support to the use of smaller bones in certain DVI circumstances, they may additionally show utility in the case of a single individual burial or in a mass grave lacking commingling. Therefore, the purpose of this research was to understand patterns of intra-individual and inter-individual skeletal DNA preservation in a multi-individual burial and how these patterns are shaped by burial factors, including moisture and microbial loading. Microbial DNA is often co-extracted with human DNA, and microbes are often implicated as important mediators of human DNA degradation and PCR inhibition [7,8,110,175]. Because of this, quantities of human DNA were directly compared with patterns of co-extracted bacterial and fungal DNA. Moreover, for

comparability with previous research, the same full demineralization extraction procedure used by Hines et al. [9] and Mundorff and Davoren [7] was used in the present study.

Materials and Methods

Sample Site and Skeletal Processing

In February 2013, a multi-individual grave was placed at the Anthropology Research Facility (ARF) at the University of Tennessee, Knoxville (UTK) with the purpose of understanding patterns of skeletal DNA preservation in a buried environment. The grave was approximately two meters by two meters, with a depth of 0.7 meters. One female and two males (Table S3.1) with similar ages at death, who had been donated to the Department of Anthropology's Body Donation Program, were placed inside the grave stacked in a cross formation; the individual at the base of the grave (A) was oriented West to East, with her head placed in the West. The middle individual (B) was placed North to South, and the shallowest body, individual (C), was oriented West to East. Plastic mesh was placed between donors to prevent commingling. The grave was backfilled and left undisturbed until excavation and disinterment in March 2017.

During disinterment, soils were collected with depth throughout the grave and along lateral transects extending away from the grave. Two types of soil controls were also collected at depths of 0 and 0.3 m, as discussed in Keenan et al. [56]. Soil biogeochemical analyses and micro- and macro-faunal counts were conducted in the Department of Bioengineering and Soil Science and reported in Keenan et al. [56]. Mapping, including depth information, was collected via hand mapping, LIDAR scanning, and FARO 3-dimensional imaging technologies. Human remains were collected in paper bags and stored at room temperature prior to processing. Decomposition material, debris, and soil were gently removed using a soft toothbrush and warm water at the Forensic Anthropology Center (FAC). Because of adipocere formation on individual A, bones of the upper and lower torso were removed by way of dissection and then cleaned with warm water. All skeletal elements were stored in cardboard boxes for approximately 4-6 months prior to skeletal sampling.

Skeletal Selection and Sampling

To represent all skeletal types, a total of 49 bones per skeleton were selected for DNA analysis based on previous research conducted by Mundorff and Davoren [5]. The carpals were represented by the capitate only. To understand variation in human DNA quality and quantity by sample site within a single bone, 19 bones per individual were sampled at 2 different sites on the same bone, and 3 bones per individual were sampled from 3 sites. In addition, to understand variation from a single sampling site, replicate samples were collected from a single sampling site from three different sites on the same three bones for each individual (i.e., humerus, tibia, and femur) (Table 3.1). Left elements were generally sampled, with the exception of a single patella, which was sampled from the right side of the body. Elements were inventoried, marked for sampling, and photographed prior to sampling.

A Dremel® rotary tool was used to remove approximately 1-2 mm from the outer surface of each bone at the area marked for sampling. The same area was then cleaned with 10% bleach followed by 70% ethanol; bones were set to dry for a minimum of 12 hours prior to sampling. All bones were sampled in a designated clean lab facility, the Molecular Anthropology Labs at UTK. A standard drill with a 9.5 mm masonry bit was used to extract ~0.2 g of bone powder per

Table 3.1: Skeletal Sampling Strategy.

Body Region	Skeletal Element	Sample / Individual	Total DNA Samples
Skull	Frontal	1	3
	Temporal	1	3
	Maxilla	1	3
	Parietal	1	3
	Occipital	1	3
	Mandible	1	3
Upper Torso	Cervical Vertebrae	2	6
	1st Rib	2	6
	Middle Rib	2	6
	Sternum	1	3
	Clavicle	2	6
	Scapula	1	3
Lower Torso	Thoracic Vertebrae	1	3
	Lumbar Vertebrae	1	3
	11th or 12th Rib	1	3
	Sacrum	1	3
	Ilium	1	3
	Ischium	1	3
	Pubis	1	3
Leg	Femur	6	18
	Tibia	6	18
	Fibula	1	3
	Patella	2	6
Arm	Humerus	6	18
	Radius	2	6
	Ulna	2	6
Hand	Metacarpal 1	1	3
	Metacarpal 2	1	3
	Metacarpal 3	1	3
	Metacarpal 4	2	6
	Metacarpal 5	1	3
	1st Proximal Phalanx	1	3
	2nd Middle Phalanx	1	3
	1st Distal Phalanx	2	6
	Capitate	1	3

Table 3.1 (continued)

Body Region	Skeletal Element	Sample / Individual	Total DNA Samples
Foot	Metatarsal 1	1	3
	Metatarsal 2	2	6
	Metatarsal 3	1	3
	Metatarsal 4	2	6
	Metatarsal 5	2	6
	1st Proximal Phalanx	1	3
	1st Distal Phalanx	1	3
	Calcaneus	2	6
	Talus	2	6
	Navicular	2	6
	Cuboid	2	6
	1st Cuneiform	2	6
	2nd Cuneiform	2	6
	3rd Cuneiform	2	6

sample. Samples were weighed and immediately frozen using liquid nitrogen and stored at -80°C prior to DNA testing. Samples were sent to Bode Cellmark Forensics, Lorton, VA for human DNA testing including extraction, amplification, STR fragment separation, and analysis.

DNA Extraction

Skeletal DNA was extracted from ~0.2 g of bone powder using a full demineralization procedure, with the additional purification step as per Amory et al. (2012). This resulted in a total elution volume of 50 µL.

DNA Quantification

The human DNA quantification was performed on a 7500 Real-Time PCR System with the Quantifiler™ Trio system and the HID 1.2 analysis software (Applied Biosystems™). The quantification reactions were set up as half volume reactions (11.5 µl) with 2 µL of template. DNA degradation levels were assessed by dividing the quantity of DNA from the small 80 bp amplicon by that from the large 214 bp amplicon, resulting in a DNA degradation index (D.I.). The presence of PCR inhibitors was evaluated by the threshold cycle (C_T) value of the internal positive control. Quantities were normalized per gram of bone powder (ng gbp^{-1}).

The Femto™ Bacterial DNA Quantification Kit and Femto™ Total Fungal Quantification Kit (Zymo Research) were used to quantify total bacterial and total fungal DNA, respectively, per manufacturer's instructions. Samples were quantified in triplicate, while standards were measured in duplicate. At least three no template controls were included in each 96-well plate. Bacterial and fungal assays were performed in the Department of Biosystems Engineering and Soil Science at UTK on a BioRad CFX96™ Real-Time PCR Detection System. Quantities are reported as total gene abundances per gram of bone powder (gene gbp^{-1}).

Total DNA from bone was measured using the Quant-iT™ PicoGreen™ dsDNA Assay Kit (Invitrogen). The assay was performed using reduced volumes of 200 µL and measured on a 96-well microplate reader. Samples were run in duplicate, including five standards, ranging from 0 µg mL^{-1} to 1.0 µg mL^{-1}; DNA concentrations are reported as nanograms per gram of bone powder.

Short Tandem Repeat (STR) Amplification, Separation, and Genotyping

All DNA extracts were amplified on a GeneAmp 9700 system using the GlobalFiler™ PCR Amplification Kit (Applied Biosystems). The amplification was performed at 29 cycles and targeted 1 ng of input DNA, where possible, or 15 µL for samples that had less than 0.06 ng/µL. Following amplification samples were prepared for capillary electrophoresis by taking 1 µL of amplified PCR product, mixing in 0.4 µL GeneScan™ 600 LIZ® dye Size Standard v2.0 (Applied Biosystems) and 9.6 µL HiDi™ formamide (Applied Biosystems) then heating for 5 minutes at 95 degrees and placing on ice for 5 minutes. Samples were injected on an ABI3500 XL fragment analyzer and genotyped using the GeneMapper® ID-X Software v.1.5 (Applied Biosystems®) using a peak detection threshold of 125 RFU.

Data Analysis and Statistics

Human DNA yields were reported based on the measured quantity of the small autosomal target from the Quantifiler™ Trio DNA Quantification Kit; these yields per gram of bone powder were then used to establish a relative ranking of bone samples based on human DNA quantity. DNA quality was determined using the degradation index, described above. To further examine DNA quality, the percentage of recovered alleles, defined as the number of successfully amplified alleles in a sample divided by the total number of alleles possible for a given individual, was calculated by bone type for each individual and averaged across individuals. A two-factor analysis of variance test (ANOVA) was used to assess statistical differences in log transformed human DNA concentrations between individuals (A, B, and C) and body region (skull, arm, hand, upper torso, lower torso, leg, foot). Statistical assumptions including normality and homogeneity of variance were calculated using the D'Agostino Normality Test from the package fBasics (v. 3042.89) and Levene's Test from the package car (v. 3.0.2), respectively. Tukey's HSD test for multiple comparisons was used post-hoc to the two-factor ANOVA to determine group differences. Non-parametric Kruskal-Wallis tests were used to assess statistical differences in log transformed bacterial gene abundances, log transformed fungal gene abundances, log transformed total DNA concentrations, degradation indices, and the percentage of recovered alleles between individuals and body regions. Conover's test for multiple comparisons was used as a post-hoc to Kruskal-Wallis using the package PMCMR (v. 4.3) to determine group differences; a Bonferroni correction was applied to reduce the effects of type I error. All analyses were performed in R v. 3.5.0 [146].

To develop a sampling rank order of bones similar to Mundorff and Davoren [7], the mean DNA yield by bone type was calculated, and means were sorted by the percentage of STRs recovered followed by human DNA concentration, thereby considering both the quantity and quality of recovered human DNA rather than quantity alone.

The average relative florescent units (RFUs) per allele were also assessed as an additional indicator of STR quality. The RFU per allele was calculated as the sum of the heterozygous peak heights and homozygous peak heights divided by the total of successfully amplified alleles.

Results

Decomposition State

The individuals were stacked in a single grave, which resulted in disparate states of decomposition relative to depth. Upon disinterment, the lower portion of the grave was saturated with water, however, at the time of internment the water table had not been reached. Individual C, which was closest to the ground surface (shallowest) was skeletonized with no adipocere and little soft tissue present (Figure 3.1A). The middle body, Individual B, was partially skeletonized, with adipocere and some skin and soft tissue present, especially in the upper torso, hands, and feet (Figure 3.1B). The deepest body, Individual A, was the least decomposed due to extensive adipocere formation. The upper and lower torso including the proximal one third of the femora and humeri, exhibited pinkish decomposing muscle tissue encased in skin and adipocere; the hands, feet, and lower segments of the arm (radius and ulna) and leg (tibia and fibula) were mostly skeletonized with minimal amounts of soft tissue or adipocere. The skull was primarily skeletonized, with preserved brain tissue (Figure 3.1C).

DNA by individual and body region

Human DNA yield and total DNA concentrations were significantly different between individuals (Human: DF = 2, $F = 6.93$, $p = 0.001$; Total: DF = 2, $X^2 = 16.0$, $p < 0.001$) and body region (Human: DF = 6, $F = 15.437$, $p < 0.001$; Total: DF = 6, $X^2 = 41.4$, $p < 0.001$), with human DNA yield exhibiting a significant interaction effect (Human: DF = 12, $F = 2.21$, $p = 0.01$). Individual C had greater quantities of human DNA than either A ($p = 0.001$) or B ($p < 0.05$), while individual A had significantly lower total DNA concentrations than either C ($p < 0.001$) or B ($p = 0$ .001) (Figure 3.2A; Table S3.2). Human DNA concentrations from the foot were significantly greater than all body regions except for the lower torso ($p < 0.001$), while human DNA concentrations of the arm were significantly lower than human DNA concentrations from all body regions except the head ($p < 0.01$) (Figure 3.3A-3.3B). Similarly, total DNA concentrations in the arm were significantly lower than total DNA concentrations from all other body regions, again, excluding the head ($p < 0.05$) (Figure 3.3C-3.3D).

Degradation indices significantly differed by individual (DF = 2, $X^2 = 93.9$, $p < 0.001$) (Figure 3.2E); human DNA from individual B was significantly more degraded than human DNA from A ($p < 0.001$) or C ($p < 0.001$) (Table S3.2). The occipital and the first proximal phalanx of the hand from B had much higher degradation indices than all other bones (Figure S3.1).

Bacterial gene abundances were significantly different by individual (DF = 2, $X^2 = 52.3$, $p < 0.001$) and body region (DF = 6, $X^2 = 18.2$, $p < 0.01$), though the only regions that were significantly different were the hand and the arm ($p < 0.01$). The hand, on average, had greater 16S rRNA gene copies (Figure 3.3E-3.3F). Fungal gene abundances were neither significant by individual ($p > 0.05$) nor body region ($p > 0.05$) (Figure 3.2C). Neither bacterial DNA nor fungal DNA were significant predictors of human DNA concentrations when tested using linear regression ($p > 0.05$).

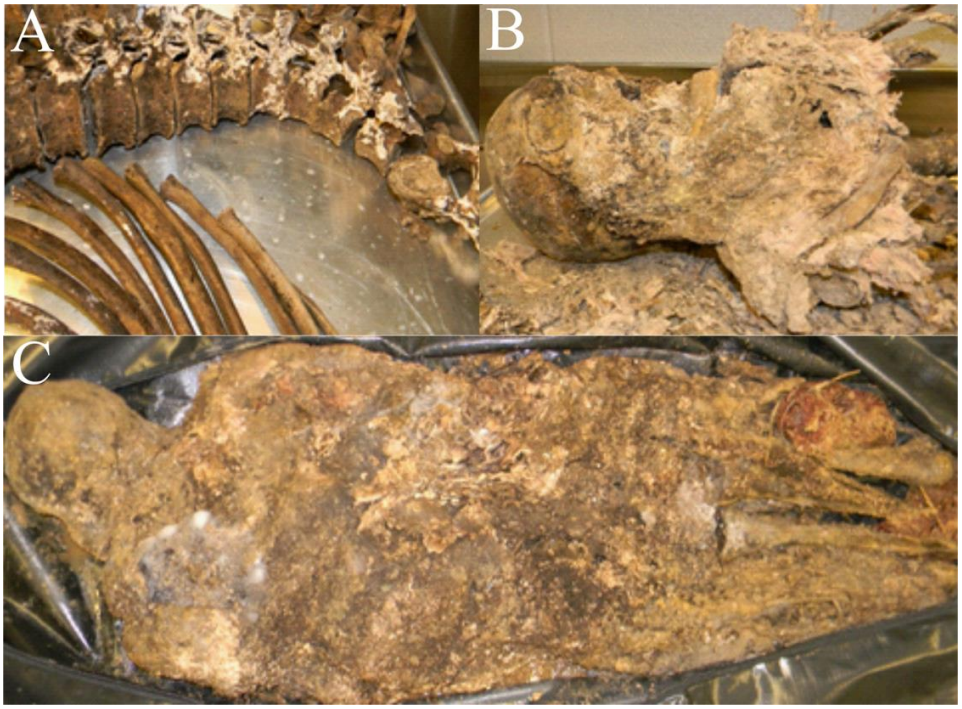

Figure 3.1: **Adipocere formation and soft tissue preservation on disinterred remains. (A) Individual C was mostly skeletonized with minimal amounts of adipocere present on the hands, feet, and vertebral column. (B) Individual B had moderate soft tissue preservation and adipocere development, especially on the torso. (C) Individual A exhibited extensive adipocere formation; a hard shell formed with underlying preserved tissue. A bloom of white fungus can be seen in the image that occurred upon storage in a walk-in cooler (~2ºC).**

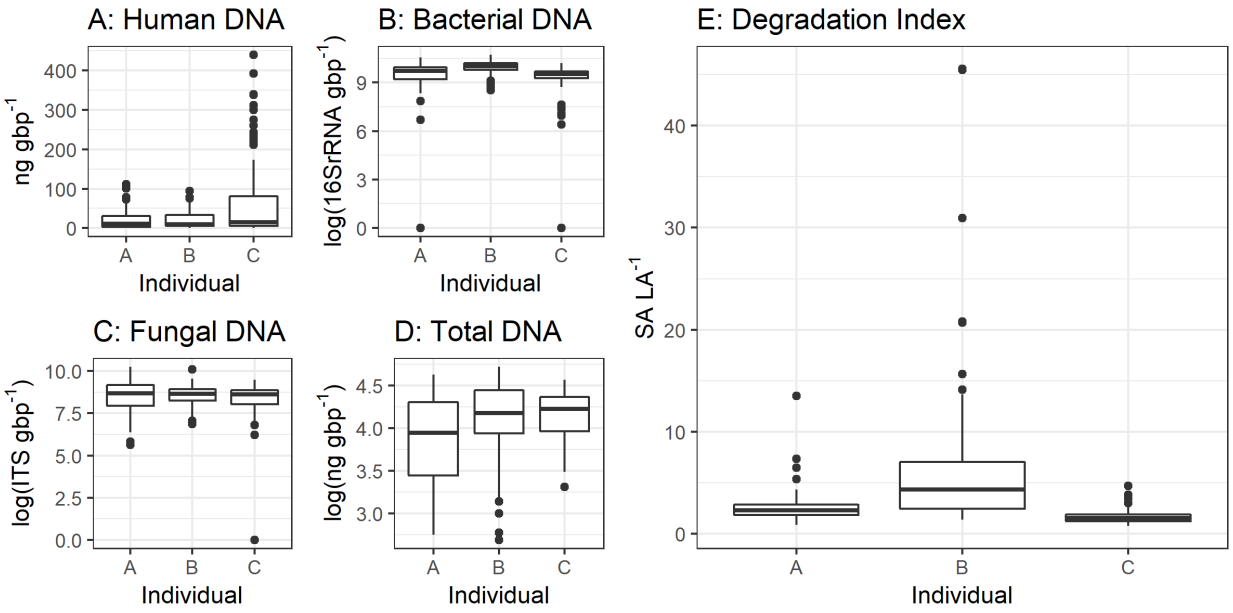

Figure 3.2: DNA quantitation by individual. (A) Human DNA concentration by individual. (B) Bacterial and (C) fungal gene abundances by individual. (D) Total DNA concentration by individual. (E) Degradation Index, as the ratio between the small human autosomal target (SA) and the large human autosomal target (LA) by individual.

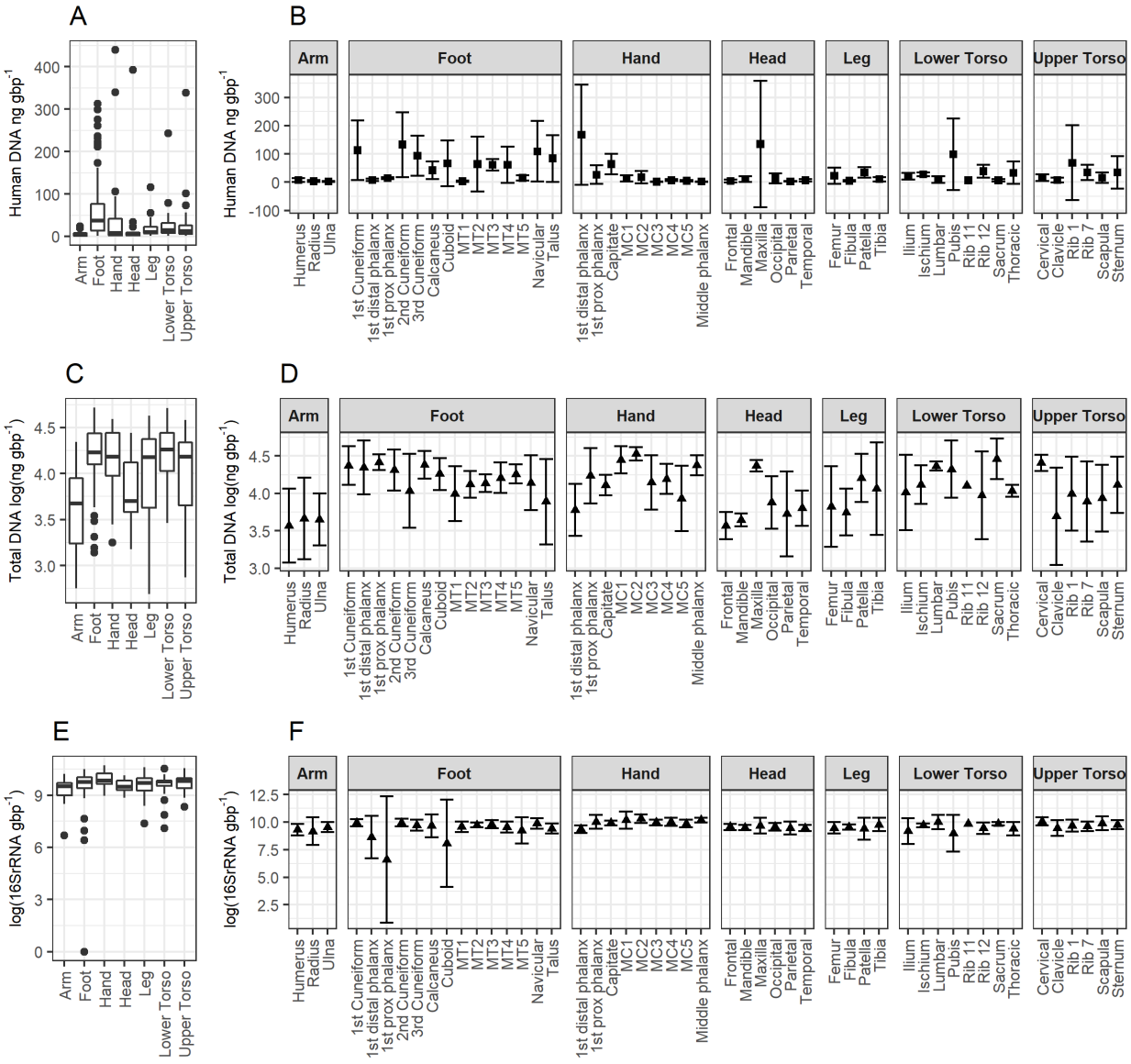

Figure 3.3: **DNA quantitation by body region**. **(A) Human DNA concentrations by body region (B) Human DNA concentrations averaged by bone across individuals and visualized by body region. (C) Total DNA concentrations by body region. (D) Total DNA concentrations averaged by bone across individuals and visualized by body region. (E) Bacterial gene abundances by body region. (F) Bacterial gene abundances averaged by bone and visualized by body region. Error bars indicate standard deviation.**

PCR Inhibition

Samples were minimally affected by PCR inhibition; only a single sample, from the proximal tibia of individual B, had a threshold cycle (C_T) value of greater than 30 for the internal positive control.

Multi-Site Differences in Human DNA

Human DNA concentrations varied by site on a single bone (Figure S3.2). The maximum difference in human DNA concentration for individual A between sampling sites on a single bone, when only two sampling sites were considered, was 83.23 ng gbp^{-1} for the 2nd cuneiform. In contrast, the minimum difference in human DNA concentration was observed in the radius (0.2803 ng gbp^{-1}), which was sampled at the distal end and at the midshaft. The ulna also showed only a small difference (< 1 ng gbp^{-1}) between proximal and midshaft sampling sites for individual A. These patterns in the ulna and radius were consistent for individuals B and C. For individual B, the maximum difference in human DNA concentration by sampling site was observed in the calcaneus (66.00 ng gbp^{-1}), while in C, the maximum difference was found for rib 1 (326.8 ng gbp^{-1}). The middle rib of individual A also showed a large difference in human DNA concentration between sampling sites at the center and vertebral end (65.09 ng gbp^{-1}), with the center having a larger concentration of human DNA; the opposite was observed in rib 1 of C; the vertebral end had a much larger concentration than the center.

When considering bones that were sampled from three sites (i.e., humerus, femur, and tibia), human DNA concentrations varied the greatest by sample site in the femur (Figure 3.4). The head of the femur had higher concentrations of human DNA than the midshaft or distal end for all individuals. Variation in human DNA concentration within a single sample site was generally low (standard deviation < 5.0 ng gbp^{-1}), with the exception of the femoral heads of C and A, the superior articular facet (tibial plateau) of the tibia of B, the humeral head of C, and the midshaft of the tibia of B. Approximately 66.7% of sites sampled twice at the same site, had a standard deviation less than 2.0 ng gbp^{-1}, and 44.4% of sites with multiple sampling events had a standard deviation less than 1.0 ng gbp^{-1}. Total DNA concentrations were variable by sampling site in the humerus, femur, and tibia. Total DNA was greater in both the humeral and femoral heads compared with their respective midshaft and distal end.

The degradation index (D.I.) demonstrated the greatest variation in the humerus, femur, and tibia of individual B, with the greatest degradation index noted for the femoral head of B. The degradation index also varied within a single sampling site, with the greatest variation noted in the femoral head and superior articular facet of the tibia in B.

STR Analysis

While the percentage of STRs recovered did not significantly differ by individual, they did significantly differ by body region, when data from all individuals were combined (DF = 6, F = 4.997, p = 7.9e-05), which following post-hoc analysis, was influenced by the arm. The arm had the poorest STR recovery rate (mean: 73.1%, Std. Dev.: 22.58 %); this was significantly lower than all other body regions ($p < 0.01$), except for the head and the lower torso (Table 3.2; Figure 3.5). The foot was the most successful body region, with the highest STR recovery rate (mean 94.15%, Std. Dev.: 16.33%) even though, the 1st distal phalanx of the foot consistently performed poorly across all three individuals (Figure 3.4). Intra and inter-locus balance and RFUs/allele were also greatest in the foot (Min:max: mean 81.34%, Std. Dev. 5.89%; RFUs/allele: Mean 3357.07 RFU, Std. Dev. 1840.26 RFU) (Table 3.2).

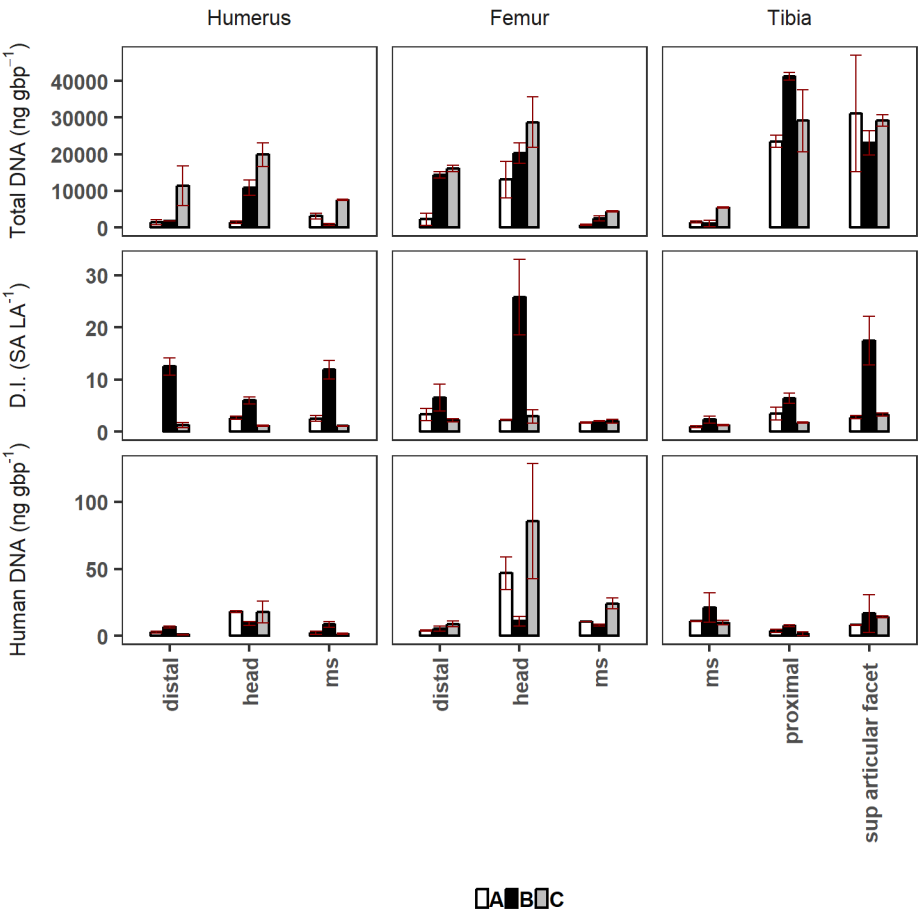

Figure 3.4: Intra-bone variation and variation in technical replicates in total DNA, degradation index (D.I.) and human DNA for the humerus, femur, and tibia. Sampling sites are on the x-axis; "ms" refers to the mid-shaft, while "sup" refers to superior. The superior articular facet of the tibia is synonymous with the tibial plateau. "A", "B", and "C" are the individuals sampled.

Table 3.2: **Mean STRs recovered (%) and mean RFUs/allele by body region**

Body Region	STR (%)	Std. Dev.	RFUs/allele	Std. Dev.
Arm	73.10	22.58	1124.43	1338.73
Foot	94.15	16.33	3357.07	1840.26
Hand	90.24	17.38	2148.45	1502.46
Head	87.79	19.57	1568.67	1477.16
Leg	89.44	17.54	1980.71	1294.20
Lower Torso	86.10	21.90	2095.41	1359.26
Upper Torso	91.73	17.65	2755.39	1809.47

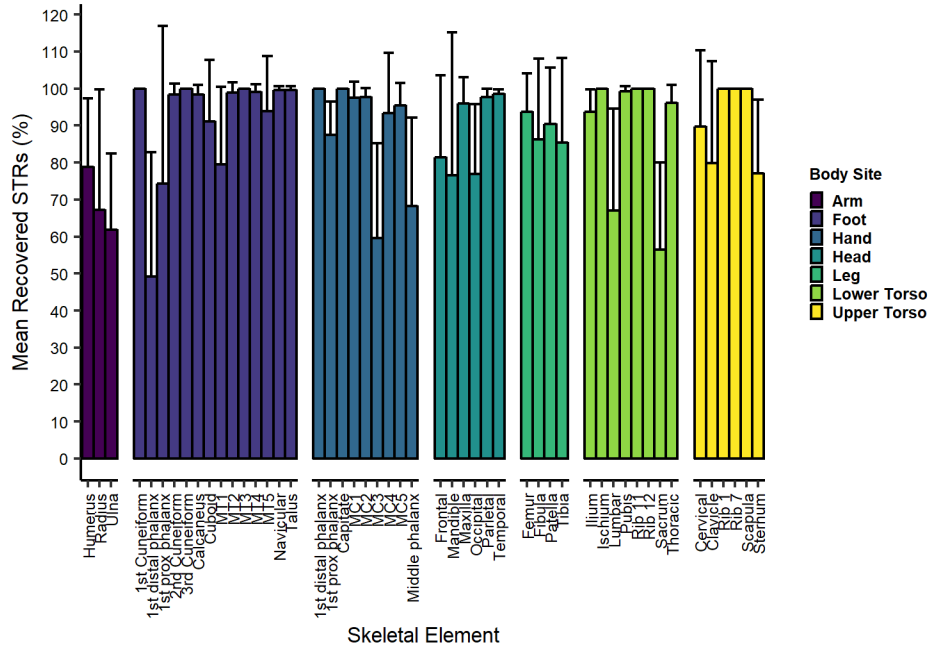

Figure 3.5: Mean STR recovery (%) by bone type across three individuals (n=3).

Several samples (26.3%; 65 out of 247) contained contaminant peaks or other artifacts within resulting STR profiles. The following autosomal STR loci showed artifact/contaminant intrusion: SE33, vWA, D13S317, TPOX, D2S1338, D3S1358, D18S51, D8S1179, TH01, D19S433, and DYS391. While the origin of these peaks remains unknown, at least two have been characterized as known GlobalFiler™ artifacts (GlobalFiler™, Applied Biosystems, Carlsbad, CA) (Figure 3.6). Bones of the foot were impacted the most by contaminant intrusion.

Discussion

Individuals in this study showed significant differences in mean human DNA concentrations. Therefore, a rank order of skeletal elements by percentage of STRs recovered and human DNA concentration was created by individual, with the top ten highest scoring bones (Table 3.3). Using STR completeness and human DNA yield as criteria, the cuneiforms exhibited the best performance; the 1st cuneiform and 3rd cuneiform ranked among the top ten highest performing bones for all individuals, while the 2nd cuneiform ranked high for at least two individuals (Table 3.3). In fact, foot bones occupy nearly half of the top ranked bones, with 5/10, 4/10, and 7/10 for individuals A, B, and C, respectively. Other top-ranking bones were from the hand and upper and lower torso, with a rib and a hand bone ranked in the top 10 for each individual; of these, only the capitate was observed among the top-ten highest ranking bones across more than one individual. *Not a single long bone ranked in the top 10 for any individual.* Though human DNA concentrations were fairly variable by sample site in bones of the feet, similar to Mundorff and Davoren [5] the quantity and quality of human DNA recovered from bones of the feet, on average, were much higher than bones from other regions of the body.

Small bones of the feet have also performed well in other research [9,109]. A previous microscopic analysis from surface remains indicated that this may be due to the survival of remnant tissues, including those of hematopoietic origin [107]. Bones of the feet are weight bearing and because of this undergo extensive bone remodeling, not only because these bones experience external force more directly but also because they are impacted by high levels of pressure from interstitial fluids [176]. While this would certainly increase hematopoiesis in the feet, remodeling is also likely to result in the release of DNA into the newly forming bone matrix with the cyclical cell death of osteoclasts and osteoblasts with continual bone destruction and formation, as first speculated by Campos et al. [77]. Unlike hematopoietic tissue, released DNA into the surrounding matrix during bone remodeling would be more likely to confer protection following death. Alternatively, there could be something unique about foot microbial communities that results in a greater degree of skeletal DNA preservation. If enteric gut microbes are major players in skeletal preservation as previously suggested [82], the increased distance from the gut may relate to skeletal DNA survival. In addition, bones of the feet, as well as being exposed to mechanical stress, have less tissue biomass in life than other bones of the body. Because of this, they are prone to mummification rather than decomposition, conferring a level of protection exposed bones do not benefit from [20]. This would not only impact microbial motility but would also likely encourage the formation of specific postmortem microbiome, with a greater influence from soil taxa.

The temporal bone was not among the top ten highest ranking bones for any single individual, which may be in part due to the location of sampling in the present study, above the external auditory meatus. Though human DNA yields from sampled temporal bones were low, unlike other cranial bones, the temporal bone resulted in complete and nearly complete STR

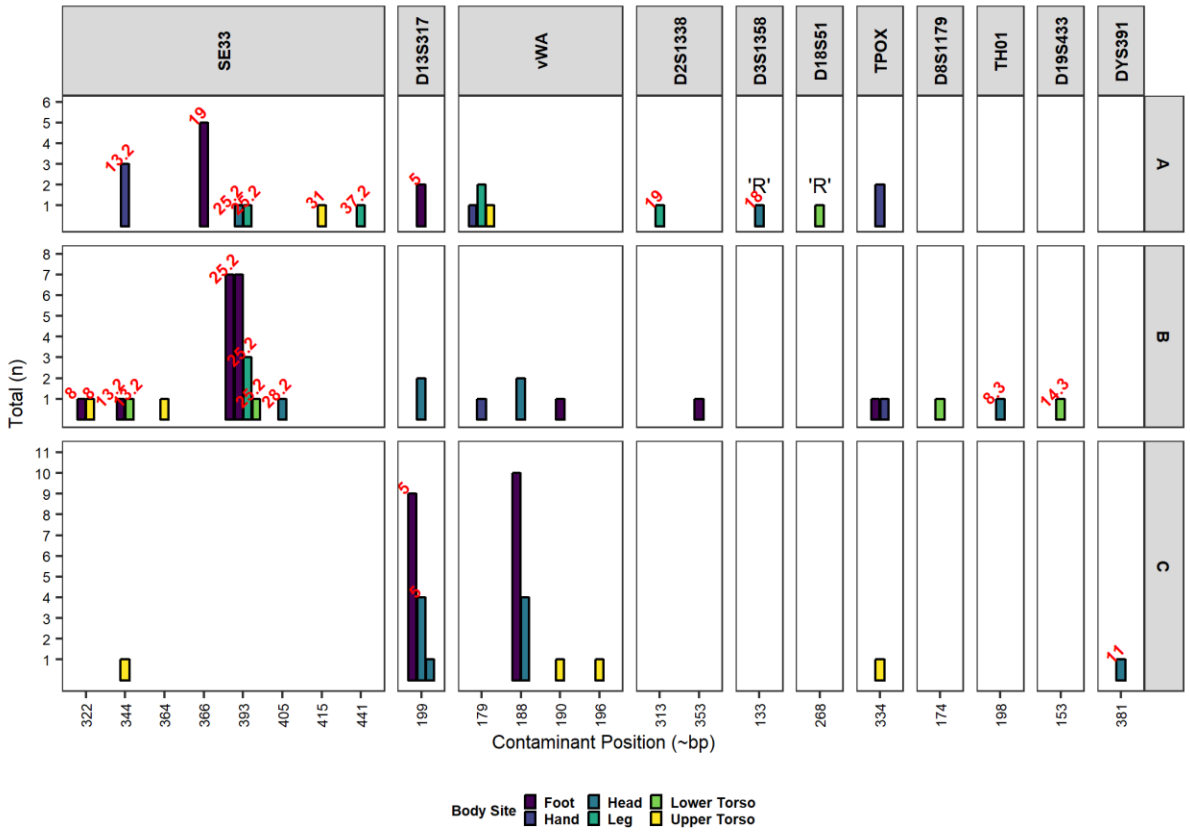

Figure 3.6: Number of artifacts and contaminants present in STR profiles by body region and individual. "R" refers to reported artifacts known to the GlobalFiler™ kit. Resulting STR repeat lengths are reported in red; positions without red size indicators were "off-ladder".

Table 3.3: Rank order of skeletal elements by % STR recovered and human DNA (ng gbp^{-1})

Individual	*Body Region*	*Bone*	*Bacterial log(gene gbp^{-1})*	*Std. Dev.*	*Fungal log(gene gbp^{-1})*	*Std. Dev.*	*Human (ng gbp^{-1})*	*Std. Dev.*	*Total log(ng gbp^{-1})*	*Std. Dev.*	*D.I.*	*Std. Dev.*	*STR (%)*	*Std. Dev.*
A	Upper Torso	Sternum	9.40	NA	5.82	NA	101.39	NA	3.68	NA	2.30	NA	100.00	NA
A	Lower Torso	Thoracic	9.80	NA	10.25	NA	78.57	NA	3.96	NA	4.17	NA	100.00	NA
A	Foot	2nd Cuneiform*	10.04	0.18	9.45	0.05	69.48	58.85	4.43	0.06	4.46	2.85	100.00	0.00
A	Foot	MT3*	10.03	NA	8.34	NA	69.24	NA	4.17	NA	2.25	NA	100.00	NA
A	Lower Torso	Rib 12	9.09	NA	6.69	NA	55.03	NA	3.56	NA	3.75	NA	100.00	NA
A	Hand	Capitate*	9.77	NA	7.37	NA	49.18	NA	4.03	NA	3.02	NA	100.00	NA
A	Foot	1st Cuneiform**	9.77	0.07	9.17	0.03	47.44	3.29	4.29	0.22	1.78	0.38	100.00	0.00
A	Lower Torso	Pubis	9.74	NA	8.20	NA	43.61	NA	3.88	NA	2.15	NA	100.00	NA
A	Foot	3rd Cuneiform**	10.03	0.06	8.87	0.39	43.54	11.17	4.23	0.12	2.54	0.22	100.00	0.00
A	Foot	Navicular	9.58	0.51	8.62	0.16	40.09	16.29	3.78	0.43	2.03	0.53	100.00	0.00
B	Hand	1st distal phalanx*	9.73	0.14	8.45	0.08	75.88	25.63	4.03	0.09	1.73	0.10	100.00	0.00
B	Foot	3rd Cuneiform**	10.08	0.04	8.70	0.03	56.30	8.11	4.45	0.10	9.57	3.97	100.00	0.00
B	Foot	1st Cuneiform**	10.35	0.15	8.68	0.06	44.90	11.87	4.66	0.08	3.45	0.63	100.00	0.00
B	Hand	MC2	10.55	NA	9.05	NA	42.21	NA	4.59	NA	2.63	NA	100.00	NA
B	Foot	MT3*	9.97	NA	8.67	NA	38.58	NA	4.23	NA	2.77	NA	100.00	NA
B	Hand	Capitate*	10.18	NA	7.27	NA	37.04	NA	4.02	NA	1.60	NA	100.00	NA

Table 3.3 (continued)

Individual	*Body Region*	*Bone*	*Bacterial log(gene gbp^{-1})*	*Std. Dev.*	*Fungal log(gene gbp^{-1})*	*Std. Dev.*	*Human (ng gbp^{-1})*	*Std. Dev.*	*Total log(ng gbp^{-1})*	*Std. Dev.*	*D.I.*	*Std. Dev.*	*STR (%)*	*Std. Dev.*
B	Lower Torso	Ischium	9.78	NA	8.96	NA	31.74	NA	4.27	NA	1.82	NA	100.00	NA
B	Lower Torso	Ilium	9.90	NA	7.60		30.28	NA	4.12	NA	2.26	NA	100.00	NA
B	Upper Torso	Rib 7	10.05	0.13	7.93	0.56	24.73	20.96	4.18	0.05	1.65	0.12	100.00	0.00
B	Hand	MC1	10.66	NA	9.32	NA	23.33	NA	4.57	NA	3.33	NA	100.00	NA
C	Head	Maxilla	8.86	NA	7.48	NA	392.86	NA	4.29	NA	1.32	NA	100.00	NA
C	Hand	1st distal phalanx*	9.00	0.06	7.98	0.11	390.00	70.71	3.96	0.06	1.93	0.59	100.00	0.00
C	Foot	2nd Cuneiform*	9.55	0.06	8.67	0.06	272.40	56.21	3.98	0.05	1.44	0.18	100.00	0.00
C	Foot	1st Cuneiform**	9.68	0.14	9.17	0.15	246.56	40.21	4.16	0.08	1.55	0.22	100.00	0.00
C	Foot	Navicular	9.64	0.03	9.05	0.27	236.28	89.33	4.17	0.12	1.57	0.24	100.00	0.00
C	Foot	3rd Cuneiform**	9.08	0.05	8.19	0.44	180.82	44.02	3.43	0.16	1.41	0.12	100.00	0.00
C	Foot	Talus	9.40	0.00	8.88	0.30	179.55	80.63	4.17	0.09	1.80	0.41	100.00	0.00
C	Upper Torso	Rib 1	9.87	0.03	9.08	0.35	174.92	231.08	4.35	0.16	1.99	1.12	100.00	0.00
C	Foot	MT2	9.51	0.04	8.59	0.15	153.18	152.30	4.07	0.24	1.46	0.14	100.00	0.00
C	Foot	Cuboid	9.22	0.28	8.66	0.33	149.20	103.82	4.15	0.03	1.52	0.52	100.00	0.00

**Shared across two individuals. **Shared across all three individuals.*

profiles; two individuals demonstrated drop-out of a single allele, while the third individual had a complete (100%) STR profile. In addition, the degradation index remained below 2 for all three individuals, and in A and B, the temporal bone was among the top ten highest performing bones based solely on the degradation index. The petrous portion of the temporal bone has shown exceptional preservation in ancient DNA research, which has been ascribed to its increased density, the greatest of any bone, which is required to protect the inner ear [15,116,118,119]. In relatively modern contexts, the petrous portion has shown greater DNA typing success than other cranial bones when testing for mtDNA [108] and was ranked highly, prioritized after tarsals, when considering nuclear DNA typing using STRs [9]. While the petrous portion of the temporal bone may yield high quality DNA from forensically relevant remains, more research is needed to determine its utility for decreased time intervals (<20 years) and various contexts.

As supported across multiple studies [5,6,8,9,109], bones of the arm and skull, with the exclusion of the maxilla from individual C, yielded the poorest human DNA results, with low concentrations and reduced quality scores. Bones of the leg, including the femur and tibia, were not among the highest-ranking skeletal elements. Interestingly, the midshaft of the femur did not produce the highest human DNA yields, rather the femoral head, which is more cancellous and likely contains more hematopoietic tissue, resulted in the greatest human DNA yields from the femur in all three individuals. Taken together, these results have implications for skeletal sampling from buried remains. First, for graves containing a single individual or multiple individuals who are not commingled, tarsals should be prioritized over other bones for DNA sampling and analysis. Moreover, if the femur is sampled, and the postmortem interval is under five years, and the femoral head is intact without exhibiting evidence of degradation, the femoral head should be prioritized for DNA sampling over the femoral midshaft.

While individuals were placed in the same grave to minimize the effects of differential environments, their differences in decompositional states were likely influenced by depth within the burial, environmental and enteric microbes, and hydrolytic enzyme activity. The deposition environment is an important predictor of skeletal degradation and skeletal DNA degradation; low temperature, moisture, and microbial activity favor skeletal DNA preservation, while the opposite, including drastic environmental fluctuations, promote DNA degradation [97,135,137]. Because individuals were stacked, bones from each individual spanned multiple depths. Individual C was first observed at approximately 27 cm below surface (FARO) and extended to a depth of 55 cm (hand measurement); remains from individual B spanned 34 cm and 62 cm, while individual A spanned between depths of 42 cm and 62 cm (Figure S3.4). Depth is an important indicator of microbial composition, structure, and function, related to changes in edaphic features including soil composition, oxygen availability, carbon source, temperature, moisture, etc. [177,178]. Human DNA concentrations did not correlate with microbial gene abundances; though, this may have been influenced by a delay between the time at which the remains were disinterred and the time at which the bones were sampled for DNA. Also, the quantity of microbes able to colonize bone may be of little importance; rather, changes in community composition and microbial interactions, may be more indicative of human DNA preservation in buried remains.

In a separate study, we examined changes in soil geochemistry within the grave, including pH, moisture, microbial respiration, dissolved organic carbon, dissolved organic nitrogen, and extracellular enzyme potentials, among others [56]. Despite observing high concentrations of labile organic sources including dissolved organic carbon and nitrogen at the grave base (70-75 cm), likely as pooled inputs from all three sets of remains, shifts in enzyme

potentials – including increases in N-acetyl-β-glucosamindase and decreases in phosphodiesterase and leucine aminopeptidase – indicate a more recalcitrant functionality for microbial communities closer to the grave base. This activity was likely mediated by oxygen availability, with the base of the grave saturated, anoxia was prevalent here; in contrast, at 40 cm and above the saturated zone, soils were oxic. In addition, potential collagenase activity, as an indicator of collagen degradation, which makes up a large portion of the organic content of bone, demonstrated increased concentrations at depths of 30 and 40 cm, indicating an increase in potential collagen degradation [56]. Collagen degradation facilitates release of bound DNA from either collagen fibrils or hydroxyapatite [11,77], which is why collagen degradation has been used as an indicator for skeletal DNA degradation [78,96,170].

Together, these observations would lead us to expect lower human DNA concentrations in the bones of C and B than in the bones of A, yet paradoxically, we saw significantly greater human DNA concentrations in C, the only fully skeletonized individual. The probable cause of this pattern is the increase in moisture with depth in the grave; the base of the grave was completely saturated at the time of excavation, and several elements from A and B were submerged. Water can be devastating to skeletal preservation [96,179]. Increased moisture encourages microbial growth, though complete saturation deters growth [30]. Moreover, water augments dissolution of the inorganic component, hydroxyapatite, of bone and the subsequent degradation of the organic component, collagen, releasing bound DNA from both the hydroxyapatite [76,77,179] and mineralized collagen fibrils [77]. With completely submerged bones, the possibility of leaching of nucleic acids into the external environment cannot be ignored, as nucleic acids are soluble in water [179], and the fluctuation of the water table and hydraulic potential of the burial in this study over time remain unknown. DNA from non-mineralized osteoid containing osteoblasts, osteoclasts, and bone lining cells [77], is likely consumed early in the decomposition process by colonizing microbes, due to ease of access, and likely is not the primary source of skeletal DNA in this study.

Conclusion

The present study indicates that bones of the feet should be considered as priority sources for skeletal DNA sampling and analysis from buried non-commingled remains. While the sample size in the current study was small, the patterns observed align well with those in previous research [5,9,109]. Though bones of the feet may be more challenging to re-associate in cases of commingled individuals, there are other circumstances in which this would not be problematic, such as the case of a single-person burial or multiple person burial without commingling. Moreover, we acknowledge that the mechanism(s) of skeletal DNA preservation likely shift(s) with time, as does the diagenetic profile of bone [78], and so the observed patterns may not be reflective of postmortem intervals greater than four years. However, patterns from surface and buried remains suggest otherwise [5,9].

Funding

This project was supported by Award No. 2016-DN-BX-0178, awarded by the National Institute of Justice, Office of Justice Programs, U.S. Department of Justice. The opinions, findings, and conclusions or recommendations expressed in this article are those of the authors and do not necessarily reflect those of the Department of Justice.

Acknowledgements

We would like to thank DeBruyn and Mundorff lab members and faculty/staff at the Forensic Anthropology Center for guidance and assistance with the excavation process. We would also like to thank Katie Corcoran and Christina Malone for collecting LIDAR and FARO scans of the grave. Lastly, we would like to thank the donors, without whom this research would not be possible.

Appendix II

Table S 3.1: Donor information

Individual	Weight (kg)	Manner of Death	Sex	Position in Grave
A	60.3	Natural/Cervical Cancer	Female	Bottom
B	70.8	Natural	Male	Middle
C	51.7	Cardiac Arrest/ End stage Lung Cancer	Male	Top

Table S3.2: **Summary statistics (Human DNA, Total DNA, and Degradation Index)**

	Human DNA (ng gbp^{-1})			***Total DNA (log(ng gbp^{-1}))***			***Degradation Index (SA LA^{-1})***		
	Mean	**Min.**	**Max.**	**Mean**	**Min.**	**Max.**	**Mean**	**Min.**	**Max.**
A	20.79	0.454	111.1	3.841	2.752	4.627	2.762	0.8677	13.51
B	20.74	0.477	94.00	4.094	2.692	4.719	6.899	1.369	45.56
C	71.89	0.675	440.0	4.145	3.312	4.565	1.712	0.790	4.721

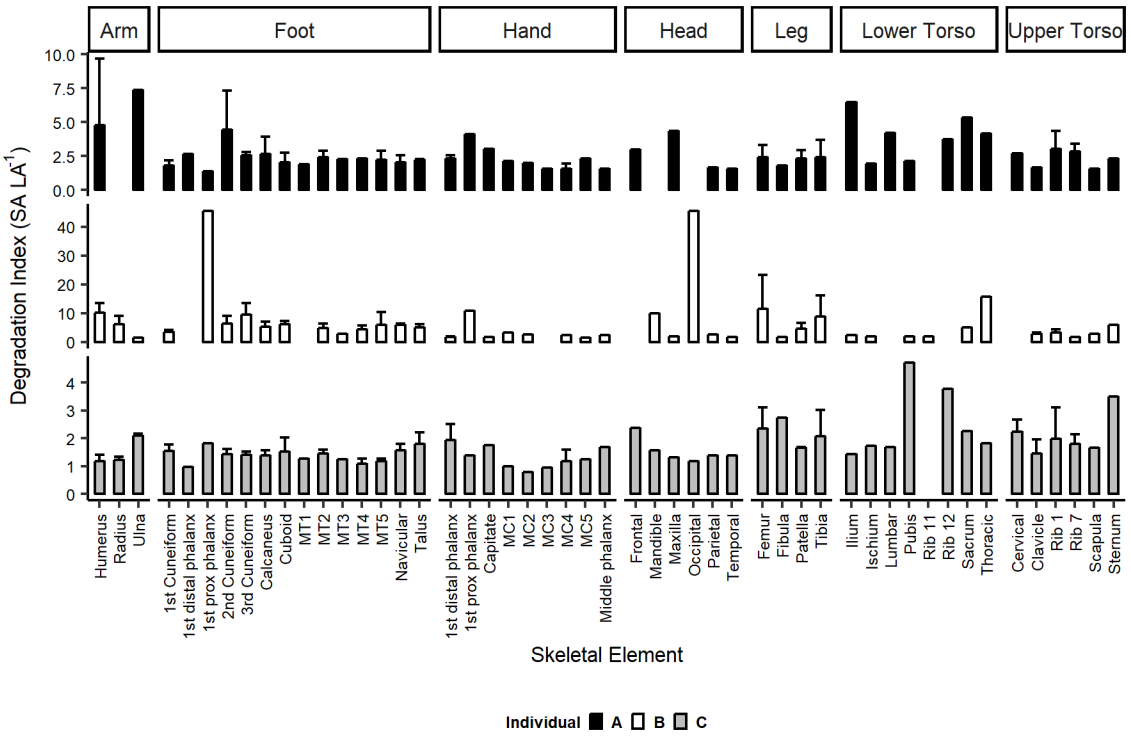

Figure S 3.1: Degradation index by skeletal element. The degradation index was calculated by dividing the concentration of the small human autosomal target (SA in ng gbp^{-1}) by the concentration of the large human autosomal target (LA in ng gbp^{-1}) and averaging by skeletal element. Results were separated by individual; error bars are present only for bones with more than one sample per individual and represent standard deviation.

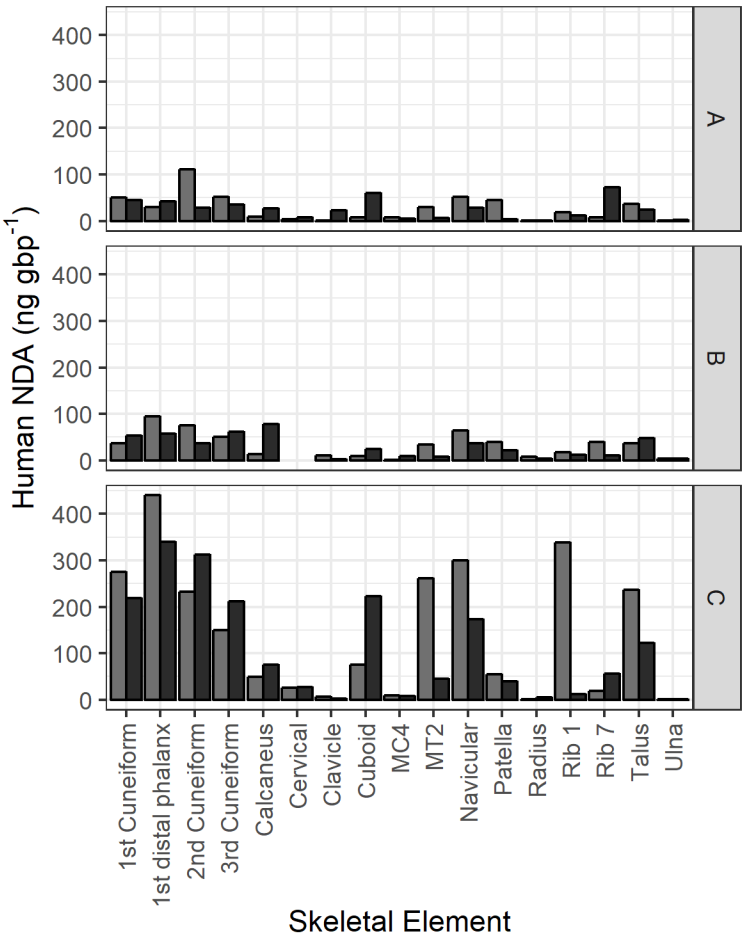

Figure S 3.2: **Multi-site differences in human DNA yield (ng gbp^{-1}). Bones were sampled from two sample sites, represented by grey and black, from three individuals "A", "B", and "C". Human DNA was normalized to nanograms per gram of bone powder (gbp).**

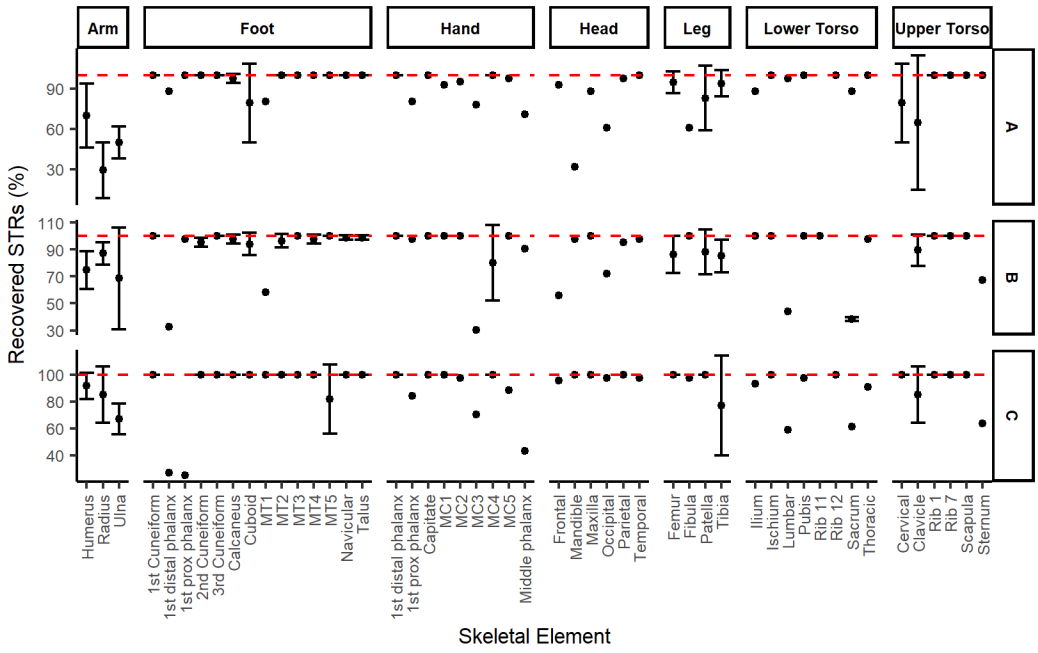

Figure S 3.3: Mean short tandem repeat (STR) recovery (%) by bone type for each individual (A, B, C).

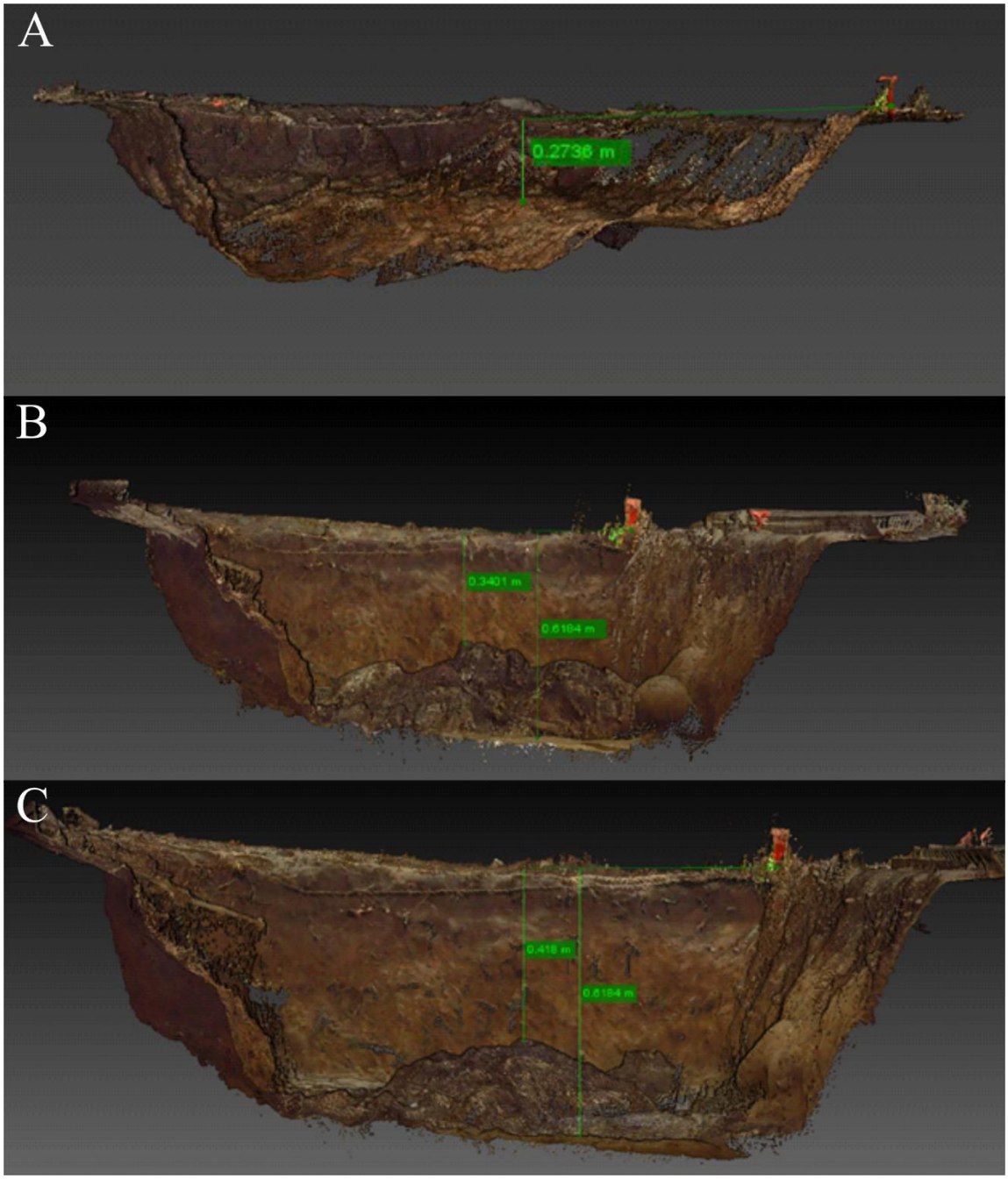

Figure S 3.4: **FARO depth profile by individual. (A) Top individual (Individual C), (B) Middle individual (Individual B), and (C) Bottom individual (Individual A). Measurments in green indicate the span of depths by individual. Individual C only has a single measurement, the depth at which bone was first uncovered, because a second scan was not able to be taken when this individual was fully uncovered.**

CHAPTER 4
THE POST-MORTEM BONE MICROBIOME: IMPLICATIONS FOR DNA SURVIVABILITY IN BURIED REMAINS

Abstract

Bone is a type of ecological input capable of supporting a dynamic ecosystem of both microscopic and macroscopic scavengers and other incidental taxa, which influence its survivability over time. Previously, we identified key taxa associated with patterns of bone DNA survivability in surface remains using random forest modeling, but models were only minimally effective, complicated by intra-individual and inter-individual variation in bone microbial communities. Subsurface skeletal preservation is modulated by the grave geochemical environment and microbial ecology and is less amenable to environmental perturbations that result in microbial community dispersion. In this study, we examined differences in microbial community composition and structure between surface and buried remains and used these differences to identify potential bone degraders related to human skeletal DNA survival. Bacterial and archaeal communities were sequenced using 16S rRNA gene amplicon sequencing of DNA extracts from 256 bone samples and 27 soil samples. Sequences were compared to previously sequenced surface bone samples and freely available, human-gut associated samples from the American Gut Project. Random forest modeling was used to predict amplified sequence variants (ASVs) associated with human DNA concentration in both surface and subsurface remains. Surface bone microbial communities showed greater shared identity with soil samples in microbial community composition and abundance, while subsurface communities demonstrated more proximate associations with gut samples following NMDS analyses of Bray-Curtis dissimilarities and weighted UniFrac distances. SIMPER analyses and random forest modeling, implicated *Clostridium* spp. and *Pseudomonas* spp., as putative bone colonizers in surface and subsurface bones. This research is the second of its kind to survey microbial communities from all bone types within and between individuals using next generation sequencing, and therefore, expands on our knowledge of microbial bone colonizers, including colonizers important in a subsurface deposition environment.

Introduction

Skeletal DNA preservation varies by bone type, and weight-bearing cortical bones are generally preferentially sampled for DNA-based identification over small, cancellous elements [6–9]. However, previous research examining inter-individual and intra-individual variation in skeletal preservation by bone type in surface and buried remains has shown that small bones of the foot, specifically tarsal bones, outperform dense, cortical bones in DNA quality (STR recovery) and quantity [5,180]. Though the causative agent(s) driving these patterns largely remain unknown, moisture availability and microbial composition and structure have been the primary factors implicated [180].

Following deposition, skeletal DNA preservation is influenced by the mechanics of bone diagenesis, including chemical and/or biological modification. Soil geochemistry and site hydrology are equally important to microbial degradation [11,67] and can influence the composition and abundance of microbes present in a given environment [35]. Dissolution and recrystallization are influenced by moisture availability, pH, and bone porosity. Following autolysis, once-occupied pore spaces in living bone become accessible to water, ionic exchange, and microorganisms [74]. Water movement through bone is driven by diffusion, hydraulic flow, and recharge [179]. Because bioapatite is not in equilibrium with the surrounding environment, it readily exchanges ions along a diffusion gradient. When the environment is saturated, movement

is limited by the rate of diffusion, and dissolution of hydroxyapatite is not as extensive. However, when site hydrology fluctuates, water continuously moves in and out of pore spaces, exposing the bone to chemically unsaturated water, increasing the rate of inorganic dissolution while simultaneously increasing bone porosity. This process is further influenced by environmental pH, with acidic environments promoting dissolution and alkaline environments encouraging preservation [67,179]. Whether hydroxyapatite undergoes dissolution and recrystallization is important to organic preservation including collagen and DNA. As hydroxyapatite dissolves, it releases bound DNA and exposes collagen to hydrolytic enzyme activity by microbial collagenases [67,76].

Previously, we applied random forest models to microbial data from surface decomposed remains to identify important OTUs related to human skeletal DNA concentration. Though the models were minimally successful, key taxa associated with patterns of DNA survivability included *Clostridium* sp., unclassified *Dermacoccaceae* sp., *Paracoccus* sp., and *Actinotalea* sp. [181]. Because factors modulating the rate and trajectory of decomposition differ between subsurface and surface environments, and putrefactive bacteria have been implicated in bone degradation [82–84], we expect microbial community composition and structure to have a greater influence on the state of decay of subsurface remains.

On the surface, decedents are exposed to more variable environmental conditions including changes in temperature, humidity, precipitation, arthropod activity, UV exposure, and scavenging [17,80], which would influence microbial community composition and structure. In fact, in surface remains, Deinococcus-Thermus, a group comprised of extremophiles, was observed in greater than 2% relative abundance in cranial elements, likely related to the duration of exposure [181]. Burials are less amenable to environmental perturbations. Rather, subsurface environments are influenced by soil composition, moisture, depth, microbial ecology, and other edaphic parameters. Unlike surface sites, burials preclude access by scavengers and insects and minimize temperature effects [27,28]. In addition, microbial communities in surface remains clustered by anatomical region, which we hypothesized to be related to micro-environmental differences in the soil and distance from the gut [181]. Soil samples were not collected from surface deposition localities and so could not be tested.

The primary goal of this study was to examine differences in microbial community composition and structure between surface and buried remains and relate these differences to patterns of skeletal DNA survival. Random forest models were generated to not only identify important taxa associated with patterns of human skeletal DNA preservation in subsurface bones but also those shared across surface and subsurface environments. Special attention was allocated to the post-mortem foot microbiome. Tarsals of the foot have consistently yielded human DNA of high quality and quantity [5,9,180]. Though this may be related to bone remodeling processes in vivo [176], there could be a unique post-mortem foot microbiome, potentially related to the physical distance between bones of the foot and the gut. Moreover, soil samples collected from within and outside of the grave and gut samples from the American Gut Project (AGP) were used to elucidate the impact of environmental and enteric microorganisms on the post-mortem bone microbiome.

Materials and Methods

Sample Description

Grave Samples

In 2013, three human individuals, two males and one female, were interred in a multi-individual grave, at the Anthropology Research Facility (ARF) at the University of Tennessee, Knoxville (UTK) to understand inter-individual and intra-individual patterns of skeletal DNA degradation. Individuals were willfully donated to the Department of Anthropology for decomposition research at the ARF and osteological research as skeletonized remains in the William M. Bass Donated Skeletal Collection. Individuals (A, B, and C) were stacked in the grave to replicate a realistic scenario. Individual A was located at the grave base; B was in the middle, and C was the shallowest. A second grave was excavated and backfilled simultaneously without interring additional human remains to serve as a disturbance control. Both graves were approximately 2 m x 2 m x 0.7 m and were located in an area of the ARF not previously used for decomposition research. Additional off-grave control soil samples were collected approximately 5 m from any decomposition locality and were not disturbed prior to collection. Graves were excavated in 2017, four years following interment. Remains were disinterred at the time of excavation.

Soil samples were collected at four depths (0-5 cm, 30-35 cm, 70-75 cm, and 80-85 cm) within the perimeter of the grave and at two depths (0-5 cm, 30-35 cm) along three lateral transects extending away from the grave. An additional soil sample was collected from within the rib cage of individual C at ~ 40 cm. Soil samples were sent to the Department of Biosystems Engineering and Soil Sciences for soil biological and geochemical testing. Variables tested included pH, conductivity, enzymatic potentials (leucine aminopeptidase, N-acetyl-glucosaminidase, collagenase, and phosphodiesterase), soil gravimetric moisture, microbial respiration, ammonium, nitrification potential, dissolved organic nitrogen, dissolved organic carbon, and nitrate. Soils were also tested for total fungal and bacterial gene abundances, human-associated *Bacteroides* gene abundances, and soil nematode abundance and composition. In depth details on soil collection, analyses (including DNA extraction methodology), and results have been reported in Keenan et al. [56]. DNA extracts from a subset of these samples were sent for next generation sequencing (n = 27) (Table S4.1).

In addition, the same forty-nine bones from each individual, representing all skeletal element types, were sampled for human DNA, total DNA, and total bacterial and fungal gene abundances. Of these 49 bones, 19 bones were sampled at two sites, and 3 bones (i.e., humerus, femur, and tibia) were sampled at three sites. Sampling sites from the femur, tibia, and humerus were sampled twice. The outer surface of all sampling sites was mechanically (i.e., Dremel® rotary tool) and chemically (i.e., 10% bleach and 70% EtOH) treated prior to sampling. Bones were sampled using a handheld drill with a 9 mm masonry bit at slow speeds (< 100 rpm) (Figure 4.1). Samples were sent to Bode Cellmark Forensics, Lorton, Virginia, for DNA extraction and human DNA testing (e.g., Quantifiler™ Trio DNA Quantification, GlobalFiler™ PCR Amplification, etc.). Extracts were returned to UTK for total DNA quantitation and total bacterial and fungal gene quantification. Methods including skeletal DNA extraction, human DNA testing, and microbial gene quantification are reported in Emmons et al. [180]. All skeletal DNA extracts used in Emmons et al. [180] were also used in the current study to assess bacterial and archaeal community composition and structure (n = 256).

Figure 4.1: **Left radius from individual C. The outer surface of the bone was mechanically removed using a Dremel® rotary tool; the sample sites, two, shown by arrows, were chemically cleaned using 10% bleach and 70% ethanol. Bone powder was collected using a hand-held drill with a 9 mm masonry bit. Samples were processed in a designated clean-lab suite of the Molecular Anthropology Laboratories at UTK.**

Comparative Samples

Two additional data sets were included for comparative purposes. First, DNA sequences from subsurface (buried) remains were compared directly to sequences from skeletal DNA extracts from three individuals who had decomposed on the ground surface (n = 162). Samples were sequenced on an Illumina MiSeq platform targeting the V3-V4 region of the 16S rRNA gene using 300 PE chemistry and have previously been characterized by [181]. Second, sequence data associated with samples from human feces (n = 53), sebum (n = 2), saliva (n = 6), and hair (n = 1) and associated metadata were accessed from the American Gut Project (AGP) (Qiita Accession ID 10317), a crowd-sourced project including thousands of samples from multiple body sites, with emphasis on fecal donations from civilians/scientist participants [123]. Samples were chosen based on age (between 50-70 yrs.) and state of residence (TN, GA, AL, WA, and VA) to reflect demographic information from deceased individuals (Table 4.1). Sample and prep IDs as well as other demographic information are located in Table S4.2. American Gut samples were processed and sequenced according to Earth Microbiome Project (EMP) protocols using 150 PE chemistry on a MiSeq Illumina Platform (Primers 515F–806R) [182].

Next Generation Sequencing Analysis

DNA extracts from gravesoil and skeletal samples were sent for next generation sequencing at the Center for Environmental Biotechnology (CEB), UTK. Library preparation was performed by the CEB using the Nextera DNA Library Prep Kit according to manufacturer instructions. Primers used were consistent with EMP protocols (515F–806R), targeting the V4 region of the 16S rRNA gene [182]. Samples were sequenced on an Illumina MiSeq System using 250 PE chemistry. Two PCR blanks and one positive control (ZymoBIOMICS Microbial Community DNA Standard, Zymo Research) were included in each run.

Table 4.1: **Demographics of skeletonized individuals.**

ID	Project	Sample Type	Weight (kg)	Age (yrs)	Medical History	Sex	Residence
SA	Surface	Bone	104	50	Diabetes, alcoholic, substance abuser	Male	TN/AL
SC	Surface	Bone	127	69	Diabetes, Cardiac issues	Male	TN
SB	Surface	Bone	80	47	High cholesterol, Arthritis	Male	TN
B	Grave	Bone	70	63	COPD	Male	VA
A	Grave	Bone	60	68	Cancer	Female	WA
C	Grave	Bone	52	63	Cancer, Coronary Artery Dx	Male	GA/AL

Sequence reads were processed using the QIIME 2™ next-generation microbiome bioinformatics platform (v. qiime2-2019.1) (QIIME2 Development Team, 2018) [183]. Read quality was assessed using QIIME2 demux; reads were quality filtered, denoised, chimeras removed, and demultiplexed using DADA2 [184]. Primers from grave samples, soil and bone, were trimmed using the –trim-left function of the DADA2 plugin. Because bone samples from the comparative surface data set targeted V3-V4, sequences were trimmed, including primer removal, using EMP primers (515F–806R) targeting V4 using the QIIME2 cutadapt plugin prior to DADA2 [143]. Sequencing runs were denoised independently and merged. While most reads were trimmed to ~253 bp, there was variation in read length (min = 144 bp, max = 425 bp, mean = 263 bp), which resulted in 35,756 unique features (n = 507). Read loss also varied by data set following denoising. Grave samples experienced a total read loss of 13.1%. Similar to previously reported values, total reads from surface bones were reduced by 64.1% [181]. AGP samples saw a reduction in total reads by 30.4%.

Features, or amplified sequence variants (ASVs), were classified using a fitted classifier (classify-sklearn) using the SILVA ribosomal RNA database v132 (silva-132-99-515-806-nb-classifier.qza) [185]. Feature and taxonomic data were exported to R (v. 3.5.0) [146] for statistical analyses and visualization using phyloseq (v.1.20.0) [186]. ASVs identified as mitochondria, chloroplasts, and eukaryotes were filtered from the data set, as well as unidentified ASVs at the phylum-level; this resulted in 27,551 ASVs. ASVs not observed across a minimum of 0.5% of samples (~2) were also removed, resulting in 10,581 ASVs. Samples were rarefied to an even depth of 10,000 reads to account for uneven library sizes [187] prior to alpha and beta diversity measurements including ordination methods and visualizations based on ordination methods. While this depth resulted in sample loss (32 samples removed; Table S4.3) and a reduction in the number of ASVs (ntaxa = 10,484), rarefaction curves indicate that a depth of 10,000 reads adequately captures species richness for the majority of samples (Figure S4.1). Tooth samples and positive controls were removed prior to data analysis, resulting in a total sample size of 453. Bray-Curtis and weighted UniFrac were computed for beta diversity analyses. Alpha diversity metrics (Inverse Simpson and observed richness) were computed using a subsampling approach, in which richness and diversity metrics were computed for a total of 100 iterations, each scaled to even depth. Due to inherent differences between data sets (AGP,

surface bone, and grave) and variation in sequence length as a result of next generation sequencing analysis, ASVs were combined at the genus-level when all datasets were combined.

Data Analysis

Data analyses, excluding random forests models, were conducted in R (v. 3.5.0) [146]. Kruskal-Wallis tests were used to assess statistical significance in alpha diversity metrics with false discovery rate corrected p-values to account for multiple comparisons. Group differences in beta diversity metrics (weighted UniFrac and Bray-Curtis) were assessed visually using non-metric multidimensional scaling (NMDS) and statistically using permutational multivariate analysis of variance tests (PERMANOVA), with a total of 900 permutations (vegan v. 2.5-3) [188]. Multiple PERMANOVAs were performed; groups tested included project type (AGP, surface bone, and grave), sample type (human-gut, human-oral, bone, soil), bone environment (surface and subsurface), individual (A, B, C, SA, SB, and SC), grave individual (A, B, and C), and anatomical region / body site (skull, upper torso, arm, lower torso, leg, foot). Tests for homogeneity of multivariate dispersion were also applied to grouping variables; 999 permutations were used.

SIMPER, similarity percentages, followed by non-parametric Kruskal-Wallis tests with false discovery rate (FDR) corrected p-values, were used to determine ASVs significantly contributing to Bray-Curtis dissimilarities between grave individuals and anatomical regions (seq-scripts release v. 1.0) [148]. ASVs were considered significant when significance was below a conservative alpha of 0.05. Random forest (RF) models were generated using Python (v. 3.5.2) and scikit-learn (v. 0.19.2) to identify important ASVs related to human DNA concentration. To reduce noise, taxa not present in more than 1% (4) of samples were eliminated from the data and data was rarefied to an even depth of 10,000 reads (ntaxa = 6,612). RF models were conducted on two datasets: 1) combined surface and subsurface bone samples (n = 384) and 2) subsurface bone samples (n = 247). ASVs were merged at the genus level for the combined data set, while all ASVs were included in the model when only subsurface bone samples were considered. Data were randomly split into training (2/3) and testing (1/3) sets. Success was measured in terms of mean absolute error, accuracy, and linear modeling of actual versus predicted data. Accuracy was calculated as the mean average percentage error subtracted from 100 %.

Results

Bone/Soil Bacterial and Archaeal Community Composition

Thirty-eight bacterial and archaeal phyla were identified in subsurface bone samples. Dominant taxa (mean relative abundance > 2%) included Proteobacteria (30.3 – 75.9%), Firmicutes (1.9 – 41.1%), Actinobacteria (1.7 – 24.0%), and Bacteroidetes (3.8 – 20.8%). This compared to thirty-six phyla in surface bones, with dominant representatives from Proteobacteria (21.1 – 59.4%), Actinobacteria (2.29 – 36.0%), Bacteroidetes (4.8 – 25.7%), Firmicutes (2.4 – 35.2%), Planctomycetes (0.1 – 10.4%), and Patescibacteria (0.03 – 10.6%). A total of 33 phyla were observed in soil samples, including controls and off-grave samples. Dominant taxa included Proteobacteria (21.1 – 59.0%), Actinobacteria (10.6 – 33.5%), Verrucomicrobia (0.9 – 34.2%), Acidobacteria (0.6 – 14.9), Firmicutes (0.4 – 18.2%), Chloroflexi (1.8 – 7.1%), Bacteroidetes (2.0 – 10.2%), and Planctomycetes (0.4 – 4.0%) (Figure S4.2).

Alpha Diversity

Samples from the AGP, on average, had the lowest bacterial diversity and richness estimates, while soils had the greatest (Table S4.4). Bone samples showed intermediate species diversity and richness. Differences by sample type (bone, gut, soil) were statistically significant (Richness: X^2 = 121.3, DF = 2, p < 2.2e-16; Inverse Simpson: X^2 = 81.5 DF = 2, p < 2.2e-16). Though richness did not significantly differ by bone deposition environment (surface vs. subsurface), mean bacterial diversity in surface bone (mean = 44.3) was greater than mean diversity in subsurface (buried) bone (mean = 28.3) (X^2 = 28.7, DF = 1, p = 8.59e-08). Richness was highly diverse among individuals (X^2 = 145.9, DF = 5, p < 2.2e-16). Samples from C had the greatest mean species richness (all comparisons p < 1.0e-5, includes surface individuals), while A had the lowest (all comparisons p < 0.001). A and B had similar degrees of diversity, which were significantly lower than all other individuals (all comparisons p < 0.001). C had significantly greater diversity estimates than A and B (p < 1.0e-10), which were similar to surface individuals, especially SB and SC. Microbial species diversity and richness was variable by bone type, but some trends did present. For example, bones of the lower torso and upper torso of A had some of the lowest richness and diversity estimates, while bones from the skull and foot had some of the highest. Bones of the arm had the lowest richness and diversity estimates of B and C, while bones of the lower torso had the highest richness and diversity estimates in these same individuals. Though mean diversity estimates from bones of the feet were intermediate to other anatomical regions, mean richness estimates were ranked second highest after the lower torso in B and C (Figure S4.3).

Beta Diversity: Sample Type, Individual, and Anatomical Region

Bacterial and archaeal communities were significantly different by project (AGP, Grave, and Surface) and sample type (soil, human gut, human oral, and bone) using a PERMANOVA on beta diversity metrics (i.e., Bray-Curtis and weighted UniFrac) (Table 4.2). Bone communities, including bones from surface and subsurface contexts, were more similar to each other than they were to soil or human-associated communities (Figure 4.2). When considering phylogenetic distance using weighted UniFrac, communities from buried individuals A and B, and especially A, showed greater distance from soil samples and increased similarity with human-associated communities from living donors. This pattern was reaffirmed compositionally by comparing relative abundance at the phylum-level (Figure 4.2C). A Venn diagram was used to track the number of genera shared between the human gut, surface bone, subsurface bone, and soil. Excluding taxa shared between soil and human gut samples, a total of 37 taxa (22.8% of genera originating from the gut) were shared between subsurface bone and human gut samples, while 282 genera (57.2% of genera originating from the soil) were shared between subsurface bone and soil, leaving the origin of 579 genera from decaying human bone unknown (Figure 4.3).

Among bone communities, beta diversity was affected by the bone deposition environment (surface vs. subsurface) and differences between individuals (A, B, C, SA, SB, SC). Individuals deposited on the ground surface clustered more closely with individual C, the shallowest individual in the multi-individual grave (Figure 4.2). When assessing samples from the grave project in isolation, bacterial and archaeal communities demonstrated significant differences by individual (A, B, and C) and anatomical region (skull, upper torso, arm, hand, lower torso, leg, and foot) (Table 4.2). This was, in part, influenced by differences in group variance. All factorial variables tested, with the exclusion of project, showed significant

Table 4.2: PERMANOVAs (999 permutations), assessing between sample differences (beta-diversity) using two metrics (Bray-Curtis dissimilarities and weighted UniFrac phylogenetic distances)

Distance Metric	Test	*F* statistic	*p* – value	Degrees of Freedom
Bray-Curtis	Project	38.0	0.001	2
	Type	17.2	0.001	3
	Surface / Subsurface Bones	36.5	0.001	1
	Individual (excludes AGP)	16.6	0.001	4
	Individual (Grave)	27.6	0.001	2
	Body Site (Grave)	6.47	0.001	6
	Individual*Body Site	4.90	0.001	12
Weighted UniFrac	Project	43.5	0.001	2
	Type	22.1	0.001	3
	Surface / Subsurface Bones	34.3		
	Individual (excludes AGP)	17.2	0.001	4
	Individual (Grave)	24.0	0.001	2
	Body Site (Grave)	6.18	0.001	6
	Individual*Body Site	4.46	0.001	12

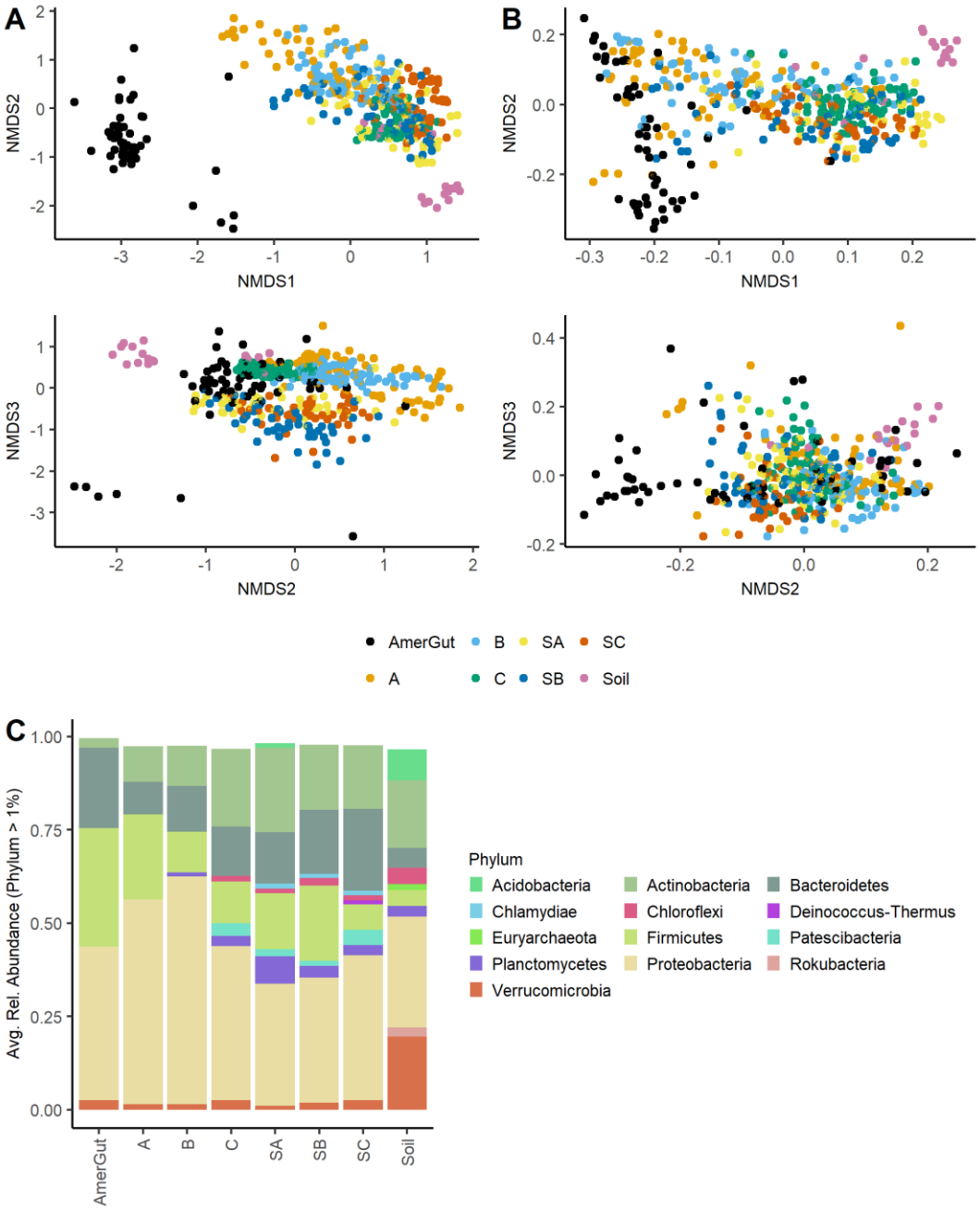

Figure 4.2: Non-metric multidimensional scaling and community composition in human bone, human-associated samples, and soils. Individuals included those from the grave (A, B, C) and those from the surface (SA, SB, SC), as well as individuals associated with the American Gut Project (AmerGut). (A) NMDS on Bray-Curtis dissimilarities (Stress = 0.110, k = 3, n = 453, ntaxa = 1,563) (B) NMDS on weighted UniFrac distances (Stress = 0.111, k = 3, n = 453, ntaxa = 1,563). ASVs were combined at the genus-level prior to ordination.

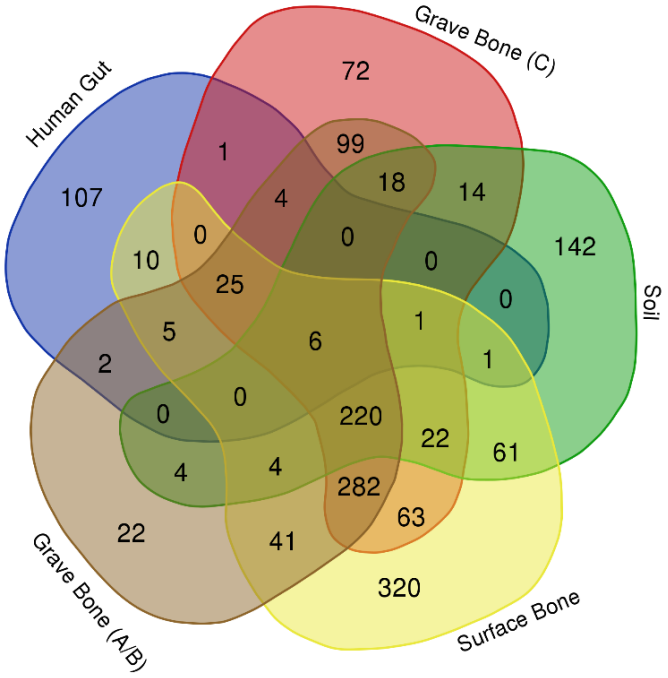

Figure 4.3: **Venn diagram of shared genera across groups (surface bone, subsurface bone, gut-associated samples, and soil). Subsurface individuals (A, B, and C) were split into two groups based on UniFrac distances and NMDS ordinations. A total of 1,546 genera were included in the analysis; samples were rarefied to an even depth of 10,000 reads. ASVs not found in at least 0.05% of samples were removed. Soil samples at a depth of 70 cm were excluded, and only gut samples from the AGP were included. Output was generated using http://bioinformatics.psb.ugent.be/cgi-bin/liste/Venn/calculate_venn.htpl.**

differences in group variance following tests for homogeneity of multivariate dispersion on Bray-Curtis dissimilarities ($p < 0.01$).

Bones that had decomposed on the surface and those at the shallowest grave depths showed greater similarity with soil samples (Figure 4.2; Figure 4.4). Though soil communities formed a distinct cluster; five soil samples (3 samples from a depth of 70 cm, 1 from a depth of 40 cm, and 1 from a depth of 30 cm) were closely associated with bone samples, all clustering with C (Figure 4.4A). Combined soil geochemistry analysis with weighted UniFrac, indicate an oligotrophic functionality for communities at 70 cm, with increased N-acetyl-glucosaminidase, leucine aminopeptidase, and cellulobiosidase potentials, despite significant quantities of pooled dissolved organic carbon and dissolved organic nitrate (Figure 4.4B). In addition, though microbial communities were significantly different by anatomical region, this was conflated by individual differences (Table 4.2). When visualized using NMDS on Bray-Curtis dissimilarities, bones of the feet were the only samples that demonstrated clear clusters across all three subsurface individuals (Figure 4.4; Figure S4.4).

Similarity Percentages (SIMPER)

Significant ASVs contributing to Bray-Curtis dissimilarities between individuals were from the following families: Streptomycetaceae, Ruminococcaceae, Enterobacteriaceae, Burkholderiaceae, Rhizobiaceae, Pseudomonadaceae, Clostridiaceae I, Aquaspirillaceae, Rhodanobacteraceae, and Rhodocyclaceae. ASVs with increased relative abundances in A and B compared to C included *Azospira* sp., *Caproiciproducens* sp., unclassified *Clostridiaceae* spp., and *Microvirgula* sp., while C was enriched in *Rhodanobacter* sp. and *Streptomyces* sp.

Because the feet demonstrated unique communities compared to other body sites (Figure 4.4), SIMPER analyses by anatomical region were focused on the post-mortem foot microbiome. Individuals were examined independently. Relative to other body regions, the foot of individual A had decreased abundances of *Clostridium sp.* (sensu stricto I), *Caproiciproducens* sp., *Clostridium tetani* (sensu stricto 15), unclassified Clostridiaceae sp., *Microvirgula* sp., and *Pseudomonas* sp. In contrast, increased abundances of *Streptomyces sp.*, *Sphingomonas* sp., and *Mycobacterium* sp. were observed (Figure S4.6A). The foot of individual B, similarly, demonstrated increased abundances of the same *Sphingomonas* sp. ASV and an additional ASV identified as *Streptomyces* sp. B also saw increased abundances of *Tardiphaga sp*. Moreover, some of the same ASVs important to the foot of individual A were also observed driving dissimilarity between the foot of B and other anatomical regions, including a reduction in abundance of unclassified Clostridiaceae *sp.*, *Clostridium* sp. (sensu stricto I), *Pseudomonas* sp., and *Microvirgula* sp. Interestingly, the foot, hand, and skull, demonstrated increased abundances of an uncultured *Thermomicrobium* sp (Figure S4.6B).

Amplified sequence variants (ASVs) driving differences by body site in C were dissimilar from A and B (Figure 4.4). The foot of C saw increased abundances of *Parafilimonas* sp., *Hathewaya* sp., *Flavisolibacter* sp., *Dokdonella* sp., *Rhodanobacter* sp., and *Terrimonas* sp. (YJ03), and decreased abundances of *Clostridium* sp. (sensu stricto 5), *Pseudomonas* sp., unclassified *Paludibacteraceae* sp., unclassified Enterobacteriaceae sp., and unclassified Burkholderiaceae sp (Figure S4.6C).

Random Forests Models

Random forest modeling (RF) was used to identify taxa predictive of human DNA concentrations across multiple depositional environments (i.e., surface and subsurface). RF

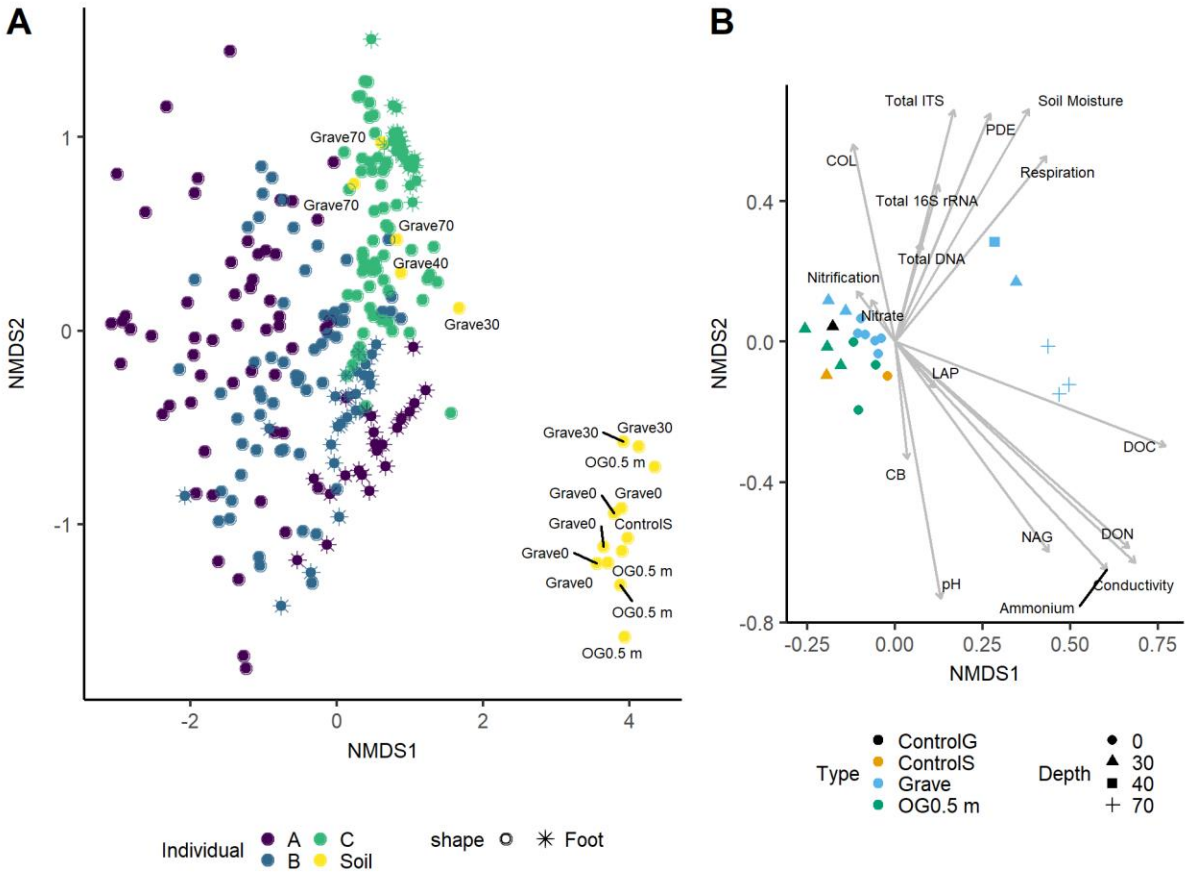

Figure 4.4: **(A) Non-metric multidimensional scaling using Bray-Curtis dissimilarities of subsurface human bone samples and associated soils (Stress = 0.127, k = 2, n = 259, ntaxa = 5,915). Soil samples are labeled by location [on-grave (Grave) or off-grave (OG 0.5 m)], depth within the grave (Grave 0 cm, 30 cm, 40 cm, and 70 cm), and type, including controls (ControlS). (B) NMDS of soils on weighted UniFrac distances with combined geochemistry using the envfit function from the package vegan (Stress = 0.06, k = 2, n = 22, ntaxa = 2,869). Soil samples were rarefied to an even depth of 7,000 reads to include more soil samples in the analysis; taxa were assessed at the level of ASV.**

modeling including both subsurface and surface bones demonstrated an accuracy of 53.4% (MAE = 2.34 ng/gbp, $R^2 = 0.43$, $p = 3.63e\text{-}13$, n = 383, ntaxa = 1100). Important predictors of skeletal DNA concentration included the genera *Azospira* and *lamia.* Other important predictors spanned 7 phyla (Actinobacteria 13%, Bacteroidetes 11%, Epsilonbacteraeota 3%, Firmicutes 21%, Patescibacteria 3%, FBP 3%, Verrucomicrobia 5%, and Proteobacteria 42%). Of these, 13% (5 of 38) were from the order Clostridiales, with 8% (3) identified as Clostridia spp. In addition, 18% of important predictors were from the order Betaproteobacteriales, with 11% from the family Burkholderiaceae (*Massilia* spp., *Aquabacterium* spp., *Pseudorhodoferax* spp., and *Achromobacter* spp. (Figure 4.5).

RF models did not improve when excluding surface bone samples; rather, accuracy was reduced by 1.59% (MAE = 2.45 ng/gbp, Accuracy = 51.8%, $R^2 = 0.40$, $p = 3.0e\text{-}08$). Important predictor taxa were from the phyla Actinobacteria (14%), Bacteroidetes (4%), Epsilonbacteraeota (4%), Firmicutes (18%), Planctomycetes (4%), Verrucomicrobia (4%), and Proteobacteria (54%). Of these, the order Clostridiales comprised 14% of total predicted taxa. The most important predictor taxa were *Aneurinibacillus* sp. (Firmicutes; importance = 0.07), *Dechlorosoma* sp. (Proteobacteria; importance = 0.05), and *Azospira* sp. (Proteobacteria; importance = 0.03) (Figure S4.5).

Discussion

Bacterial/Archaeal Community Differences Between Surface and Subsurface Bones

Surface and subsurface bones showed interesting differences in bacterial/archaeal community composition. While bones from both deposition environments were heavily influenced by Proteobacteria, Actinobacteria, Bacteroidetes, Firmicutes, and Patescibacteria, additional colonizers of surface remains included Planctomycetes, Chloroflexi, Chlamydiae, and Deinococcus-Thermus (Figure 4.2C; Figure S4.2). Within Chlamydiae, the order Chlamydiales dominated, with major representatives from *Neochlamydia* and *Candidatus protochylamydia*. The orders Thermomicrobiales, mainly composed of an unclassified JG30-Kf-CM45, and Caldilineales dominated the phylum Chloroflexi. Chlamydiae includes obligate intracellular bacteria associated with a diverse range of hosts including arthropods, mammals- including humans - and amoeba [189]. The two dominant genera sequenced from surface bone are likely amoebic endosymbionts, potentially of *Acanthamoeba* spp. and *Hartmannella* spp., free-living, potentially bacterivorous amoeba found in diverse habitats [190,191]. The presence of Deinococcus-Thermus and Chloroflexi in surface bones, both of which include thermophilic members, potentially reflects extreme changes in the surface deposition environment, including temperature, moisture, and UV irradiation.

Though surface and subsurface environments were significantly different using Bray-Curtis dissimilarities and weighted UniFrac distances, microbial communities from bone appear to coalesce at a junction between human-associated gut communities and soil microbial communities, indicating a shared community of mixed origin. Surface bone microbial communities shared greater similarities with soil samples in microbial community composition and abundance, while subsurface communities demonstrated more proximate associations with gut samples. Excluding individual C, this was also true of diversity analyses. This lends support to claims that prolonged exposure to putrefactive enteric bacteria increases the likelihood of skeletal degradation [82–84]; A and B had significantly lower mean human DNA concentrations than C [180]. In contrast, and in alignment with surface observations, Damann et al. (2015)

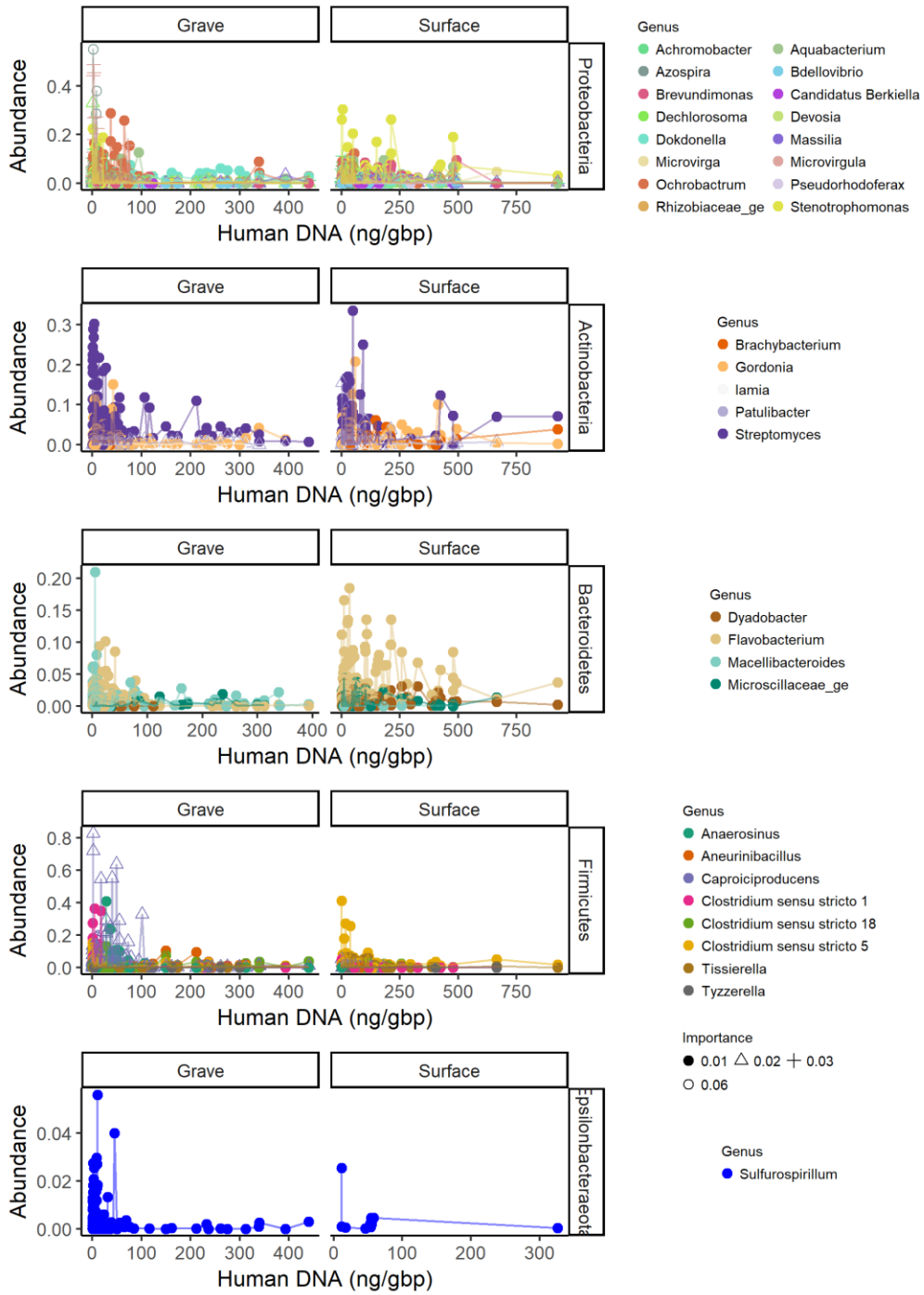

Figure 4.5: Important ASVs associated with surface and subsurface skeletal DNA concentration, as predicted using Random Forest Modeling. Excluded phyla include Patescibacteria, Verrocomicrobia, and FBP. Importance is a fraction (0.01 = 1%) and represents the importance of a given taxa to the RF model.

observed shifts in surface exposed bone-associated communities with postmortem-interval, reflecting a convergence with soil communities over time. Similarly, Metcalf et al. (2016) found that a minimum of 40% of microbial (archaeal and bacterial) decomposers could be linked to the soil environment, initially found at low abundances prior to decomposition.

Many bone colonizers were not observed in either soil or gut samples (Figure 4.3). Though microbial populations could have multiple additional origins (water, skin, hair, etc.), this was likely an effect of the sequencing process. For unknown reasons, soil samples had a much lower read distribution (~30,000 reads) than bone samples; population migrations would be better identified with deeper sequencing. Additionally, soil samples at depths below 30 cm were removed from Venn diagram analyses because these samples were heavily influenced by decomposition byproducts. These samples included all soils collected at depths below 30 cm; therefore, our Venn diagram analysis lacked a large subset of soil microbes interacting with decomposing remains.

Interestingly, microbial communities from individual C diverged from A and B, demonstrating greater similarity with SA, SB, and SC. Potential factors responsible for this divergence include depth, oxygen availability, soil composition, pH, moisture, arthropod activity, and temperature. Individual C was first uncovered at a depth of 27 cm. Diurnal and seasonal temperature fluctuations as well as necrophagous insect activity have been observed in burials with depths less than 30.5 cm [28]. In addition, changes in soil geochemistry within the grave indicate a shift in oxygen availability below 40 cm, coinciding with a change in community functionality, which was reflected in soil enzymatic potentials. Increases in N-acetyl-β-glucosaminidase and decreases in phosphodiesterase and leucine aminopeptidase at the grave base, point to a more oligotrophic community [56]. Microbial communities from individuals A and B showed greater dispersion, potentially as a stacking effect. Materials pooled to the grave base, primarily as a result of gravitational forces. Soil encompassing individuals were disturbed during interment, decreasing soil compaction, and thereby promoting increased drainage to the grave base, creating a water bucket and sponge-like effect [192,193]. This was reflected in the microbial communities at the grave base and from within the rib cage of Individual C, which deviated from the communities of other soils and were more similar, in community composition and abundance to bone samples presumed to have greater influence from soil (i.e., bones from C, SA, SB, and SC).

Identifying Bone Degraders Using Skeletal DNA Preservation

We previously speculated about the potential impact of groundwater and its associated effects on differences in DNA survivability between individuals [180]. Though the grave base was saturated at the time of disinterment, the lack of organic preservation, as indicated by decreased human DNA concentrations (Table S4.5) is indicative of fluctuating water levels within the grave. Seasonally water-logged sites demonstrate poor skeletal preservation [139], which is expected given the mechanisms of bone diagenesis and the impact of water [11,179].

Nevertheless, we were still interested in identifying microbial taxa associated with high and low levels of human DNA preservation. The most important taxa identified by our most successful random forest model, which incorporated data from both surface and subsurface bone samples, were *Azospira* spp. (importance = 0.06) and *Microvirgula* spp. (importance = 0.03). Both showed increased abundances when human DNA concentrations were low. *Azospira* spp. includes diazotrophic microaerophilic nitrogen fixers [194], while *Microvirgula* spp. is

comprised of facultative aerobic denitrifying taxa, capable of using both oxygen and nitrogen oxides as terminal electron acceptors [195].

More interestingly, we saw increased relative abundances of several Firmicutes with decreasing human DNA concentrations including *Clostridium sensu stricto 1, Clostridium sensu stricto 5, Capoiciproducens,* and *Aneurosinus*. *Clostridium sensu stricto I* has a putative gut origin. It was not observed in soils presumed to be unaffected by decomposition and was disproportionately observed in bones of the arm from individuals' A and B (Figure S4.7). The humerus, ulna, and radius consistently yield poor human DNA results in DNA testing and analysis [5,7–9], indicating that species from this genus may play a role in skeletal degradation. The origin of these bacteria, though possibly from the human gut, ultimately remains unknown. It is possible that *Clostridium sensu stricto I* is naturally found at depths greater than 30 cm. Regardless of its origin, *Clostridum* spp. includes known collagenase producers and therefore, has the capability to actively degrade bone collagen [35]. In fact, the first isolated collagenase was from *Clostridium histolyticum* (Harrington, 1996). *Clostridium sensu stricto 5* also presents a compelling relationship with human DNA survival, decreasing in relative abundance as human DNA concentration increased in both surface and subsurface bones (Figure 4.5).

Multiple collagenase-producing bacteria and fungi have been isolated using enrichment cultures under "burial conditions" (temperatures = 10°C) in the past, and include *Trichonella sp.*, *Pseudomonas* spp., *Penicillium* spp., *Fusarium* sp., *Cladosporium* sp., *Xanthomonas* sp., and *Aeromonas* sp. [70]. None of which, were identified as important taxa associated with skeletal DNA preservation in this study using RF modeling. Other potential bone degraders identified using random forest modeling include *Flavobacterium,* S*ulfurosporillium, Gordonia, Streptomyces*, *Ochrobactrum,* and *Macellibacteroides*. The challenge is deciphering primary bone degraders from secondary or tertiary beneficiaries and other syntrophic bacteria as well as incidental taxa. For example, *Aquabacterium,* a genus commonly isolated from freshwater biofilms [197], was identified as an important predictor of human skeletal DNA degradation. This relationship is likely coincidental; these bacteria are found in water and water enhances skeletal DNA degradation.

In addition to collagenolytic activity, microorganisms can exploit the inorganic components of hydroxyapatite directly through the production of organic acids [79], which would release bound DNA from hydroxyapatite. Phosphate solubilizing bacteria (PSB), in particular, are likely suspects in hydroxyapatite dissolution. Soil genera known to solubilize inorganic P include but aren't limited to *Pseudomonas, Enterobacter, Bacillus, Rhizobium, Agrobacterium, Micrococcus, Aereobacter, Erwinia, Streptomyces, Nocardia* [198], and *Gordonia* [199].

The Post-mortem Foot Microbiome

Previously, we showed that microbial communities clustered by anatomical site in surface exposed remains [181]. In contrast, the post-mortem human foot was the only anatomical region that exhibited close clustering among microbial communities in a subsurface environment (Figure S4.5). This is a probable consequence of the experimental design. Individuals were stacked in the grave, making the decomposition of each individual interdependent with the decomposition of all other individuals in the grave. While a stacking scenario is more realistic of forensic events, it made it more challenging to disentangle potential variables effecting differential skeletal DNA degradation. The feet were physically isolated from the major points of decomposition (i.e., the torso) and pooled water (i.e., Northwest side of grave). This does not

negate the possibility that a unique foot microbiome is related to disproportionately increased human DNA preservation in bones of the feet. Tarsals have shown high success rates across a number of deposition environments [9]. We previously indicated that this was likely due to extensive bone remodeling, hematopoiesis, and mummification [180]. While the first two are still valid, the last can be evaluated through a more critical assessment of the microbial ecology of foot bone colonizers. Limited moisture availability for microbial growth and motility is likely a critical factor [30]. Taxa with increased abundances in the feet and driving their dissimilarity from other anatomical sites include a wide-array of environmental taxa: *Streptomyces sp.*, *Sphingomonas* sp., and *Mycobacterium* sp., *Tardiphaga* sp., *Parafilimonas* sp., *Hathewaya* sp., *Flavisolibacter* sp., *Dokdonella* sp., *Rhodanobacter* sp., and *Terrimonas* sp. (YJ03). Thus, the preservation of skeletal DNA in the foot may be related to limited putrefactive exposure.

However, this relationship is by no means simple. Several top-ranking bones from buried individuals were from the upper and lower torso [180]. These regions are closest to the gut and are exposed to greater levels of putrefactive bacteria during decomposition. If putrefactive bacteria promote skeletal degradation as hypothesized [82–84], bones from the torso should exhibit some of the lowest concentrations of human DNA. We attribute these contradictory patterns to the preservative effects of adipocere. Adipocere (a.k.a. grave wax) forms from the hydrogenation of fatty acids to hydroxy fatty acids. This process has been linked to *Clostridium perfringens* and generally increases the alkalinity of the environment [200,201]. Intermittent water-logging, anoxia, and saturation [201,202] due to stacking, as observed in the grave, would promote adipocere formation, which decreases the rate of putrefactive processes. However, bacterial translocation occurs early in decomposition; inoculated *S. aureus* was observed throughout different organ systems in as little as 1 hour using a rodent model [85]. The rapidity of bacterial migration in human remains has been deduced through the study of the thanatomicrobiome [203]. Results indicate bacterial detection in organ systems in as little as 20 hours, with all organ systems affected by approximately 50 hours [38,49]. Therefore, it is plausible that putrefactive bacteria continue to degrade certain regions of the body even when adipocere formation is extensive in other regions.

Additionally, bones of the feet from all three individuals exhibited decreased abundances of *Clostridium* spp. and *Pseudomonas* spp., complementing random forest results. As discussed above, these taxa are linked to collagenolytic and phosphate solubilizing abilities. *Pseudomonas* spp. is particularly interesting, as it has been experimentally linked to biofilm formation and hydroxyapatite dissolution and is a common pathogen associated with osteomyelitis [94,95].

Conclusions

This research represents our second attempt to predict microbial bone degraders from human skeletal DNA concentration using random forest modeling. It also expands our original survey of bone colonizers to include the subsurface environment. Random forest models from buried remains demonstrated greater success than those applied to surface remains, and models were even stronger when including both deposition environments. Results showed an inverse relationship between *Clostridium* spp., a genus composed of known collagen degraders, as well as *Flavobacterium*, S*ulfurosporillium*, *Gordonia*, *Streptomyces*, *Ochrobactrum*, and *Macellibacteroides*, and human skeletal DNA degradation. Both *Streptomyces* spp. and *Gordonia* spp. are known phosphate solubilizing bacteria [198,199], capable of degrading hydroxyapatite directly through organic acid production. Similarly, *Pseudomonas* spp., which

was observed in disproportionately decreased abundances in bones of the foot, may also be important to skeletal DNA degradation. Colonization by one or more of these taxa is a potential mechanism through which skeletal DNA is degraded and/or released from bone. Additionally, data from this study indicate an important role for enteric microorganisms of the human gut in skeletal DNA preservation as initially hypothesized by Bell et al. [84]. This research furthers our understanding of post-mortem bone colonization by microbes and its effects on human DNA preservation.

Appendix III

Table S 4.1: **Soil Samples sent for NGS**

Sample ID	Sample Type	Provenience	Depth (cm)
MGR2170021	Soil	0.5 m off grave	0
MGR2170023	Soil	0.5 m off grave	30
MGR2170037	Soil	0.5 m off grave	0
MGR2170039	Soil	0.5 m off grave	30
MGR2170053	Soil	0.5 m off grave	0
MGR2170055	Soil	0.5 m off grave	30
MGR2170005	Soil	Control Grave	0
MGR2170007	Soil	Control Grave	30
MGR2170001	Soil	Control	0
MGR2170003	Soil	Control	30
MGR2170057	Soil	Grave	0
MGR2170059	Soil	Grave	0
MGR3170002	Soil	Grave	0
MGR3170003	Soil	Grave	0
MGR3170004	Soil	Grave	0
MGR3170005	Soil	Grave	0
MGR3170006	Soil	Grave	30
MGR3170007	Soil	Grave	40
MGR3170008	Soil	Grave	30
MGR3170009	Soil	Grave	30
MGR3170026	Soil	Grave	70
MGR3170027	Soil	Grave	85
MGR3170028	Soil	Grave	70
MGR3170029	Soil	Grave	85
MGR3170030	Soil	Grave	70

Table S 4.1 (continued)

Sample ID	Sample Type	Provenience	Depth (cm)
MGR3170031	Soil	Grave	70
MGR3170032	Soil	Grave	85

Table S 4.2: **Samples from the American Gut Project (Qiita 10317)**

Prep ID	Sample ID	Age	Residence	weight (kg)	Sample Type
1115	10317.000002261	52	TN	70	Stool
	10317.000002262	54	TN	74	Stool
	10317.000003439	50	TN	58	Stool
	10317.000001812	56	WA	70	Stool
	10317.000001830	58	WA	79	Stool
	10317.000002211	69	GA	63	Stool
	10317.000002219	61	GA	47	Stool
	10317.000002220	66	GA	71	Stool
	10317.000001194	60	VA	63	Stool
	10317.000001826	68	WA	82	Stool
	10317.000002884	60	WA	49	Stool
1116	10317.000001281	61	TN	78	Stool
	10317.000001286	55	TN	52	Stool
	10317.000004656	58	GA	46	Stool
	10317.000001205	54	VA	76	Stool
	10317.000001861	68	VA	72	Stool
	10317.000002114	67	VA	126	Stool
	10317.000004830	67	WA	125	Stool
	10317.000004831	68	WA	144	Stool
	10317.000005910	67	WA	60	Stool
1122	10317.000013020	67	TN	97	Stool
	10317.000014979	52	TN	68	Stool
	10317.000014111	56	GA	83	Stool
	10317.000001187	57	VA	55	Stool
	10317.000010744	57	VA	63	Stool
	10317.000010909	59	VA	53	Stool
	10317.000007023	60	AL	72	Stool
	10317.000014974	69	AL	104	Mouth
	10317.000002113	67	VA	124	Stool

Table S 4.2 (continued)

Prep ID	Sample ID	Age	Residence	weight (kg)	Sample Type
	10317.000003433	63	VA	113	Stool
	10317.000009166	67	VA	96	Stool
	10317.000013009	63	WA	88	Stool
1130	10317.000002259	52	TN	70	Mouth
	10317.000009767	63	TN	28	Stool
	10317.000003440	50	TN	58	Mouth
	10317.000002111	57	VA	79	Stool
	10317.000002112	58	VA	92	Stool
	10317.000001811	55	WA	77	Stool
	10317.000002221	60	GA	63	Mouth
	10317.000002222	60	GA	63	Stool
	10317.000002157	60	VA	79	Stool
	10317.000006078	64	VA	56	Stool
	10317.000007009	64	VA	97	Stool
	10317.000007010	64	VA	97	Mouth
	10317.000004651	67	WA	64	Stool
	10317.000005702	68	WA	84	Stool
	10317.000005703	68	WA	84	Stool
	10317.000005911	67	WA	60	Mouth
	10317.000006071	60	WA	56	Stool
1133	10317.000002260	52	TN	70	Forehead
	10317.000009586	57	TN	60	Stool
	10317.000003441	50	TN	58	Right Hand
	10317.000009403	58	GA	70	Stool
	10317.000009594	52	VA	53	Stool
	10317.000003983	59	WA	104	Stool
	10317.000005738	57	WA	85	Stool
	10317.000007012	64	VA	97	Hair
1158	10317.000009768	63	TN	28	Stool
	10317.000022443	52	TN	59	Stool
	10317.000022444	55	TN	92	Stool
	10317.000022520	51	TN	77	Stool
	10317.000026437	57	AL	87	Stool

Table S 4.3: **Excluded data. Data not included in most analyses. The reason (R or E) refers to purposeful exclusion (E) or exclusion due to rarefaction (R) at a depth of 10,000 reads.**

Reason	Sample ID	Run	Project	Type	Individual	Body Site	Bone
R	bone10010	G1	Grave	Bone	A	Lower Torso	Ilium
R	bone10030	G1	Grave	Bone	A	Arm	Humerus
R	bone10039	G1	Grave	Bone	A	Arm	Radius
R	bone10069	G1	Grave	Bone	A	Skull	Parietal
R	PCRblank1	G1	Grave	Negative Control	Seq	Blank	Blank
R	PCRblank2	G1	Grave	Negative Control	Seq	Blank	Blank
E	ZymoControl	G1	Grave	Positive Control	Seq	Control	Control
R	PCRblank3	G2	Grave	Negative Control	Seq	Blank	Blank
R	PCRblank4	G2	Grave	Negative Control	Seq	Blank	Blank
E	ZymoControl2	G2	Grave	Positive Control	Seq	Control	Control
R	30028	G3	Grave	Bone	C	Foot	1st prox foot phalanx
R	MGR2170003	G3	Grave	Soil	Soil	ControlS	ControlS
R	MGR2170005	G3	Grave	Soil	Soil	ControlG	ControlG
R	MGR2170007	G3	Grave	Soil	Soil	ControlG	ControlG
R	MGR2170023	G3	Grave	Soil	Soil	OG0.5 m	OG0.5 m
R	MGR2170039	G3	Grave	Soil	Soil	OG0.5 m	OG0.5 m
R	MGR2170057	G3	Grave	Soil	Soil	Grave	Grave0
R	MGR3170027	G3	Grave	Soil	Soil	Grave	Grave85
R	MGR3170029	G3	Grave	Soil	Soil	Grave	Grave85
R	MGR3170030	G3	Grave	Soil	Soil	Grave	Grave70
R	MGR3170032	G3	Grave	Soil	Soil	Grave	Grave85
R	PCRblank5	G3	Grave	Negative Control	Seq	Blank	Blank
R	PCRblank6	G3	Grave	Negative Control	Seq	Blank	Blank
E	ZymoControl3	G3	Grave	Positive Control	Seq	Control	Control
E	3939-JMD-0048	S1	Surface	Bone	SA	Tooth	maxillary lateral incisor L
E	3939-JMD-0049	S1	Surface	Bone	SA	Tooth	maxillary canine L
E	3939-JMD-0050	S1	Surface	Bone	SA	Tooth	maxillary 1st premolar
E	3939-JMD-0051	S1	Surface	Bone	SA	Tooth	maxillary molar
E	3939-JMD-0052	S1	Surface	Bone	SA	Tooth	mandibular canine L
E	3939-JMD-0053	S1	Surface	Bone	SA	Tooth	mandibular 1st premolar L
E	3939-JMD-0100	S2	Surface	Bone	SC	Tooth	maxillary lateral incisor L
E	3939-JMD-0101	S2	Surface	Bone	SC	Tooth	maxillary canine L
E	3939-JMD-0102	S2	Surface	Bone	SC	Tooth	maxillary 1st premolar
E	3939-JMD-0103	S2	Surface	Bone	SC	Tooth	maxillary molar

Table S 4.3 (continued)

Reason	Sample ID	Run	Project	Type	Individual	Body Site	Bone
E	3939-JMD-0104	S2	Surface	Bone	SC	Tooth	mandibular canine L
E	3939-JMD-0105	S2	Surface	Bone	SC	Tooth	mandibular 1st premolar L
E	3939-JMD-0153	S2	Surface	Bone	SB	Tooth	maxillary lateral incisor L
E	3939-JMD-0154	S2	Surface	Bone	SB	Tooth	maxillary canine L
E	3939-JMD-0155	S2	Surface	Bone	SB	Tooth	maxillary 1st premolar
E	3939-JMD-0156	S2	Surface	Bone	SB	Tooth	maxillary molar
E	3939-JMD-0157	S2	Surface	Bone	SB	Tooth	mandibular canine L
E	3939-JMD-0158	S2	Surface	Bone	SB	Tooth	mandibular 1st premolar L
E	3939-JMD-0159	S2	Surface	Bone	SB	Tooth	mandibular lateral incisor R
E	3939-JMD-0160	S2	Surface	Bone	SB	Tooth	mandibular lateral incisor R
E	3939-JMD-0161	S2	Surface	Bone	SB	Tooth	mandibular lateral incisor R
R	10317	1115	AmGut	human-gut		Stool	
R	10317	1115	AmGut	human-gut		Stool	
R	10317	1122	AmGut	human-gut		Stool	
R	10317	1122	AmGut	human-gut		Stool	
R	10317	1122	AmGut	human-gut		Stool	
R	10317	1130	AmGut	human-oral		Mouth	
R	10317	1133	AmGut	human-skin		Forehead	
R	10317	1133	AmGut	human-skin		Hand	
R	10317	1133	AmGut	human-gut		Stool	

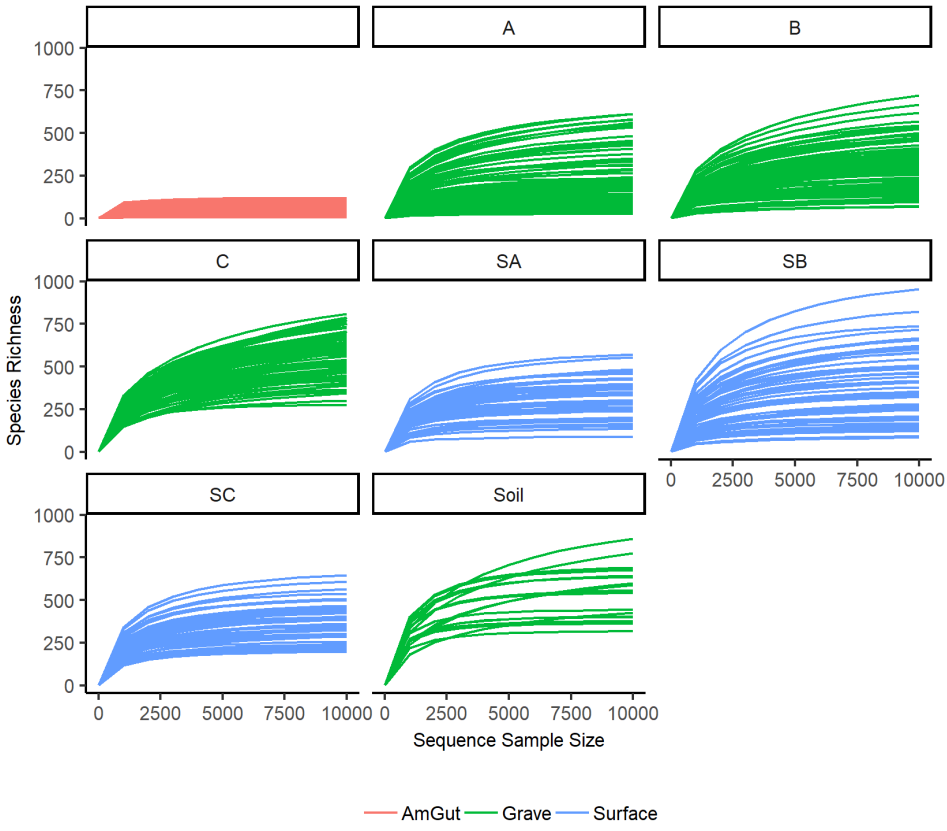

Figure S 4.1: Rarefaction Curves by individual with a sequencing depth of 10,000. Facets represent individuals (SA, SB, SC, A, B, C) or sample type (soil and AGP). Each line represents a sample. Species richness refers to observed OTUs.

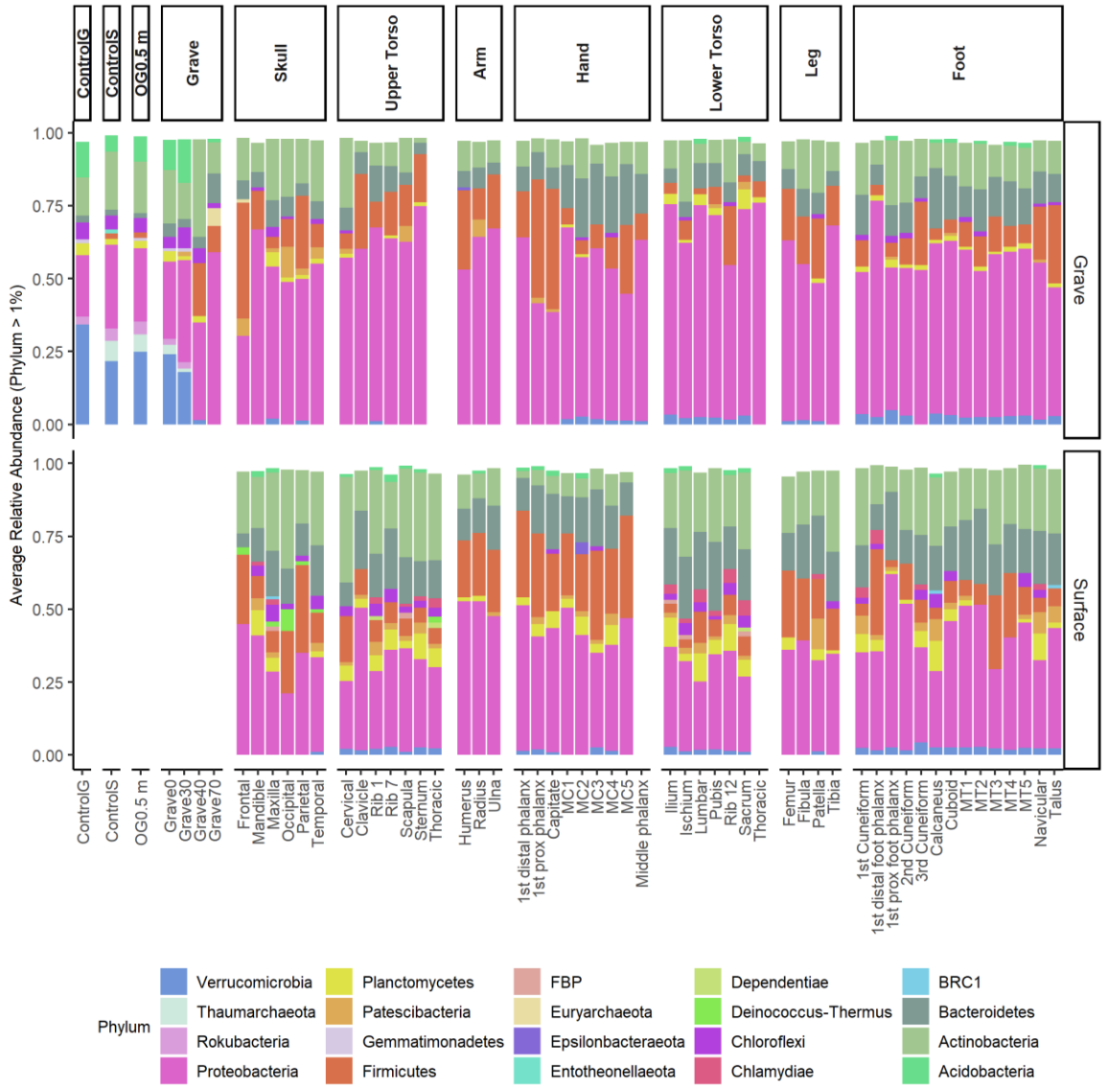

Figure S 4.2: **Bone bacterial and archaeal community composition. Samples were averaged by bone type and soil type, as indicated by the x-axis. Soil samples include those collected with depth in the grave ("Grave"; depths = 0, 30, 40, 70), those collected 0.5 m off grave("OG0.5 m"), and Control soils, disturbed and undisturbed ("ControlG","ControlS"). All samples with less than 7,000 reads were filtered from the data set prior to visualization**

Table S 4.4: Alpha diversity metrics by individual (A, B, C, SA, SB, SC) and sample type (AmerGut and Soil).

Measure	Individual	Mean	Std. Dev.	Max.	Min.
Richness	AmerGut	65.21	27.62	118.34	10.77
	A	229.09	160.95	619.04	25.97
	B	308.01	146.08	713.43	71.44
	C	567.42	122.70	828.69	276.43
	SA	313.88	115.60	575.40	87.99
	SB	402.77	215.47	938.04	86.34
	SC	377.07	111.03	655.45	195.11
	Soil	546.25	156.96	862.81	314.60
Inverse Simpson	AmerGut	7.69	7.46	24.69	1.03
	A	19.87	20.96	109.90	1.97
	B	19.61	15.84	88.44	1.64
	C	45.14	24.72	115.98	5.12
	SA	33.26	23.49	108.36	5.42
	SB	47.40	39.40	198.88	3.32
	SC	51.71	28.02	118.26	12.95
	Soil	75.00	46.99	168.65	16.15

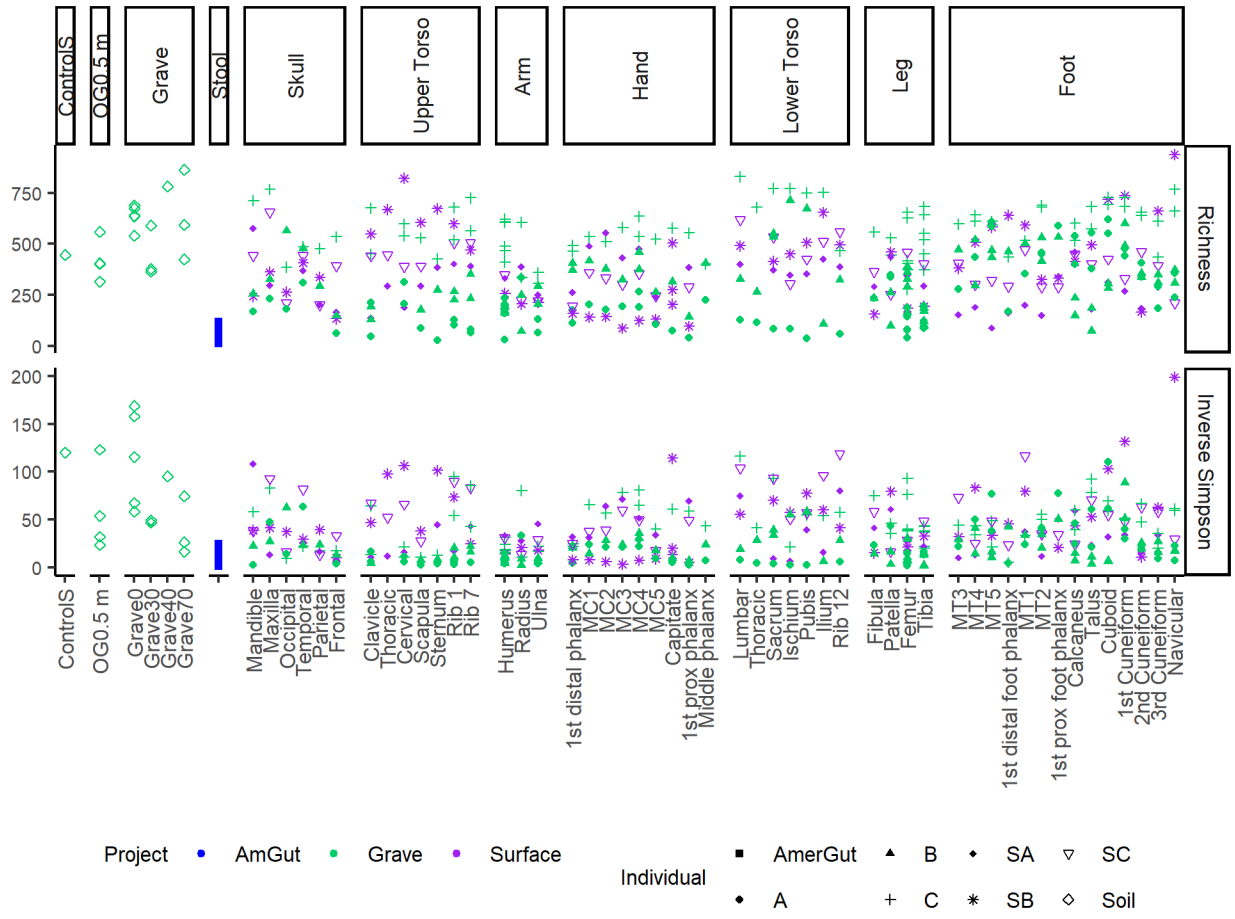

Figure S 4.3: Alpha diversity estimates by sample.

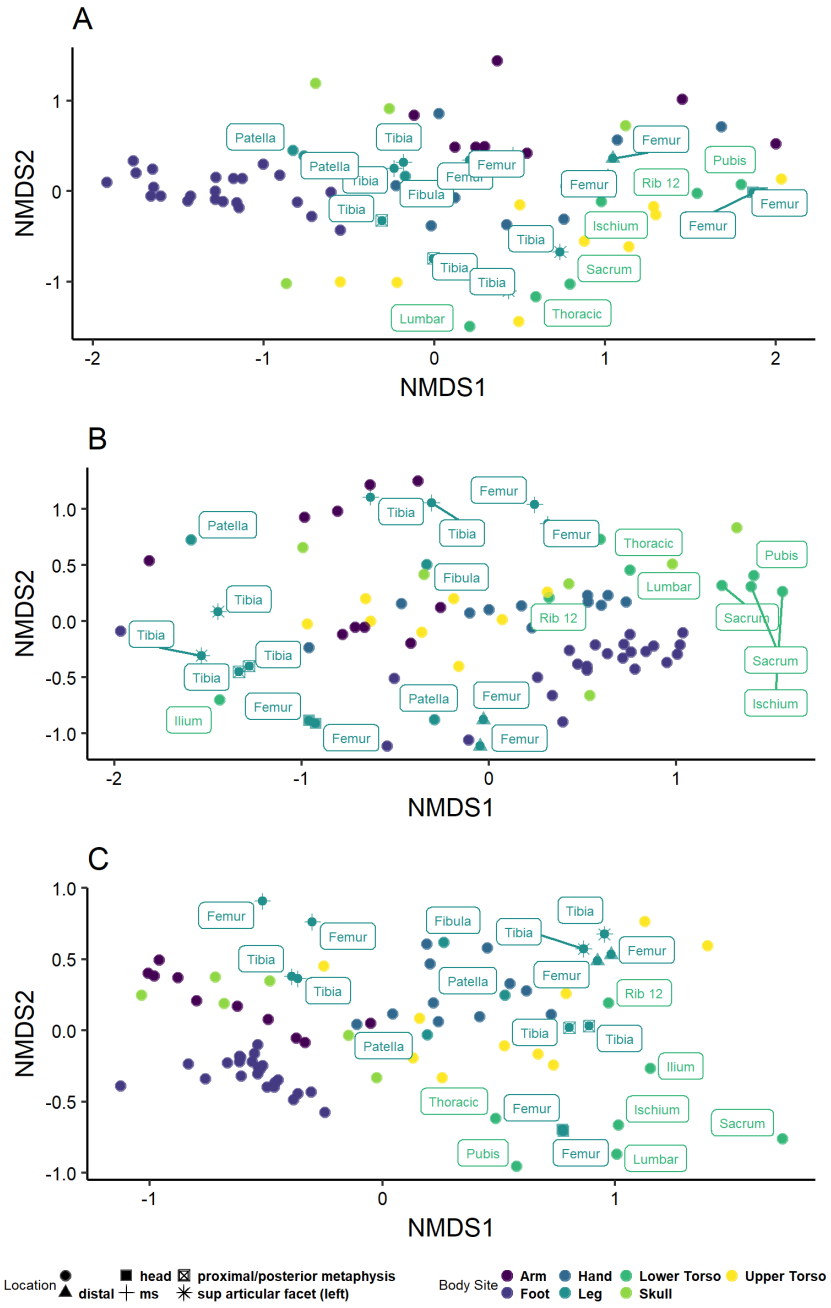

Figure S 4.4: **NMDS of Bray-Curtis dissimilarities of subsurface bones by anatomical region. (A) NMDS ordination of individual A (Stress = 0.162, k = 2, n = 78). (B) NMDS ordination of individual B (Stress = 0.153, k = 2, n = 82). (C) NMDS ordination of individual C (Stress = 0.172, k = 2, n = 82).**

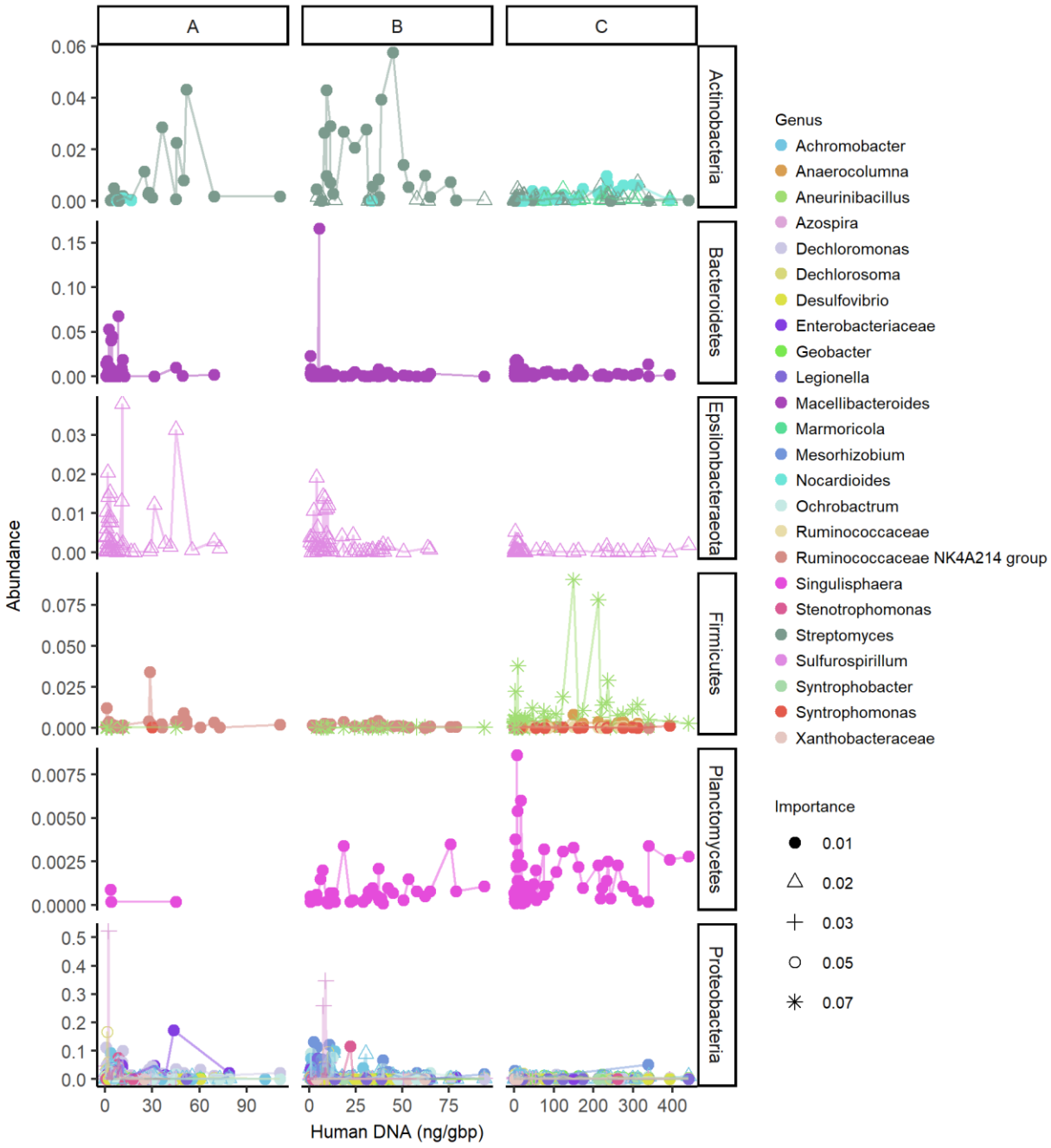

Figure S 4.5: **Important ASVs associated with subsurface skeletal DNA concentration, as predicted using Random Forest Modeling and visualized by individual and phylum. Abundance refers to relative abundance in a given sample; important taxa with relative abundances less than 0.01% were filtered from the data. Importance is the fraction of importance to the model (0.01 = 1% importance). Verrucomicrobia were excluded from the visualization.**

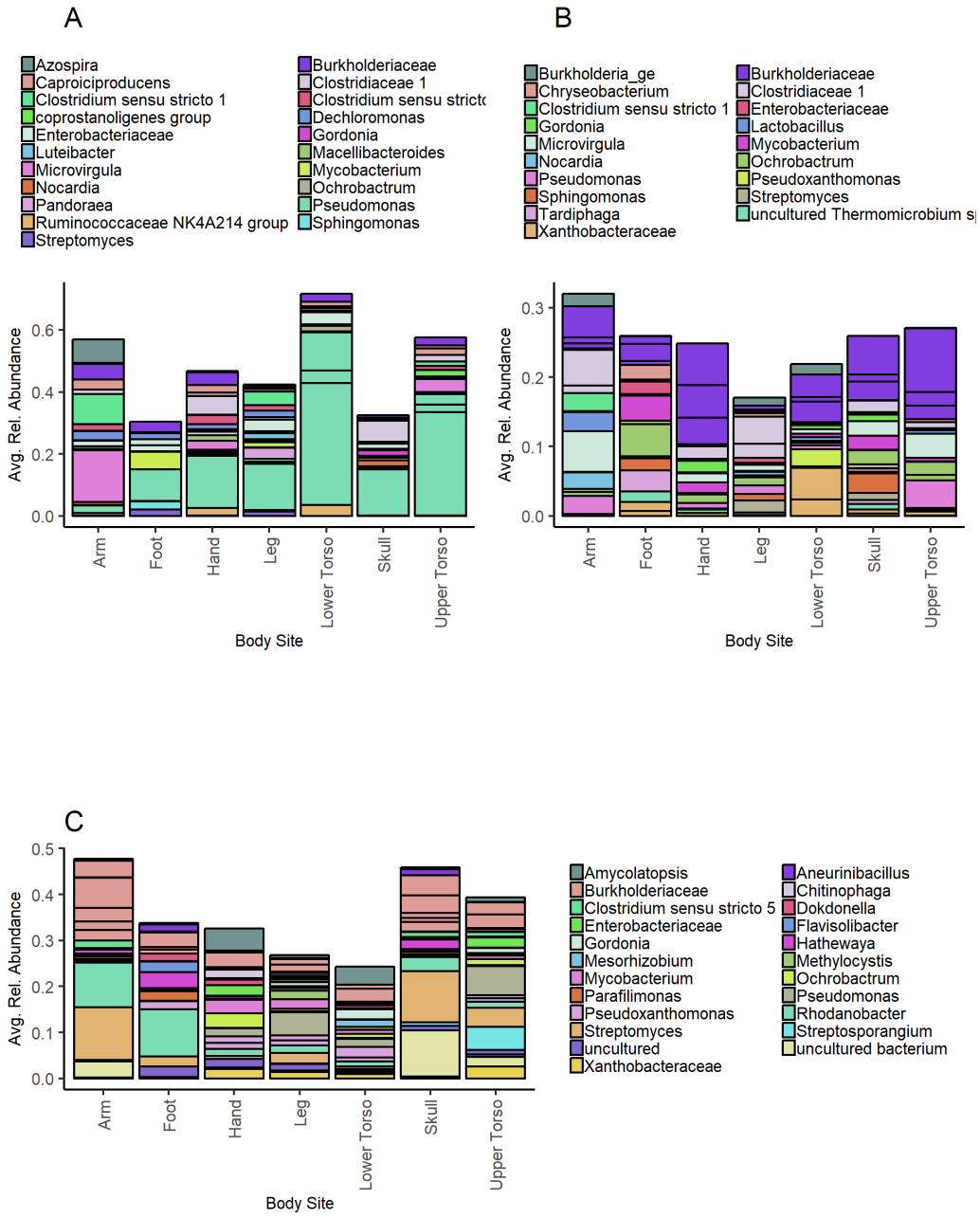

Figure S 4.6: SIMPER results by individual and anatomical region. Results are colored by genus, with black divisions separators denoting ASV. Relative abundances were averaged by body site. (A) Simper results for individual A. (B) Simper results for individual B, and (C) simper results for individual C.

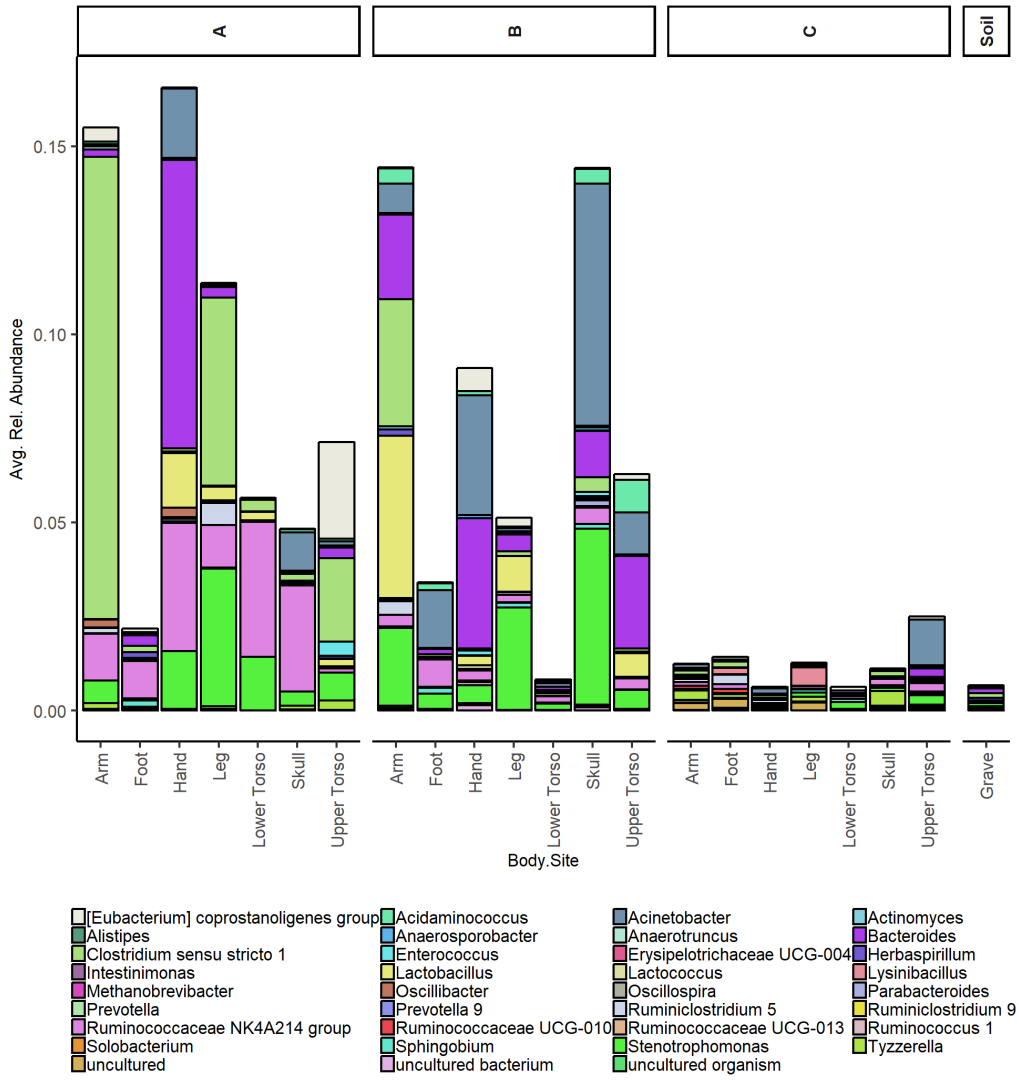

Figure S 4.7: Putative human-associated gut genera.

Table S 4.5: Human DNA concentrations by individual and deposition environment.

Project	Individual	Mean	Std. Dev	Max	Min
Grave	A	21.29	24.44	111.10	0.69
	B	20.74	21.02	94.00	0.48
	C	72.60	108.50	440.00	0.68
Surface	SA	46.79	72.96	477.50	0.00
	SB	145.89	177.74	926.00	10.90
	SC	93.94	124.87	493.48	0.00

CHAPTER 5
CONCLUSIONS, LIMITATIONS, AND FUTURE DIRECTIONS

Conclusions

In this dissertation I explored intra-individual and inter-individual patterns of DNA preservation by skeletal element type and interpreted these patterns using site-specific taphonomic variables including soil geochemistry and microbial ecology. Through this exploration, all objectives and questions raised in the introduction have been addressed and several key findings have emerged.

Key findings

1) Human DNA concentrations in buried remains varied by individual and anatomical region, and this variation, along with differences in STR recovery, could be used to create recommendations for skeletal DNA sampling from buried remains. Bones of the feet, specifically the cuneiforms, exhibited the best performance in human DNA testing and are recommended for skeletal DNA sampling when remains are buried and non-commingled.
2) Not a single long bone ranked among the top 10 most successful elements for human DNA testing for any individual. When considering bones that were sampled from multiple sites, total DNA was greater in both the humeral and femoral heads compared with their respective midshaft and distal ends.
3) Total bacterial and fungal gene abundances in bone, as a proxy for microbial loading, were not reliable predictors of human DNA concentration. Rather specific bacteria including *Clostridium* spp., which includes known collagenase-producers, as well as a suite of other taxa from the phyla Bacteroidetes, Proteobacteria, Planctomycetes, Firmicutes, and Actinobacteria have demonstrated inverse relationships with human DNA concentration. Colonization by one or more of these taxa is a potential mechanism through which skeletal DNA is degraded and/or released from bone.
4) Enteric microorganisms from the human gut likely play an important role in skeletal DNA preservation.
5) The deposition environment, specifically site hydrology, had a noticeable impact on patterns of skeletal DNA preservation. Though DNA preservation was significantly different between surface and subsurface remains (Figure 5.1), the feet demonstrated consistently high human DNA concentrations.

Patterns of skeletal DNA preservation in buried remains

Despite evidence that human tarsals have shown high DNA typing success from buried environments [9], we hypothesized that human skeletal DNA concentrations would be lower in predominantly cancellous elements recovered from a subsurface environment. This was not supported. Even among buried remains, bones of the foot yielded some of the highest concentrations of skeletal DNA. Though the mechanism driving this pattern remains unknown, we have proposed multiple interconnected and competing mechanisms in chapters III and IV. These include: (1) bones of the feet undergo extensive remodeling [176], which increases hematopoiesis and osteoclastic activity that stimulates the release of cellular DNA into the

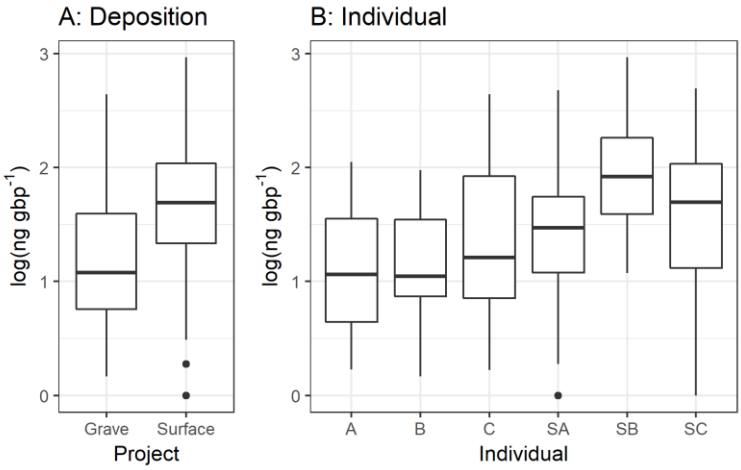

Figure 5.1: **Human DNA concentrations by depositional environment and individual. Data was log transformed. Human DNA concentrations were significantly different by depositional environment following an independent t-test (*p* = 1.43e-12) and individual following an ANOVA (p < 2e-16).**

surrounding bone matrix for eventual stabilization by hydroxyapatite (See Campos et al. [77]). (2) Bones of the feet harbor a unique foot microbiome following death, influenced by their distance from the gut and their tendency to mummify rather than liquify during decomposition. (3) In a grave environment plagued with intermittent water-logging, spatial positioning protected foot bones from multiple submersion events, decreasing the likelihood of hydroxyapatite dissolution and DNA release.

Based on the first mechanism, bones of the foot would start with a disproportionately high reservoir of human DNA due to activity and pressure in life. Previous research has observed remnant cellular material in close association with the trabeculae of foot bones [107]. This indicates that this material is not undergoing rapid degradation in the deposition environment, which likely relates to the second mechanism. Because feet lack a large amount of soft tissue, they tend to mummify rather than liquify during decomposition. This suggests that bones of the feet may lack the moisture necessary for microbial growth and motility, which is important for decomposition [30]. In addition, mummified skin may have a protective effect, delaying colonization by environmental microbes, especially phosphate solubilizing bacteria and fungi. The last mechanism is specific to the experimental site. As noted on several occasions, water is devastating to bone preservation [179]. Therefore, less exposure to water increases the likelihood of preservation. Because the pore structure of bone determines which portions of the bone interact with water [179], the spatial location of the feet in relatively dry areas of the grave likely impacted observed patterns in DNA success. An alternative pattern may have emerged had the feet been in a relatively wet area of the grave; though, this needs to be tested. Nevertheless, the physical/geochemical profile of the grave should be considered prior to making any DNA sampling decisions.

Prolonged and intermittent exposure to water was likely the primary factor related to skeletal DNA preservation in this research. Bones of individual A were submerged at the time of excavation and disinterment, and extensive adipocere formation on the same individual indicates decomposition in an anoxic, high moisture environment [204], which is further supported by

changes in soil geochemistry below depths of 40 cm [56]. Movement in and out of bone pore spaces increases the rate of inorganic dissolution [179].

Bone Colonizers and Degraders

A large number of microbial bone colonizers were extracted and sequenced using next generation sequencing technology from post-mortem human bone. Bones from both deposition environments were heavily influenced by Proteobacteria, Actinobacteria, Bacteroidetes, Firmicutes, and Patescibacteria. Bones deposited on the surface were additionally impacted by amoebic endosymbionts from the phylum Chlamydiae, and potential thermophiles from the phyla Chloroflexi and Deinococcus-Thermus. The presence of putative extremophiles in surface remains was interesting but not surprising, reflecting extreme changes in the surface deposition environment in temperature, moisture, and UV irradiation.

Random forest modeling was used to identify taxa predictive of human DNA concentration. RF models from both the surface and subsurface environment were generated, and the model was improved when including data from both deposition environments. RF models identified several putative taxa related to bone degradation. Among them, *Clostridium* spp., *Gordonia* spp., and *Streptomyces* spp. have the most potential, as these either have collagenolytic or phosphate solubilizing functions. SIMPER results further elucidated a potential role for *Pseudomonas* spp., which showed disproportionately lower relative abundances in bones of the feet, is implicated in osteomyelitis, and is a known phosphate solubilizing bacteria [95].

Limitations

Results suffered several limitations as a consequence of the experimental design. First and foremost, buried individuals were stacked in the grave, making it challenging to disentangle factors affecting differential decomposition. Though this was more realistic of a forensic scenario, use of multiple single burials would ease data interpretations. Second, remains were excavated over the course of a week, which exposed successive soil layers to new conditions, potentially shifting microbial community functionality within the grave. A similar problem was discussed in Child [35] in regard to archaeological sites. Once disinterred, remains were transported to the FAC, where they were stored on metal racks to undergo gentle washing and were then placed in cardboard boxes pending sampling. As indicated by Mircea et al. [87] there are drastic differences between the depositional environment and the storage environment that could influence degradation prior to sampling. Specifically, Mircea et al. [87] recovered several putative storage related fungal species including *S. chartarum*, *P. chrysogenum*, *A. versicolor*, and *P. pannorum*. Individual A was removed from the grave and placed in a body bag at 2°C. When long bones were later removed from storage, a noticeable fungal bloom was present on the remains. A blue fungal growth was also visible on the remains of B prior to gentle washing (Figure 5.2).

Third, several intrinsic factors - skeletal morphology, microanatomy, pathology, trauma, age, trace element composition, and sex - also relate to skeletal preservation [98]. Research presented here included willfully donated individuals to the William M. Bass Donated Skeletal Collection. The collection includes deceased individuals, and as such, demographics are skewed toward the old. In addition, deleterious health factors resulting in the death of donated individuals may also influence skeletal preservation. For example, the vertebral column of individual B was completely fused and bones from this individual were generally more brittle.

Figure 5.2: **Fungal bloom on individual A (left) following storage at 2°C and fungal growth (red arrows) on individual B (right) following storage at 22°C.**

Lastly, data analysis was primarily exploratory and was heavily influenced by our choice of molecular target, DNA. DNA can provide information regarding presence versus absence, but it cannot tell us anything about activity. Because of this, it is difficult to discern incidental taxa - taxa that are present and inactive - from taxa that are actively degrading bone. This is an issue that has long plagued microbial ecology – linking structure and function. Microbial dormancy through endospore formation among Gram positive bacteria [205] and microbial DNA bound to hydroxyapatite as a result of previous colonization [167] are particularly worrisome and can bias our interpretations.

Moreover, 16S rRNA gene amplicon sequencing results in amplification bias, with overrepresentation by some taxa and under representation by others, augmented by differences in 16S rRNA copy number per genome. A mock community sample from Zymo research (ZymoBIOMICS Microbial Community DNA Standard) was incorporated into subsurface sequencing runs. The reported "theoretical composition" included 12% of the following taxa: *Listeria monocytogenes*, *Pseudomonas aeruginosa*, *Bacillus subtilis*, *Escherichia coli*, *Salmonella enterica*, *Lactobacillus fermentum*, *Enterococcus faecalis*, and *Staphylococcus aureus*, and 2% composition from *Saccharomyces cerevisiae*, and *Cryptococcus neoformans*. Though mock communities were consistent across all three runs, *Listeria*, *Pseudomonas*, and *Microbacterium* were overrepresented (Figure 5.3).

All post-sequencing analyses will influence obtained results, and questions concerning data treatment are heavily debated. For example, some researchers suggest rarefying datasets to even depth [187], while others warn against it [206]. ASVs were screened using a prevalence threshold of 0.05% or 1% and were then combined at the genus level when all datasets were included in analyses. This along with rarefying to a depth of 10,000 reads resulted in a loss of potentially important taxa. Alternative practices (i.e., metagenomics) could provide strain level resolution that would ultimately be more informative, especially when identifying potential bone degraders.

In addition, though 18S rRNA gene amplicon sequencing was applied to surface remains, the use of 300 paired end chemistry to sequence a 576 bp target resulted in problems with downstream sequencing analysis. Sequence quality steadily declined at the ends of forward and reverse reads, resulting in increased sequencing errors. This made it exceptionally challenging to

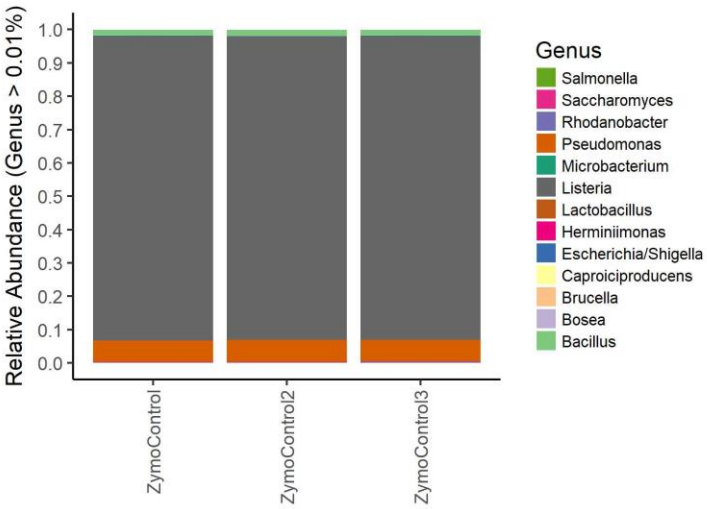

Figure 5.3: Community composition of positive controls from 3 MiSeq sequencing runs.

merge forward and reverse paired end reads, which consequently influenced read loss. Therefore, this research suffers from a lack of data regarding microbial eukaryotic bone colonizers and degraders. Collagenolytic fungal species have been cultured from degraded archaeological bone [70], while others can produce acids that target hydroxyapatite [79].

Future directions

This research represents a first step in understanding the dynamics of bone colonizing microbes, as such it leaves room for multiple avenues of additional research. First, while bacterial communities were the primary focus of this dissertation, fungal and other microbial eukaryotes are important to bone degradation. Therefore, this research would be greatly improved with the inclusion of high quality microbial eukaryotic and fungal datasets. Moreover, while we were able characterize who is colonizing bone, we could only speculate on their functional capabilities. Metatranscriptomic or metabolomic data could help us resolve important functional information. This could also be paired with more controlled experimental analysis, focusing on a few organisms. The study of biofilm formation and its relationship to skeletal degradation is particularly compelling (See Junka et al. [94,95]).

In addition, including multiple time points in future research would improve our ability to decipher primary, secondary, and tertiary degraders. This would also benefit by complementary analyses using microscopy to visualize microbial degraders and potential destructive foci. Lastly, the role of putrefactive bacteria in skeletal degradation and its timing could potentially be resolved through additional bacterial translocation studies, similar to Burcham et al. [85] but focused on the skeleton.

REFERENCES

[1] E. Hagelberg, I.C. Gray, A.J. Jeffreys, Identification of the skeletal remains of a murder victim by DNA analysis, Nature. 352 (1991) 427–429. doi:10.1038/352427a0.
[2] B.C. Smith, D.L. Fisher, V.W. Weedn, G.R. Warnock, M.M. Holland, A Systematic Approach to the Sampling of Dental DNA, 1993. www.astm.org (accessed November 25, 2018).
[3] T. Christian Boles, C.C. Snow, E. Stover, Forensic DNA Testing on Skeletal Remains from Mass Graves: A Pilot Project in Guatemala, 1995. www.astm.org (accessed November 25, 2018).
[4] S. Andelinović, D. Sutlović, I. Erceg Ivkosić, V. Skaro, A. Ivkosić, F. Paić, B. Rezić, M. Definis-Gojanović, D. Primorac, Twelve-year experience in identification of skeletal remains from mass graves., Croat. Med. J. 46 (2005) 530–539.
[5] A. Mundorff, J.M. Davoren, Examination of DNA yield rates for different skeletal elements at increasing post mortem intervals., Forensic Sci. Int. Genet. 8 (2014) 55–63. doi:10.1016/j.fsigen.2013.08.001.
[6] S. Edson, J. Ross, M. Coble, T. Parson, S. Barritt, Naming the Dead- Confronting the Realities of Rapid Identification of Degraded Skeletal Remains, Forensic Sci. Rev. 16 (2004) 63–90.
[7] M.D. Leney, Sampling skeletal remains for ancient DNA (aDNA): A measure of success, Hist. Archaeol. 40 (2006) 31–49.
[8] A. Milos, A. Selmanović, L. Smajlović, R.L.M. Huel, C. Katzmarzyk, A. Rizvić, T.J. Parsons, Success rates of nuclear short tandem repeat typing from different skeletal elements., Croat. Med. J. 48 (2007) 486–493.
[9] D. Hines, M. Vennemeyer, S. Amory, R. Huel, I. Hanson, C. Katzmarzyk, T. Parsons, Prioritized Sampling of Bone and Teeth for DNA Analysis in Commingled Cases, in: Commingled Hum. Remain. Methods Recover. Anal. Identif., Elsevier Inc, 2014: pp. 275–305.
[10] S.L. Forbes, Potential determinants of postmortem and postburial interval of buried remains., in: M. Tibbett, D.O. Carter (Eds.), Soil Anal. Forensic Taphon. Chem. Biol. Eff. Buried Hum. Remain., CRC Press, 2009: pp. 225–246.
[11] M.J. Collins, C.M. Nielsen-Marsh, J. Hiller, C.I. Smith, J.P. Roberts, R. V. Prigodich, T.J. Wess, J. Csapo, A.R. Millard, G. Turner-Walker, The survival of organic matter in bone: a review, Archaeometry. 44 (2002) 383–394. doi:10.1111/1475-4754.t01-1-00071.
[12] D.J. Levy-Booth, R.G. Campbell, R.H. Gulden, M.M. Hart, J.R. Powell, J.N. Klironomos, K.P. Pauls, C.J. Swanton, J.T. Trevors, K.E. Dunfield, Cycling of extracellular DNA in the soil environment, Soil Biol. Biochem. 39 (2007) 2977–2991. doi:10.1016/j.soilbio.2007.06.020.
[13] K.M. Nielsen, P.J. Johnsen, D. Bensasson, D. Daffonchio, Release and persistence of extracellular DNA in the environment., Environ. Biosafety Res. 6 (2007) 37–53. doi:10.1051/ebr:2007031.
[14] F.E. Damann, D.E. Williams, A.C. Layton, Potential Use of Bacterial Community Succession in Decaying Human Bone for Estimating Postmortem Interval , , J. Forensic Sci. 60 (2015) 844–850. doi:10.1111/1556-4029.12744.
[15] L.M. Misner, A.C. Halvorson, J.L. Dreier, D.H. Ubelaker, D.R. Foran, The correlation between skeletal weathering and dna quality and quantity, J. Forensic Sci. 54 (2009) 822–828. doi:10.1111/j.1556-4029.2009.01043.x.
[16] M.M.E.M.E. Jans, C.M.M. Nielsen-marsh, C.I.I. Smith, M.J.J. Collins, H. Kars,

Characterisation of microbial attack on archaeological bone, J. Archaeol. Sci. 31 (2004) 87–95. doi:10.1016/j.jas.2003.07.007.
[17] R.W. Mann, W.M. Bass, L. Meadows, Time since death and decomposition of the human body: variables and observations in case and experimental field studies., J. Forensic Sci. 35 (1990) 103–111.
[18] D.O. Carter, D. Yellowlees, M. Tibbett, Cadaver decomposition in terrestrial ecosystems, Naturwissenschaften. 94 (2007) 12–24. doi:10.1007/s00114-006-0159-1.
[19] H. Gill-King, Chemical and ultrastructural aspects of decomposition, Forensic Taphon. Postmortem Fate Hum. (1997). http://www.crcnetbase.com/doi/abs/10.1201/9781439821923.sec2 (accessed May 2, 2017).
[20] T. Simmons, P.A. Cross, R.E. Adlam, C. Moffatt, The influence of insects on decomposition rate in buried and surface remains, J. Forensic Sci. 55 (2010) 889–892. doi:10.1111/j.1556-4029.2010.01402.x.
[21] J.A. Payne, A Summer Carrion Study of the Baby Pig Sus Scrofa Linnaeus, Ecology. 46 (1965) 592–602.
[22] G.D. De Jong, W. Wyatt Hoback, L.G. Higley, Effect of Investigator Disturbance in Experimental Forensic Entomology: Carcass Biomass Loss and Temperature, J. Forensic Sci. 56 (2011) 1556–4029. doi:10.1111/j.1556-4029.2010.01552.x.
[23] Y. Jeong, L.M. Jantz, J. Smith, Investigation into Seasonal Scavenging Patterns of Raccoons on Human Decomposition, J. Forensic Sci. 61 (2016) 467–471. doi:10.1111/1556-4029.12992.
[24] A.C. Smith, The Effects of Sharp-Force Thoracic Trauma on the Rate and Pattern of Decomposition, J. Forensic Sci. 59 (2014) 319–326. doi:10.1111/1556-4029.12338.
[25] R. Miller, The Affects of Clothing on Human Decomposition: Implications for Estimating Time Since Death, Masters Theses. (2002). https://trace.tennessee.edu/utk_gradthes/856 (accessed February 4, 2019).
[26] A. Dautartas, M.W. Kenyhercz, G.M. Vidoli, L. Meadows Jantz, A. Mundorff, D.W. Steadman, Differential Decomposition Among Pig, Rabbit, and Human Remains, J. Forensic Sci. (2018). doi:10.1111/1556-4029.13784.
[27] W.C. Rodriguez, Decomposition of Buried and Submerged Bodies, in: M.H. Sorg, W.D. Haglund (Eds.), Forensic Taphon. Postmortem Fate Hum. Remain., CRC Press, 1997.
[28] W.C. Rodriguez, W.M. Bass, Decomposition of Buried Bodies and Methods That May Aid in Their Location, 30 (1985) 836–852.
[29] R.W. Merritt, R. Snider, J.L. de Jong, M. Eric Benbow, R.K. Kimbirauskas, R.E. Kolar, Collembola of the Grave: A Cold Case History Involving Arthropods 28 Years After Death, J. Forensic Sci. 52 (2007) 1359–1361. doi:10.1111/j.1556-4029.2007.00568.x.
[30] D.O. Carter, D. Yellowlees, M. Tibbett, Moisture can be the dominant environmental parameter governing cadaver decomposition in soil, Forensic Sci. Int. 200 (2010) 60–66. doi:10.1016/j.forsciint.2010.03.031.
[31] S. Fiedler, M. Graw, Decomposition of buried corpses, with special reference to the formation of adipocere., Naturwissenschaften. 90 (2003) 291–300. doi:10.1007/s00114-003-0437-0.
[32] S.L. Forbes, B.B. Dent, B.H. Stuart, The effect of soil type on adipocere formation, Forensic Sci. Int. 154 (2005) 35–43. doi:10.1016/j.forsciint.2004.09.108.
[33] M.H. Manheim, Decomposition Rates of Deliberate Burials: A Case Study of

Preservation, in: M.H. Sorg, W.D. Haglund (Eds.), Forensic Taphon. Postmortem Fate Hum. Remain., CRC Press, 1996: pp. 469–478.
[34] L.M. Swann, S.L. Forbes, S.W. Lewis, Analytical separations of mammalian decomposition products for forensic science: a review., Anal. Chim. Acta. 682 (2010) 9–22. doi:10.1016/j.aca.2010.09.052.
[35] A.M. Child, Microbial Taphonomy of Archaeological Bone, 1995. doi:10.2307/1506608.
[36] M.E. Benbow, a. J. Lewis, J.K. Tomberlin, J.L. Pechal, Seasonal necrophagous insect community assembly during vertebrate carrion decomposition, J. Med. Entomol. 50 (2013) 440–450. doi:10.1603/ME12194.
[37] J.L. Pechal, T.L. Crippen, M.E. Benbow, A.M. Tarone, S. Dowd, J.K. Tomberlin, The potential use of bacterial community succession in forensics as described by high throughput metagenomic sequencing, Int. J. Legal Med. 128 (2013) 193–205. doi:10.1007/s00414-013-0872-1.
[38] I. Can, G.T. Javan, A.E. Pozhitkov, P.A. Noble, Distinctive thanatomicrobiome signatures found in the blood and internal organs of humans., J. Microbiol. Methods. 106 (2014) 1–7. doi:10.1016/j.mimet.2014.07.026.
[39] J.L. Metcalf, Estimating the postmortem interval using microbes: Knowledge gaps and a path to technology adoption, Forensic Sci. Int. Genet. 38 (2019) 211–218. doi:10.1016/J.FSIGEN.2018.11.004.
[40] A. Belk, Z.Z. Xu, D.O. Carter, A. Lynne, S. Bucheli, R. Knight, J.L. Metcalf, Microbiome data accurately predicts the postmortem interval using random forest regression models, Genes (Basel). 9 (2018). doi:10.3390/genes9020104.
[41] J.L. Metcalf, L. Wegener Parfrey, A. Gonzalez, C.L. Lauber, D. Knights, G. Ackermann, G.C. Humphrey, M.J. Gebert, W. Van Treuren, D. Berg-Lyons, K. Keepers, Y. Guo, J. Bullard, N. Fierer, D.O. Carter, R. Knight, A microbial clock provides an accurate estimate of the postmortem interval in a mouse model system, Elife. 2 (2013) e01104. doi:10.7554/eLife.01104.
[42] S.J. Finley, M.E. Benbow, G.T. Javan, Microbial communities associated with human decomposition and their potential use as postmortem clocks, Int. J. Legal Med. (2014). doi:10.1007/s00414-014-1059-0.
[43] J.L. Metcalf, Z.Z. Xu, S. Weiss, S. Lax, W. Van Treuren, E.R. Hyde, S.J. Song, A. Amir, P. Larsen, N. Sangwan, D. Haarmann, G.C. Humphrey, G. Ackermann, L.R. Thompson, C. Lauber, A. Bibat, C. Nicholas, M.J. Gebert, J.F. Petrosino, S.C. Reed, J.A. Gilbert, A.M. Lynne, S.R. Bucheli, D.O. Carter, R. Knight, Microbial community assembly and metabolic function during mammalian corpse decomposition, Science (80-.). 351 (2016) 158–162. doi:10.1126/science.aad2646.
[44] K.A. Hauther, K.L. Cobaugh, L.M. Jantz, T.E. Sparer, J.M. Debruyn, Estimating Time Since Death from Postmortem Human Gut Microbial Communities, J. Forensic Sci. 60 (2015) 1234–1240. doi:10.1111/1556-4029.12828.
[45] J.M. DeBruyn, K.A. Hauther, Postmortem succession of gut microbial communities in deceased human subjects, PeerJ. 5 (2017) e3437. doi:10.7717/peerj.3437.
[46] E.R. Hyde, D.P. Haarmann, A.M. Lynne, S.R. Bucheli, J.F. Petrosino, The living dead: bacterial community structure of a cadaver at the onset and end of the bloat stage of decomposition., PLoS One. 8 (2013) e77733. doi:10.1371/journal.pone.0077733.
[47] J. Adserias-Garriga, | N M Quijada, | M Hernandez, | D Rodríguez Lázaro, | D Steadman, | L J Garcia-Gil, Dynamics of the oral microbiota as a tool to estimate time since death,

Mol Oral Microbiol. (2017) 32. doi:10.1111/omi.12191.
[48] G.T. Javan, S.J. Finley, T. Smith, J. Miller, J.E. Wilkinson, Cadaver Thanatomicrobiome Signatures: The Ubiquitous Nature of Clostridium Species in Human Decomposition, Front. Microbiol. 8 (2017).
[49] G.T. Javan, S.J. Finley, I. Can, J.E. Wilkinson, J.D. Hanson, A.M. Tarone, Human Thanatomicrobiome Succession and Time Since Death, Sci. Rep. 6 (2016) 29598. doi:10.1038/srep29598.
[50] K.L. Cobaugh, S.M. Schaeffer, J.M. DeBruyn, Functional and Structural Succession of Soil Microbial Communities below Decomposing Human Cadavers., PLoS One. 10 (2015) e0130201. doi:10.1371/journal.pone.0130201.
[51] R.C. Bergmann, T.K. Ralebitso-Senior, T.J.U. Thompson, An RNA-based analysis of changes in biodiversity indices in response to Sus scrofa domesticus decomposition, Forensic Sci. Int. 241 (2014) 190–194. doi:10.1016/j.forsciint.2014.06.001.
[52] L.A. Benninger, D.O. Carter, S.L. Forbes, The biochemical alteration of soil beneath a decomposing carcass, Forensic Sci. Int. 180 (2008) 70–75. doi:10.1016/j.forsciint.2008.07.001.
[53] T.B. Thomas, S.J. Finley, J.E. Wilkinson, D.J. Wescott, A. Gorski, G.T. Javan, G.T. Javan, Postmortem microbial communities in burial soil layers of skeletonized humans, J. Forensic Leg. Med. 49 (2017) 43–49. doi:10.1016/j.jflm.2017.05.009.
[54] J. Adserias-Garriga, M. Hernández, N.M. Quijada, D.R. Lázaro, D. Steadman, J. Garcia-Gil, Daily thanatomicrobiome changes in soil as an approach of postmortem interval estimation: An ecological perspective, Forensic Sci. Int. 278 (2017) 388–395. doi:10.1016/j.forsciint.2017.07.017.
[55] C.L. Lauber, J.L. Metcalf, K. Keepers, G. Ackermann, D.O. Carter, R. Knight, Vertebrate decomposition is accelerated by soil microbes, Appl. Environ. Microbiol. 80 (2014) 4920–4929. doi:10.1128/AEM.00957-14.
[56] S.W. Keenan, A.L. Emmons, L.S. Taylor, G. Phillips, A.R. Mason, A.Z. Mundorff, E.C. Bernard, J. Davoren, J.M. DeBruyn, Spatial impacts of a multi-individual grave on microbial and microfaunal communities and soil biogeochemistry, PLoS One. 13 (2018) e0208845. doi:10.1371/journal.pone.0208845.
[57] D.O. Carter, J.L. Metcalf, A. Bibat, R. Knight, Seasonal variation of postmortem microbial communities, Forensic Sci. Med. Pathol. 11 (2015) 202–207. doi:10.1007/s12024-015-9667-7.
[58] S.J. Finley, J.L. Pechal, M.E. Benbow, B.K. Robertson, G.T. Javan, & M.E. Benbow, B.K. Robertson, G.T. Javan, Microbial Signatures of Cadaver Gravesoil During Decomposition, Microb. Ecol. 71 (2016) 524–529. doi:10.1007/s00248-015-0725-1.
[59] M. Tibbett, D.O. Carter, T. Haslam, R. Major, R. Haslam, A laboratory incubation method for determining the rate of microbiological degradation of skeletal muscle tissue in soil., J. Forensic Sci. 49 (2004) 560–5. doi:10.1520/JFS2003247.
[60] D.O. Carter, M. Tibbett, Microbial decomposition of skeletal muscle tissue (Ovis aries) in a sandy loam soil at different temperatures, Soil Biol. Biochem. 38 (2006) 1139–1145. doi:10.1016/j.soilbio.2005.09.014.
[61] R.R. Parmenter, J.A. Macmahon, R.R. Parmenter1 ', J.A. Macmahon2, Carrion Decomposition and Nutrient Cycling in a Semiarid Shrub—Steppe Ecosystem Carrion decomposition and nutrient cycling in a semiarid shrub-steppe ecosystem, Source Ecol. Monogr. Ecol. Monogr. 79 (2009) 637–661. doi:10.1890/08-0972.1.

[62] J.K. Tomberlin, T.L. Crippen, A.M. Tarone, B. Singh, K. Adams, Y.H. Rezenom, M.E. Benbow, M. Flores, M. Longnecker, J.L. Pechal, D.H. Russell, R.C. Beier, T.K. Wood, Interkingdom responses of flies to bacteria mediated by fly physiology and bacterial quorum sensing, Anim. Behav. 84 (2012) 1449–1456. doi:10.1016/j.anbehav.2012.09.013.
[63] I. Szelecz, F. Sorge, C.V.W. Seppey, M. Mulot, H. Steel, R. Neilson, B.S. Griffiths, J. Amendt, E.A.D. Mitchell, Effects of decomposing cadavers on soil nematode communities over a one-year period, Soil Biol. Biochem. 103 (2016) 405–416. doi:10.1016/j.soilbio.2016.09.011.
[64] B. Singh, K.J. Minick, M.S. Strickland, K.G. Wickings, T.L. Crippen, A.M. Tarone, M.E. Benbow, N. Sufrin, J.K. Tomberlin, J.L. Pechal, Temporal and Spatial Impact of Human Cadaver Decomposition on Soil Bacterial and Arthropod Community Structure and Function, Front. Microbiol. 8 (2018) 2616. doi:10.3389/fmicb.2017.02616.
[65] I. Szelecz, B. Fournier, C. Seppey, J. Amendt, E. Mitchell, Can soil testate amoebae be used for estimating the time since death? A field experiment in a deciduous forest, Forensic Sci. Int. 236 (2014) 90–98. doi:10.1016/j.forsciint.2013.12.030.
[66] C.V.W. Seppey, B. Fournier, I. Szelecz, D. Singer, E.A.D. Mitchell, E. Lara, Response of forest soil euglyphid testate amoebae (Rhizaria: Cercozoa) to pig cadavers assessed by high-throughput sequencing, Int. J. Legal Med. 130 (2016) 551–562. doi:10.1007/s00414-015-1149-7.
[67] G. Turner-Walker, The Chemical and Microbial Degradation of Bones and Teeth, John Wiley and Sons, Ltd, 2008.
[68] D.B. Burr, O. Akkus, Bone Morphology and Organization, in: D.B. Burr, M.R. Allen (Eds.), Basic Appl. Bone Biol., 2nd ed., Elsevier Inc., 2014: pp. 3–25.
[69] H.P. Schwarcz, D. Abueidda, I. Jasiuk, The Ultrastructure of Bone and Its Relevance to Mechanical Properties, Front. Phys. 5 (2017). doi:10.3389/fphy.2017.00039.
[70] A.M.M. Child, Towards an Understanding of the Microbial Decomposition of Archaeological Bone in the Burial Environment, J. Archaeol. Sci. 22 (1995) 165–174. doi:10.1006/JASC.1995.0018.
[71] S.W. Keenan, A.S. Summers, Early diagenesis and recrystallization of bone, Geochim. Cosmochim. Acta. 196 (2017) 209–223. doi:10.1016/j.gca.2016.09.033.
[72] S. Keenan, From bone to fossil : a review of the diagenesis of bioapatite, Am. Mineral. (2016). doi:10.2138/am-2016-5737.
[73] M.J. Olszta, X. Cheng, S.S. Jee, R. Kumar, Y.-Y. Kim, M.J. Kaufman, E.P. Douglas, L.B. Gower, L.B. Gower, Bone structure and formation: A new perspective, Mater. Sci. Eng. R. (2007). doi:10.1016/j.mser.2007.05.001.
[74] C. Kendall, A. Marie, H. Eriksen, I. Kontopoulos, M.J. Collins, G. Turner-Walker, A.M.H. Eriksen, I. Kontopoulos, M.J. Collins, G. Turner-Walker, A. Marie, H. Eriksen, I. Kontopoulos, M.J. Collins, G. Turner-Walker, Diagenesis of archaeological bone and tooth, Palaeogeogr. Palaeoclimatol. Palaeoecol. 491 (2018) 21–37. doi:10.1016/j.palaeo.2017.11.041.
[75] M.M.E. Jans, Microbial bioerosion of bone-a review, in: M. Wisshak, L. Tapanila (Eds.), Curr. Dev. Bioerosion, Springer-Verlag, Berlin, 2008: pp. 397–413. doi:10.1007/978-3-540-77598-0_20.
[76] A. Gotherstrom, M.J. Collins, A. Angerbjorn, K. Liden, Bone preservation and DNA amplification, Archaeometry. 3 (2002) 395–404. doi:10.1111/1475-4754.00072.
[77] P.F. Campos, O.E. Craig, G. Turner-Walker, E. Peacock, E. Willerslev, M.T.P. Gilbert,

DNA in ancient bone - Where is it located and how should we extract it?, Ann. Anat. 194 (2012) 7–16. doi:10.1016/j.aanat.2011.07.003.
[78] C. Sosa, E. Vispe, C. Núñez, M. Baeta, Y. Casalod, M. Bolea, R.E.M. Hedges, B. Martinez-Jarreta, Association between ancient bone preservation and dna yield: a multidisciplinary approach., Am. J. Phys. Anthropol. 151 (2013) 102–9. doi:10.1002/ajpa.22262.
[79] V. Marchiafava, E. Bonucci, A. Ascenzi, Fungal Osteoclasia: a Model of Dead Bone Resorption, Calcif. Tissue Res. 14 (1974) 195–210.
[80] C.N. Trueman, D.M. Martill, The long-term survival of bone: the role of bioerosion, Archaeometry. 44 (2002) 371–382. doi:10.1111/1475-4754.t01-1-00070.
[81] C.J. Hackett, Microscopical Focal Destruction (Tunnels) in Exhumed Human Bones, Med. Sci. Law. 21 (1981) 243–265. doi:10.1177/002580248102100403.
[82] L. White, T.J. Booth, The origin of bacteria responsible for bioerosion to the internal bone microstructure: Results from experimentally-deposited pig carcasses, Forensic Sci. Int. 239 (2014) 92–102. doi:10.1016/j.forsciint.2014.03.024.
[83] T.J. Booth, An Investigation Into the Relationship Between Funerary Treatment and Bacterial Bioerosion in European Archaeological Human Bone, Archaeometry. 58 (2016) 484–499. doi:10.1111/arcm.12190.
[84] L.S. Bell, M.F. Skinnerb, S.J. Jonesa, The speed of post mortem change to the human skeleton and its taphonomic significance, Forensic Sci. Int. 82 (1996) 129–140.
[85] Z.M. Burcham, J.A. Hood, J.L. Pechal, K.L. Krausz, J.L. Bose, C.J. Schmidt, M.E. Benbow, H.R. Jordan, Fluorescently labeled bacteria provide insight on post-mortem microbial transmigration, Forensic Sci. Int. 264 (2016) 63–69. doi:10.1016/j.forsciint.2016.03.019.
[86] A. Balzer, G. Gleixner, G. Grupe, H.-L. Schmidt, S. Schramm, S. Turban-Just, In vitro decomposition of bone collagen by soil bacteria: the implications for stable isotope analysis in archaeometry, Archaeometry. 39 (1997) 415–429. doi:10.1111/j.1475-4754.1997.tb00817.x.
[87] C. Mircea, A. Vulpoi, I. Rusu, C. Radu, M. Pârvu, B. Kelemen, Exploring post-excavation degradation potential of fungal communities associated with archaeological human remains, Archaeometry. (2018). doi:10.1111/arcm.12438.
[88] L.S. Bell, A. Elkerton, Unique Marine Taphonomy in Human Skeletal Material Recovered from the Medieval Warship Mary Rose, Int. J. Osteoarchaeol. 18 (2008) 523–535. doi:10.1002/oa.952.
[89] J.T. Staley, A. Konopka, MEASUREMENT OF IN SITU ACTI\TITIES OF NONPHOTOSYNTHETIC MICROORGANISMS IN AQUATIC AND TERRESTRIAL HABITATS, Annu. Rev. Microbiol. 39 (1985) 321–346.
[90] V. Reeb, A. Kolel, T.R. McDermott, D. Bhattacharya, Good to the bone: Microbial community thrives within bone cavities of a bison carcass at Yellowstone National Park, Environ. Microbiol. 13 (2011) 2403–2415. doi:10.1111/j.1462-2920.2010.02359.x.
[91] H.I. Hollund, M.D. Teasdale, V. Mattiangeli, O.Ó. Sverrisdóttir, D.G. Bradley, T. O'connor, Pick the Right Pocket. Sub-sampling of Bone Sections to Investigate Diagenesis and DNA Preservation, Int. J. Osteoarchaeol. 27 (2017) 365–374. doi:10.1002/oa.2544.
[92] N.D. Higgs, C.T.S. Little, A.G. Glover, Bones as biofuel: a review of whale bone composition with implications for deep-sea biology and palaeoanthropology.,

Proceedings. Biol. Sci. 278 (2011) 9–17. doi:10.1098/rspb.2010.1267.
[93] H.S. Aronson, A.J. Zellmer, S.K. Goffredi, The specific and exclusive microbiome of the deep-sea bone-eating snail, Rubyspira osteovora, FEMS Microbiol. Ecol. 93 (2017). doi:10.1093/femsec/fiw250.
[94] A. Junka, P. Szymczyk, G. Ziółkowski, E. Karuga-Kuzniewska, D. Smutnicka, I. Bil-Lula, M. Bartoszewicz, S. Mahabady, P.P. Sedghizadeh, Bad to the Bone: On In Vitro and Ex Vivo Microbial Biofilm Ability to Directly Destroy Colonized Bone Surfaces without Participation of Host Immunity or Osteoclastogenesis, PLoS One. 12 (2017) e0169565. doi:10.1371/journal.pone.0169565.
[95] A.F. Junka, P. Szymczyk, D. Smutnicka, M. Kos, I. Smolina, M. Bartoszewicz, E. Chlebus, M. Turniak, P.P. Sedghizadeh, Microbial biofilms are able to destroy hydroxyapatite in the absence of host immunity in vitro, J. Oral Maxillofac. Surg. 73 (2015) 451–464. doi:10.1016/j.joms.2014.09.019.
[96] C.M. Nielsen-Marsh, R.E.M. Hedges, Patterns of Diagenesis in Bone I: The Effects of Site Environments, J. Archaeol. Sci. 27 (2000) 1139–1150. doi:10.1006/jasc.1999.0537.
[97] J. Burger, S. Hummel, B. Hermann, W. Henke, DNA preservation: a microsatellite-DNA study on ancient skeletal remains., Electrophoresis. 20 (1999) 1722–8. doi:10.1002/(SICI)1522-2683(19990101)20:8<1722::AID-ELPS1722>3.0.CO;2-4.
[98] A. Galloway, P. Willey, L. Snyder, Human Bone Mineral densities and survival of bone elements: a contemporary example, in: M.H. Sorg, W.D. Haglund (Eds.), Forensic Taphon. Postmortem Fate Hum. Remain., CRC Press, 1997.
[99] S. Haynes, J.B. Searle, A. Bretman, K.M.† Dobney, Bone Preservation and Ancient DNA: The Application of Screening Methods for Predicting DNA Survival, J. Archaeol. Sci. 29 (2002) 585–592. doi:10.1006/jasc.2001.0731.
[100] W.L. Perry, W.M. Bass, W.S. Riggsby, K. Sirotkin, The autodegradation of deoxyribonucleic acid (DNA) in human rib bone and its relationship to the time interval since death., J. Forensic Sci. 33 (1988) 144–53. http://www.ncbi.nlm.nih.gov/pubmed/3351452.
[101] C. Kaiser, B. Bachmeier, C. Conrad, A. Nerlich, H. Bratzke, W. Eisenmenger, O. Peschel, Molecular study of time dependent changes in DNA stability in soil buried skeletal residues, Forensic Sci. Int. 177 (2008) 32–36. doi:10.1016/j.forsciint.2007.10.005.
[102] R. Alaeddini, M. Ahmadi, S.J. Walsh, A. Abbas, Semi-quantitative PCR Analysis of DNA Degradation, Aust. J. Forensic Sci. 43 (2011) 53–64. doi:10.1080/00450618.2010.498026.
[103] D.R. Foran, Relative degradation of nuclear and mitochondrial DNA: An experimental approach, J. Forensic Sci. 51 (2006) 766–770. doi:10.1111/j.1556-4029.2006.00176.x.
[104] R. Alaeddini, S.J. Walsh, A. Abbas, Forensic implications of genetic analyses from degraded DNA--a review., Forensic Sci. Int. Genet. 4 (2010) 148–57. doi:10.1016/j.fsigen.2009.09.007.
[105] Latham, Madonna, DNA Survivability in Skeletal Remains, in: J. Pokines, S.A. Symes (Eds.), Man. Forensic Taphon., CRC Press, 2013.
[106] E.S.M. Iwamura, C.R.G.C.M. Oliveira, J.A. Soares-Vieira, S.A.B. Nascimento, D.R. Mu??oz, A Qualitative Study of Compact Bone Microstructure and Nuclear Short Tandem Repeat Obtained From Femur of Human Remains Found on the Ground and Exhumed 3 Years After Death, Am. J. Forensic Med. Pathol. 26 (2005) 33–44. doi:10.1097/01.paf.0000154116.30837.d5.
[107] J.M. Andronowski, A.Z. Mundorff, I. V Pratt, J.M. Davoren, D.M.L. Cooper, Evaluating

differential nuclear DNA yield rates and osteocyte numbers among human bone tissue types: A synchrotron radiation micro-CT approach, 28 (2017) 211–218. doi:10.1016/j.fsigen.2017.03.002.
[108] S.M. Edson, A.F. Christensen, S.M. Barritt, A. Meehan, M.D. Leney, L.N. Finelli, Sampling of the cranium for mitochondrial DNA analysis of human skeletal remains, Forensic Sci. Int. Genet. Suppl. Ser. 2 (2009) 269–270. doi:10.1016/j.fsigss.2009.09.029.
[109] A.Z. Mundorff, E.J. Bartelink, E. Mar-Cash, DNA preservation in skeletal elements from the world trade center disaster: Recommendations for Mass Fatality Management, J. Forensic Sci. 54 (2009) 739–745. doi:10.1111/j.1556-4029.2009.01045.x.
[110] a Alonso, S. Andelinović, P. Martín, D. Sutlović, I. Erceg, E. Huffine, L.F. de Simón, C. Albarrán, M. Definis-Gojanović, a Fernández-Rodriguez, P. García, I. Drmić, B. Rezić, S. Kuret, M. Sancho, D. Primorac, DNA typing from skeletal remains: evaluation of multiplex and megaplex STR systems on DNA isolated from bone and teeth samples., Croat. Med. J. 42 (2001) 260–266. doi:10.1016/j.seppur.2013.09.009.
[111] P. Gilbert, Marcus, Thomas, L. Rudbeck, E. Willerslev, A.J. Hansen, C. Smith, K.E.H. Penkman, K. Prangenberg, C.M. Nielsen-Marsh, M.E. Jans, P. Arthur, N. Lynnerup, G. Turner-Walker, M. Biddle, B. Kjølbye-Biddle, M.J. Collins, Biochemical and physical correlates of DNA contamination in archaeological human bones and teeth excavated at Matera, Italy, J. Archaeol. Sci. 32 (2005) 785–793. doi:10.1016/j.jas.2004.12.008.
[112] R. Alaeddini, Forensic implications of PCR inhibition--A review., Forensic Sci. Int. Genet. 6 (2012) 297–305. doi:10.1016/j.fsigen.2011.08.006.
[113] M.N. Hochmeister, B. Budowle, U. V. Borer, U. Eggmann, C.T. Comey, R. Dirnhofer, Typing of Deoxyribonucleic Acid (DNA) Extracted from Compact Bone from Human Remains, 1991. www.astm.org (accessed May 9, 2019).
[114] S.T.G. Ferreira, H.H. Kuser, R.G. Garrido, A. Trindade-Filho, K.A. Paula, M.F. Galvão, A. V. Moraes, Floods and mudslides in the State of Rio de Janeiro and a plane crash in the Brazilian Amazon rainforest: A study of two different experiences in disaster victim identification (DVI), Forensic Sci. Int. Genet. Suppl. Ser. 3 (2011) e516–e517. doi:10.1016/j.fsigss.2011.10.005.
[115] S.T.G.G. Ferreira, R.G. Garrido, K.A. Paula, R.C. Nogueira, E.S. Oliveira, A. V. Moraes, Cartilage and phalanges from hallux: Alternative sources of samples for DNA typing in disaster victim identification (DVI). A comparative study, Forensic Sci. Int. Genet. Suppl. Ser. 4 (2013) e366–e367. doi:10.1016/j.fsigss.2013.10.186.
[116] R. Pinhasi, D. Fernandes, K. Sirak, M. Novak, S. Connell, S. Alpaslan-Roodenberg, F. Gerritsen, V. Moiseyev, A. Gromov, P. Raczky, A. Anders, M. Pietrusewsky, G. Rollefson, M. Jovanovic, H. Trinhhoang, G. Bar-Oz, M. Oxenham, H. Matsumura, M. Hofreiter, Optimal Ancient DNA Yields from the Inner Ear Part of the Human Petrous Bone, PLoS One. 10 (2015) e0129102. doi:10.1371/journal.pone.0129102.
[117] K.A. Sirak, D.M. Fernandes, O. Cheronet, M. Novak, B. Gamarra, T. Balassa, Z. Bernert, A. Cséki, J. Dani, J.Z. Gallina, G. Kocsis-Buruzs, I. Kővári, O. László, I. Pap, R. Patay, Z. Petkes, G. Szenthe, T. Szeniczey, T. Hajdu, R. Pinhasi, A minimally-invasive method for sampling human petrous bones from the cranial base for ancient DNA analysis, Biotechniques. 62 (2017). doi:10.2144/000114558.
[118] E. Pilli, S. Vai, M.G. Caruso, G. D'errico, A. Berti, D. Caramelli, Neither femur nor tooth: Petrous bone for identifying archaeological bone samples via forensic approach, (2018). doi:10.1016/j.forsciint.2017.12.023.

[119] H.B. Hansen, P.B. Damgaard, A. Margaryan, J. Stenderup, N. Lynnerup, E. Willerslev, M.E. Allentoft, Comparing Ancient DNA Preservation in Petrous Bone and Tooth Cementum, PLoS One. 12 (2017) e0170940. doi:10.1371/journal.pone.0170940.
[120] E.M. Frank, A.Z. Mundorff, J.M. Davoren, The effect of common imaging and hot water maceration on DNA recovery from skeletal remains, Forensic Sci. Int. 257 (2015) 189–195. doi:10.1016/j.forsciint.2015.08.019.
[121] G. Turner-walker, The Chemical and Microbial Degradation of Bones and Teeth, in: R. Pinhasi, S. Mays (Eds.), Adv. Hum. Palaeopathology, John Wiley & Sons, Ltd, 2008: pp. 3–29.
[122] S. Amory, R. Huel, A. Bilić, O. Loreille, T.J. Parsons, Automatable full demineralization DNA extraction procedure from degraded skeletal remains, Forensic Sci. Int. Genet. 6 (2012) 398–406. doi:10.1016/j.fsigen.2011.08.004.
[123] McDonald et al. American Gut: an Open Platform for Citizen Science Microbiome Research, MSystems. 3 (2018) e00031-18. doi:10.1128/mSystems.00031-18.
[124] N.R. Shirley, R.J. Wilson, L.M. Jantz, Cadaver use at the University of Tennessee's Anthropological Research Facility, Clin. Anat. 24 (2011) 372–380. doi:10.1002/ca.21154.
[125] A.E. Magurran, Ecological Diversity and Its Measurement, Chapman & Hall 1996, 1988. https://link-springer-com.proxy.lib.utk.edu/content/pdf/10.1007%2F978-94-015-7358-0.pdf (accessed May 9, 2019).
[126] T.C.J. Hill, K.A. Walsh, J.A. Harris, B.F. Moffett, Using ecological diversity measures with bacterial communities, FEMS Microbiol. Ecol. 43 (2003) 1–11. doi:10.1111/j.1574-6941.2003.tb01040.x.
[127] M. Greenacre, Measures of Distance between Samples: Non-Euclidean, in: M. Greenacre, R. Primicerio (Eds.), Multivar. Anal. Ecol. Data, 2013. www.fbbva.eswww.multivariatestatistics.org (accessed May 9, 2019).
[128] K.R. Clarke, Nonparametric Multivariate Analyses of Changes in Community Structure, Aust. J. Ecol. 18 (1993) 117–143. doi:10.1111/j.1442-9993.1993.tb00438.x.
[129] A. Ramette, Multivariate analyses in microbial ecology, FEMS Microbiol. Ecol. 62 (2007) 142–160. doi:10.1111/j.1574-6941.2007.00375.x.
[130] C. Lozupone, R. Knight, UniFrac: a New Phylogenetic Method for Comparing Microbial Communities, Appl. Environ. Microbiol. 71 (2005) 8228–8235. doi:10.1128/AEM.71.12.8228-8235.2005.
[131] C.A. Lozupone, M. Hamady, S.T. Kelley, R. Knight, Quantitative and Qualitative Diversity Measures Lead to Different Insights into Factors That Structure Microbial Communities Downloaded from, Appl. Environ. Microbiol. 73 (2007) 1576–1585. doi:10.1128/AEM.01996-06.
[132] Z. Xu, D. Malmer, M.G.I. Langille, S.F. Way, R. Knight, Which is more important for classifying microbial communities: who's there or what they can do?, ISME J. 8 (2014) 2357. doi:10.1038/ISMEJ.2014.157.
[133] R.D. Cutler, T.C. Edwards, K.H. Beard, A. Cutler, K.T. Hess, J. Gibson, J.J. Lawler, Random Forests for Classification in Ecology, Ecol. Soc. Am. 88 (2007) 2783–2792.
[134] M.S. Megyesi, S.P. Nawrocki, N.H. Haskell, Using accumulated degree-days to estimate the postmortem interval from decomposed human remains., J. Forensic Sci. 50 (2005) 618–626. doi:10.1520/JFS2004017.
[135] J. Elsner, J. Schibler, M. Hofreiter, A. Schlumbaum, Burial condition is the most important factor for mtDNA PCR amplification success in Palaeolithic equid remains

from the Alpine foreland, Archaeol. Anthropol. Sci. 7 (2015) 505–515. doi:10.1007/s12520-014-0213-4.
[136] M. Schultz, Microscopic Structure of Bone, in: Forensic Taphon. Postmortem Fate Hum. Remain., 1997: pp. 187–199.
[137] M. Graw, H.J. Weisser, S. Lutz, DNA typing of human remains found in damp environments, Forensic Sci. Int. 113 (2000) 91–95. doi:10.1016/S0379-0738(00)00221-8.
[138] M.T.P. Gilbert, L. Rudbeck, E. Willerslev, A.J. Hansen, C. Smith, K.E.H. Penkman, K. Prangenberg, C.M. Nielsen-Marsh, M.E. Jans, P. Arthur, N. Lynneruo, G. Turner-Walker, M. Biddle, B. Kj??lbye, M.J. Collins, Biochemical and physical correlates of DNA contamination in archaeological human bones and teeth excavated at Matera, Italy, J. Archaeol. Sci. 32 (2005) 785–793. doi:10.1016/j.jas.2004.12.008.
[139] M.M.E. Jans, H. Kars, C.M. Nielsen-Marsh, C.I. Smith, A.G. Nord, P. Arthur, N. Earl, IN SITU PRESERVATION OF ARCHAEOLOGICAL BONE: A HISTOLOGICAL STUDY WITHIN A MULTIDISCIPLINARY APPROACH, Archaeometry. 44 (2002) 343–352.
[140] M. Castillo, S.M. Martín-Orúe, E.G. Manzanilla, I. Badiola, M. Martín, J. Gasa, Quantification of total bacteria, enterobacteria and lactobacilli populations in pig digesta by real-time PCR, Vet. Microbiol. 114 (2006) 165–170. doi:10.1016/j.vetmic.2005.11.055.
[141] A. Klindworth, E. Pruesse, T. Schweer, J. Peplies, C. Quast, M. Horn, F.O. Glöckner, Evaluation of general 16S ribosomal RNA gene PCR primers for classical and next-generation sequencing-based diversity studies., Nucleic Acids Res. 41 (2013) e1. doi:10.1093/nar/gks808.
[142] L.W. Hugerth, E.E.L. Muller, Y.O.O. Hu, L.A.M. Lebrun, H. Roume, D. Lundin, P. Wilmes, A.F. Andersson, Systematic design of 18S rRNA gene primers for determining eukaryotic diversity in microbial consortia, PLoS One. 9 (2014). doi:10.1371/journal.pone.0095567.
[143] M. Martin, Cutadapt removes adapter sequences from high-throughput sequencing reads kenkyuhi hojokin gan rinsho kenkyu jigyo., EMBnet.Journal. 17 (2013) 10–12. doi:10.14806/ej.17.1.200.
[144] A.M. Bolger, M. Lohse, B. Usadel, Trimmomatic: A flexible read trimming tool for Illumina NGS data, Bioinformatics. btu170 (2014).
[145] P.D. Schloss, S.L. Westcott, T. Ryabin, J.R. Hall, M. Hartmann, E.B. Hollister, R.A. Lesniewski, B.B. Oakley, D.H. Parks, C.J. Robinson, J.W. Sahl, B. Stres, G.G. Thallinger, D.J. Van Horn, C.F. Weber, Introducing mothur: Open-source, platform-independent, community-supported software for describing and comparing microbial communities, Appl. Environ. Microbiol. 75 (2009) 7537–7541. doi:10.1128/AEM.01541-09.
[146] R.C. Team, R: A language and environment for statistical computing., (2018).
[147] P.J. McMurdie, S. Holmes, Phyloseq: a bioconductor package for handling and analysis of high-throughput phylogenetic sequence data., Pac. Symp. Biocomput. (2012) 235–46. http://www.ncbi.nlm.nih.gov/pubmed/22174279 (accessed August 8, 2017).
[148] A. Steinberger, seq-scripts release v. 1.0., (2016). doi:10.5281/zenodo.1458243.
[149] D.O. Carter, M. Tibbett, Taphonomic mycota: fungi with forensic potential., J. Forensic Sci. 48 (2003) 168–171. doi:JFS2002169_481.
[150] K. Dumack, S. Flues, K. Hermanns, M. Bonkowski, Rhogostomidae (Cercozoa) from soils, roots and plant leaves (Arabidopsis thaliana): Description of Rhogostoma epiphylla

sp. nov. and R. cylindrica sp. nov., Eur. J. Protistol. 60 (2017) 76–86. doi:10.1016/j.ejop.2017.06.001.
[151] I. Szelecz, Losch, Sandra, Seppey, Christophe V.W., Lara, Enrique, Singer, David, Sorge, Franziska, Tschui, Joelle, Perotti, M. Alejandra, E.A.D. Mitchell, Comparative analysis of bones, mites, soil chemistry, nematodes and soil micro-eukaryotes from a suspected homicide to estimate the post-mortem interval, Nat. Sci. Reports. 8 (2018) 1:14.
[152] N. Theodorakopoulos, D. Bachar, R. Christen, K. Alain, V. Chapon, Exploration of Deinococcus-Thermus molecular diversity by novel group-specific PCR primers, Microbiologyopen. 2 (2013) 862–872. doi:10.1002/mbo3.119.
[153] N. Fierer, M. Hamady, C.L. Lauber, R. Knight, The influence of sex, handedness, and washing on the diversity of hand surface bacteria, Proc. Natl. Acad. Sci. 105 (2008) 17994–17999. doi:10.1073/PNAS.0807920105.
[154] C. De Filippo, D. Cavalieri, M. Di Paola, M. Ramazzotti, J.B. Poullet, S. Massart, S. Collini, G. Pieraccini, P. Lionetti, Impact of diet in shaping gut microbiota revealed by a comparative study in children from Europe and rural Africa., Proc. Natl. Acad. Sci. U. S. A. 107 (2010) 14691–6. doi:10.1073/pnas.1005963107.
[155] HMP Consortium. Structure, function and diversity of the healthy human microbiome, Nature. 486 (2012) 207–214. doi:10.1038/nature11234.
[156] N. Larsen, F.K. Vogensen, F.W.J. van den Berg, D.S. Nielsen, A.S. Andreasen, B.K. Pedersen, W.A. Al-Soud, S.J. Sørensen, L.H. Hansen, M. Jakobsen, Gut Microbiota in Human Adults with Type 2 Diabetes Differs from Non-Diabetic Adults, PLoS One. 5 (2010) e9085. doi:10.1371/journal.pone.0009085.
[157] J.L. Pechal, C.J. Schmidt, H.R. Jordan, M.E. Benbow, A large-scale survey of the postmortem human microbiome, and its potential to provide insight into the living health condition, Nat. Sci. Reports. 8 (2018). doi:10.1038/s41598-018-23989-w.
[158] J.G. Caporaso, C.L. Lauber, E.K. Costello, D. Berg-Lyons, A. Gonzalez, J. Stombaugh, D. Knights, P. Gajer, J. Ravel, N. Fierer, J.I. Gordon, R. Knight, Moving pictures of the human microbiome, Genome Biol. 12 (2011) R50. doi:10.1186/gb-2011-12-5-r50.
[159] E.E.K. Costello, C.C.L. Lauber, M. Hamady, N. Fierer, J.I. Gordon, R. Knight, Bacterial community variation in human body habitats across space and time, Science (80-.). 326 (2009) 1694–7. doi:10.1126/science.1177486.Bacterial.
[160] N. Fierer, C.L. Lauber, N. Zhou, D. McDonald, E.K. Costello, R. Knight, Forensic identification using skin bacterial communities., Proc. Natl. Acad. Sci. U. S. A. 107 (2010) 6477–6481. doi:10.1073/pnas.1000162107.
[161] S. Lax, J.T. Hampton-Marcell, S.M. Gibbons, G.B. Colares, D. Smith, J.A. Eisen, J.A. Gilbert, Forensic analysis of the microbiome of phones and shoes, Microbiome. 3 (2015) 21. doi:10.1186/s40168-015-0082-9.
[162] R.A. Nicholson, Bone Degradation, Burial Medium and Species Representation: Debunking the Myths, an Experiment-based Approach, 1996.
[163] M.A. Ghannoum, R.J. Jurevic, P.K. Mukherjee, F. Cui, M. Sikaroodi, A. Naqvi, P.M. Gillevet, Characterization of the Oral Fungal Microbiome (Mycobiome) in Healthy Individuals, PLoS Pathog. 6 (2010) e1000713. doi:10.1371/journal.ppat.1000713.
[164] C.N. Trueman, D.M. Martill, The long-term survival of bone: the role of bioerosion, Archaeometry. 44 (2002) 371–382. doi:10.1111/1475-4754.t01-1-00070.
[165] H.I. Hollund, M.D. Teasdale, V. Mattiangeli, O.Ó. Sverrisdóttir, D.G. Bradley, T. O'Connor, Pick the Right Pocket. Sub-sampling of Bone Sections to Investigate

Diagenesis and DNA Preservation, Int. J. Osteoarchaeol. 27 (2017) 365–374. doi:10.1002/oa.2544.
[166] P. Carini, P.J. Marsden, J.W. Leff, E.E. Morgan, M.S. Strickland, N. Fierer, Relic DNA is abundant in soil and obscures estimates of soil microbial diversity, BioRxiv. 53 (2016) 680840. doi:10.1101/043372.
[167] M. Brundin, D. Figdor, G. Sundqvist, U. Sjögren, DNA binding to hydroxyapatite: A potential mechanism for preservation of microbial DNA, J. Endod. 39 (2013) 211–216. doi:10.1016/j.joen.2012.09.013.
[168] M. Kamitakahara, S. Takahashi, T. Yokoi, C. Inoue, K. Ioku, Adhesion Behavior of Microorganisms Isolated from Soil on Hydroxyapatite and Other Materials, Appl. Biochem. Biotechnol. (2018) 1–10. doi:10.1007/s12010-018-2861-9.
[169] T. Bille, R. Wingrove, M. Holland, C. Holland, C. Cave, J. Schumm, Novel method of DNA extraction from bones assisted DNA identification of World Trade Center victims, Int. Congr. Ser. 1261 (2004) 553–555. doi:10.1016/S0531-5131(03)01831-4.
[170] Y.M. Coulson-Thomas, A.L. Norton, V.J. Coulson-Thomas, R. Florencio-Silva, N. Ali, S. Elmrghni, C.D. Gil, G.R.S. Sasso, R.A. Dixon, H.B. Nader, DNA and bone structure preservation in medieval human skeletons., Forensic Sci. Int. 251 (2015) 186–94. doi:10.1016/j.forsciint.2015.04.005.
[171] A.R. Gonzales, T. a Henke, S. V Hart, Mass Fatality Incidents : A Guide for Human Forensic Identification, Natl. Institue Justice. (2005) 1–79. https://www.ncjrs.gov/pdffiles1/nij/199758.pdf.
[172] M. Prinz, A. Carracedo, W.R. Mayr, N. Morling, T.J. Parsons, A. Sajantila, R. Scheithauer, H. Schmitter, P.M. Schneider, DNA Commission of the International Society for Forensic Genetics (ISFG): Recommendations regarding the role of forensic genetics for disaster victim identification (DVI), Forensic Sci. Int. Genet. 1 (2007) 3–12. doi:10.1016/j.fsigen.2006.10.003.
[173] Interpool, INTERPOL Disaster Victim Identification Guide, 2014 (2014) 127.
[174] I. Icmp, S.O.P. Aa, Standard Operating Procedure for Sampling Bone and Tooth Specimens From Human Remains, (2015) 1–19.
[175] C. Kendall, A. Marie, H. Eriksen, I. Kontopoulos, M.J. Collins, G. Turner-Walker, Diagenesis of archaeological bone and tooth, Palaeogeogr. Palaeoclimatol. Palaeoecol. 491 (2018) 21–37. doi:10.1016/j.palaeo.2017.11.041.
[176] A.G. Robling, A.B. Castillo, C.H. Turner, BIOMECHANICAL AND MOLECULAR REGULATION OF BONE REMODELING, Annu. Rev. Biomed. Eng. 8 (2006) 455–498. doi:10.1146/annurev.bioeng.8.061505.095721.
[177] K.G. Eilers, S. Debenport, S. Anderson, N. Fierer, Digging deeper to find unique microbial communities: The strong effect of depth on the structure of bacterial and archaeal communities in soil, Soil Biol. Biochem. 50 (2012) 58–65. doi:10.1016/j.soilbio.2012.03.011.
[178] C. Will, A. Thürmer, A. Wollherr, H. Nacke, N. Herold, M. Schrumpf, J. Gutknecht, T. Wubet, F. Buscot, R. Daniel, Horizon-Specific Bacterial Community Composition of German Grassland Soils, as Revealed by Pyrosequencing-Based Analysis of 16S rRNA Genes †, Appl. Environ. Microbiol. 76 (2010) 6751–6759. doi:10.1128/AEM.01063-10.
[179] R.E.M. Hedges, A.R. Millard, Bones and Groundwater: Towards the Modelling of Diagenetic Processes, 1995.
[180] A.L. Emmons, J. Davoren, J.M. DeBruyn, A.. Mundorff, Inter and intra-individual

variation in skeletal DNA preservation in buried remains. Manuscript in preparation., 2019.
[181] A.L. Emmons, S.W. Keenan, J.M. DeBruyn, J. Davoren, J. Andronowski, D. Carter, A.Z. Mundorff, Patterns of microbial colonization of human bone from surface-decomposed remains., 2019.
[182] J.G. Caporaso, C.L. Lauber, W. a Walters, D. Berg-Lyons, J. Huntley, N. Fierer, S.M. Owens, J. Betley, L. Fraser, M. Bauer, N. Gormley, J. a Gilbert, G. Smith, R. Knight, Ultra-high-throughput microbial community analysis on the Illumina HiSeq and MiSeq platforms, ISME J. 6 (2012) 1621–1624. doi:10.1038/ismej.2012.8.
[183] Bolyen et al. QIIME 2: Reproducible, interactive, scalable, and extensible microbiome data science, PeerJ Prepr. (2018). doi:10.7287/peerj.preprints.27295v1.
[184] B.J. Callahan, P.J. McMurdie, M.J. Rosen, A.W. Han, A.J.A. Johnson, S.P. Holmes, DADA2: High-resolution sample inference from Illumina amplicon data., Nat. Methods. 13 (2016) 581–3. doi:10.1038/nmeth.3869.
[185] F. Pedregosa, G. Varoquax, A. Gramfort, V. Michel, O. Grisel, M. Blondel, P. Prettenhofer, R. Weiss, V. Dubourg, J. Vanderplas, A. Passos, D. Cournapeau, Scikit-learn: Machine Learning in Python Gaël Varoquaux Bertrand Thirion Vincent Dubourg Alexandre Passos PEDREGOSA, VAROQUAUX, GRAMFORT ET AL. Matthieu Perrot, 2011. http://scikit-learn.sourceforge.net. (accessed March 15, 2019).
[186] P.J. McMurdie, S. Holmes, phyloseq: An R Package for Reproducible Interactive Analysis and Graphics of Microbiome Census Data, PLoS One. 8 (2013) e61217. doi:10.1371/journal.pone.0061217.
[187] S. Weiss, Z.Z. Xu, S. Peddada, A. Amir, K. Bittinger, A. Gonzalez, C. Lozupone, J.R. Zaneveld, Y. Vázquez-Baeza, A. Birmingham, E.R. Hyde, R. Knight, Normalization and microbial differential abundance strategies depend upon data characteristics, Microbiome. 5 (2017) 27. doi:10.1186/s40168-017-0237-y.
[188] J. Oksanen, F.G. Blanchet, F. Michael, K. Roeland, L. Pierre, M. Dan, P.R. Minchin, R.B. O'Hara, G.L. Simpson, P. Solymos, M. Henry, H. Stevens, E. Szoecs, H. Wagner, vegan: Community Ecology Package, (2018). https://cran.r-project.org/package=vegan.
[189] A. Collingro, S. Poppert, E. Heinz, S. Schmitz-Esser, A. Essig, M. Schweikert, M. Wagner, M. Horn, Recovery of an environmental chlamydia strain from activated sludge by co-cultivation with Acanthamoeba sp., Microbiology. 151 (2005) 301–309.
[190] M. Horn, M. Wagner, K.-D. Mu, E.N. Schmid, T.R. Fritsche, K.-H. Schleifer, R. Michel, Neochlamydia hartmannellae gen. nov., sp. nov. (Parachlamydiaceae), an endoparasite of the amoeba Hartmannella vermiformis, 2000. www.microbiologyresearch.org (accessed March 27, 2019).
[191] A. Collingro, E.R. Toenshoff, M.W. Taylor, T.R. Fritsche, M. Wagner, M. Horn, "Candidatus Protochlamydia amoebophila", an endosymbiont of Acanthamoeba spp, (2019). doi:10.1099/ijs.0.63572-0.
[192] B.B. Dent, M.J. Knight, Cemeteries: a special kind of landfill. The context of their sustainable management. Groundwater: sustainable solutions, in: Conf. Int. Assoc. Hydrogeol., Melbourne, 1998: pp. 451–456. file:///C:/Users/Alexandra Emmons/Downloads/Cemeteries_specialkindlandfill.pdf (accessed March 28, 2019).
[193] B.B. Dent, S.L. Forbes, B.H. Stuart, Review of human decomposition processes in soil, Environ. Geol. 45 (2004) 576–585. doi:10.1007/s00254-003-0913-z.
[194] B. Reinhold-Hurek, T. Hurek, The Genera Azoarcus, Azovibrio, Azospira and Azonexus,

in: D. Martin, S. Falkow, E. Rosenberg, K.H. Schleifer, E. Stackebrandt (Eds.), Prokaryotes, Volume 5, 2006. doi:10.1007/0-387-30745-1_42.
[195] D. Patureau, J.-J. Godon, P. Dabert, T. Bouchez, N. Bernet, J.P. Delgenes, R. Moletta, Microvirgula aerodenitrificans gen. nov., sp. nov., a new Gram-negative bacterium exhibiting co-respiration of oxygen and nitrogen oxides up to oxygen-saturated conditions, 1998. www.microbiologyresearch.org (accessed March 28, 2019).
[196] D.J. Harrington, MINIREVIEW Bacterial Collagenases and Collagen-Degrading Enzymes and Their Potential Role in Human Disease, 1996.
[197] S. Kalmbach, W. Manz, J. Wecke, U. Szewzyk, Aquabacterium gen. nov., with description of Aquabacterium citratiphilum sp. nov., Aquabacterium parvum sp. nov. and Aquabacterium commune sp. nov., three in situ dominant bacterial species from the Berlin drinking water system, Int. J. Syst. Bacteriol. 49 (1999) 769–777. www.microbiologyresearch.org (accessed March 29, 2019).
[198] R. Chander Kuhad, S. Singh, A. Singh, Phosphate-Solubilizing Microorganisms, in: Singh et al. (Ed.), Bioaugmentation, Biostimulation and Biocontrol, Springer-Verlag Berlin Heidelberg , 2011. doi:10.1007/978-3-642-19769-7_4.
[199] E. Hoberg, P. Marschner, R. Lieberei, Organic acid exudation and pH changes by Gordonia sp. and Pseudomonas fluorescens grown with P adsorbed to goethite, Microbiol. Res. 160 (2005) 177–187. doi:10.1016/J.MICRES.2005.01.003.
[200] T.G. O'Brien, A.C. Kuehner, Waxing Grave About Adipocere: Soft Tissue Change in an Aquatic Context, J. Forensic Sci. 52 (2007) 294–301. doi:10.1111/j.1556-4029.2006.00362.x.
[201] M. Ueland, H.A. Breton, S.L. Forbes, Bacterial populations associated with early-stage adipocere formation in lacustrine waters, Int. J. Legal Med. 128 (2014) 379–387. doi:10.1007/s00414-013-0907-7.
[202] S.L. Forbes, B.H. Stuart, B.B. Dent, The effect of the burial environment on adipocere formation., Forensic Sci. Int. 154 (2005) 24–34. doi:10.1016/j.forsciint.2004.09.107.
[203] G.T. Javan, S.J. Finley, Z. Abidin, J.G. Mulle, The Thanatomicrobiome: A Missing Piece of the Microbial Puzzle of Death., Front. Microbiol. 7 (2016) 225. doi:10.3389/fmicb.2016.00225.
[204] M. Ueland, H.A. Breton, S.L. Forbes, Bacterial populations associated with early-stage adipocere formation in lacustrine waters, Int. J. Legal Med. 128 (2014) 379–387. doi:10.1007/s00414-013-0907-7.
[205] J.T. Lennon, S.E. Jones, Microbial seed banks: the ecological and evolutionary implications of dormancy, Nat Rev Microbiol. 9 (2011) 119–130. doi:10.1038/nrmicro2504.
[206] P.J. McMurdie, S. Holmes, Waste Not, Want Not: Why Rarefying Microbiome Data Is Inadmissible, PLoS Comput. Biol. 10 (2014) e1003531. doi:10.1371/journal.pcbi.1003531.

VITA

Alexandra Leah Emmons was born in Mount Holly, New Jersey on April 10, 1990 to parents Alan and Brenda Emmons. One of two children, she moved to Brunswick, Georgia following her parents separation in 1994, where she eventually graduated Salutatorian from Brunswick High School in 2008. Following graduation, Alexandra relocated to Athens, Georgia, where she began attendance at the University of Georgia. Under the guidance of Dr. Maria Teresa Tersigni-Tarrant, a prominent forensic anthropologist, she received a Bachelor of Arts in Anthropology and a Bachelor of Science in Biology. In the spring of 2012, she was formally accepted to the University of Tennessee to pursue a Master of Arts degree in Anthropology with a concentration in Biological Anthropology under the leadership of Dr. Graciela Cabana. Her thesis was entitled *The Preservation and Persistence of Human DNA in Soil during Cadaver Decomposition*.

Following the defense of her thesis, Alexandra was re-accepted to the University of Tennessee to pursue a PhD in Anthropology under the guidance of Dr. Amy Mundorff. During her doctoral studies, she received an interdisciplinary minor in computational science and obtained a certificate in Disasters, Displacements, and Human Rights (DDHR).